Distributed optimization methods for the management of the security of interconnected power systems

Maxime Velay

Communauté
UNIVERSITÉ Grenoble Alpes

THÈSE

Pour obtenir le grade de

DOCTEUR DE LA COMMUNAUTÉ UNIVERSITÉ GRENOBLE ALPES

Spécialité : GENIE ELECTRIQUE

Arrêté ministériel : 25 mai 2016

Présentée par

Maxime VELAY

Thèse dirigée par **Yvon BESANGER** , G-INP
et codirigée par **Nicolas RETIERE**, UGA

préparée au sein du **Laboratoire CEA (hors LETI et LITEN)**
dans **l'École Doctorale Electronique, Electrotechnique, Automatique, Traitement du Signal (EEATS)**

Méthodes d'optimisation distribuée pour l'exploitation sécurisée des réseaux électriques interconnectés

Distributed optimization methods for the management of the security of interconnected power systems

Thèse soutenue publiquement le **25 septembre 2018**,
devant le jury composé de :

Monsieur YVON BESANGER
PROFESSEUR, GRENOBLE INP, Directeur de thèse
Monsieur ALBERTO BORGHETTI
PROFESSEUR ASSOCIE, UNIVERSITE DE BOLOGNE - ITALIE, Rapporteur
Monsieur GAUTHIER PICARD
PROFESSEUR ASSOCIE, ECOLE DES MINES DE SAINT-ETIENNE, Rapporteur
Madame SALIMA HASSAS
PROFESSEUR, UNIVERSITE LYON 1, Présidente
Monsieur NICOLAS RETIERE
PROFESSEUR, UNIVERSITE GRENOBLE ALPES, Co-directeur de thèse
Madame MERITXELL VINYALS
CHERCHEUR, CEA LIST - GIF-SUR-YVETTE, Encadrante

RÉSUMÉ DU MANUSCRIT EN FRANÇAIS

Notre société étant plus dépendante que jamais au vecteur d'énergie électrique, la moindre perturbation du transport ou de l'acheminement de l'électricité a un impact social et économique important. La fiabilité et la sécurité des réseaux électriques sont donc cruciales pour les gestionnaires de réseaux, en plus des aspects économiques. De plus, les réseaux de transport sont interconnectés pour réduire les coûts des opérations et pour améliorer la sécurité. Un des grands défis des gestionnaires des réseaux de transport est ainsi de se coordonner avec les réseaux voisins, ce qui soulève des problèmes liés à la taille du problème à résoudre, à l'interopérabilité et à la confidentialité des données.

Cette thèse vise à développer des outils d'optimisation qui répondent à un certain nombre de ces besoins. Tout d'abord, l'équilibre production-consommation doit être respecté tout en minimisant les coûts de production et en respectant les contraintes du réseau. De plus, les plannings de production doivent respecter ces contraintes dans les conditions normales, mais aussi dans l'éventualité où un équipement majeur du réseau viendrait à subir un incident. Lorsqu'il existe une incertitude liée à la production d'énergie renouvelable, le planning doit également être robuste aux erreurs de prédictions. Enfin, étant donné que les réseaux de transport sont interconnectés, il faut que les différents acteurs et notamment les gestionnaires, puissent se coordonner, tout en gardant la confidentialité et l'autonomie nécessaire, et ce, peu importe la taille du réseau.

Cette thèse se focalise principalement sur la sécurité des opérations sur les réseaux électriques, c'est pourquoi, dans le Chapitre 3, l'évolution des principales caractéristiques des blackouts, qui sont des échecs de la sécurité des réseaux, sont étudiés sur la période 2005-2016. L'objectif de cette étude consiste à déterminer quelles sont les principales caractéristiques des incidents de ces 10 dernières années, afin d'identifier ce qui devrait être intégré pour réduire le risque que ces incidents se reproduisent. L'évolution a été étudiée et comparée avec les caractéristiques des blackouts qui se sont produits avant 2005. Cette étude suit le développement d'un blackout : les *préconditions* constituent le contexte dans lequel se déroule le blackout, le ou les *éléments déclencheurs* initient une *cascade de défauts* qui peut contenir deux phases. Une fois que tout ou partie du réseau est effondré, la restauration du système, qui n'est pas étudiée en détails dans cette thèse, peut commencer.

Cette étude révèle que, contrairement à la plupart des blackouts avant 2005 [LBZR06], ces incidents ne se sont pas produits pendant des périodes de pic de consommation. Les principales préconditions identifiées dans cette étude sont, premièrement, la forte dépendance entre les régions interconnectées et ensuite, les équipements

hors-service. La dépendance entre régions est considérée comme forte si plus de 20 % de la puissance est importée ou exportée, ou si les capacités de transfert sont proches des limites de surcharges. La combinaison de ces deux conditions est particulièrement dangereuse si des lignes d'interconnexion sont hors-service. Nous notons aussi l'importance pour les gestionnaires des réseaux de transport de déterminer soigneusement la liste des équipements vulnérables, ou les contingences crédibles ou probables, ainsi que l'impact sur les réseaux voisins. Les interconnexions sont donc au centre des principales préconditions identifiées.
Les éléments déclencheurs de ces blackouts ne diffèrent pas des blackouts des périodes précédentes, on retrouve des surcharges, des courts-circuits et des pannes provenant des protections.

Nous avons ensuite étudié les cascades de défauts qui suivent ces éléments déclencheurs et principalement la vitesse de propagation. On peut, en général, distinguer deux cascades: une cascade quasi-statique, lente, et une cascade rapide qui comporte surtout des phénomènes transitoires. La durée des cascades est en fait primordiale pour les gestionnaires et en particulier la cascade quasi-statique, qui peut leur permettre de réagir aux incidents. En effet, lors de la cascade quasi-statique, des états stables sont atteints entre chaque incident donnant un temps pour agir, alors que quand la cascade rapide commence, la seule barrière pouvant stopper la propagation des incidents est le plan de défense automatique du système. L'étude de ces 9 blackouts montre que 7 d'entre eux ont commencé leur cascade par la cascade rapide sans cascade quasi-statique, ce qui est plus rapide que les blackouts des périodes précédentes puisque, pour les blackouts avant 2012, plus de la moitié ont eu un cascade quasi-statique d'après [VBC$^+$12]. Cette rapidité peut être expliquée par les dépendances entre les régions, qui, une fois séparées suite à un élément déclencheur, s'effondrent très rapidement et par les forte modifications des transferts de puissance suite à la déconnexion d'éléments fortement chargés.

En conclusion, pour réduire le risque d'apparition de blackouts il est préférable de travailler sur la prévention de ceux-ci et surtout d'éviter d'entrer dans les cascades rapides qui empêchent les gestionnaires et les réglages automatiques, notamment le réglage de fréquence, d'agir. De plus, il est important d'inclure les interactions avec les réseaux voisins, particulièrement celles pouvant mener à une séparation des régions interconnectées, ainsi que de considérer la coordination des acteurs.

Dans le cas où un incident modifie l'équilibre production-consommation, et surtout lors d'une séparation du réseau, le réglage primaire en fréquence est la première action qui permet de retrouver cet équilibre. Ce réglage est effectué localement sur chaque groupe de production par un correcteur proportionnel dépendant de la déviation en fréquence et permet donc de la stabiliser à une fréquence de fonctionnement différente. De plus, comme indiqué précédemment, il est primordial d'éviter de déclencher la cascade rapide par de la prévention coordonnée entre les différents acteurs du réseau de transport.

Pour ce faire, le Chapitre 4, présente un algorithme totalement distribué permettant de résoudre le problème préventif de " Security Constrained Optimal Power Flow " (SCOPF). Ce problème a pour but de déterminer et répartir la production de chaque générateur tout en garantissant que des contraintes de sécurité sont respectées. Ces contraintes assurent qu'après la perte de n'importe quel équipement majeur (ligne, transformateur, générateur, etc.) le nouveau point d'équilibre, atteint suite au réglage primaire en fréquence, respecte les contraintes du système.

L'algorithme développé pour résoudre ce problème d'optimisation est basé sur la structure présentée dans [CKC$^+$14], qui considère les équations de flux de puissance linéarisées, à laquelle nous avons incorporé le réglage primaire en fréquence. Cet algorithme utilise une décomposition fine du problème et est implémenté sous le paradigme multi-agent, basé sur deux catégories d'agents : les appareils et les bus. Cette décomposition procure l'autonomie et la confidentialité nécessaire aux différents acteurs du système, mais aussi, un bon passage à l'échelle par rapport à la taille du problème. Les agents sont coordonnés grâce à l' "Alternating Direction Method of Multipliers (ADMM)" qui est une méthode distribuée et itérative en trois étapes. Pour ce faire, les variables du problème d'optimisation sont dupliquées au niveau des connexions entre les bus et les appareils pour permettre une séparation artificielle du problème, et une contrainte couplante est ajoutée pour garder l'équivalence avec le problème original. Il en résulte un problème d'optimisation quasi-séparable avec d'un côté, les contraintes et objectifs indépendants entre eux des appareils, et de l'autre, les contraintes et objectifs indépendants entre eux des bus. Le Lagrangien augmenté peut alors être formé sur la contrainte couplante. L'ADMM consiste ensuite à résoudre d'abord les problèmes des appareils, c'est à dire minimiser le Lagrangien augmenté avec les variables reçues par chaque appareil. Tous les sous-problèmes des appareils peuvent être résolus en parallèle puisque ces sous-problèmes sont indépendants les uns des autres, ce qui est également le cas des sous-problèmes des bus. Puis, la deuxième étape vise à résoudre les problèmes des bus, autrement dit, à minimiser, en parallèle, le Lagrangien augmenté avec les résultats reçus des appareils voisins et considérés comme constant. Et enfin, la troisième étape consiste à mettre à jour les variables duales par les bus, avant d'envoyer ces résultats aux appareils.

De plus, un problème de consensus est ajouté et a pour but de déterminer d'une manière distribuée la réponse du réglage primaire en fréquence. En détail, un scénario est créé pour chaque contingence et la variable permettant la coordination du réglage primaire des agents est la déviation relative de la fréquence du réseau : $\alpha = \frac{\Delta f}{f_0}$, avec Δf la déviation en fréquence et f_0 la fréquence nominale du réseau. Les agents doivent donc trouver un consensus sur cette variable, qui permet de respecter l'équilibre production-consommation dans chacun des scénarios, suivant le réglage primaire, ainsi que les contraintes du réseau. En effet, la réponse du réglage primaire de chaque générateur est proportionnelle à cette déviation relative de la fréquence. Les sous-problèmes d'optimisation des agents bus et appareils sont faciles à résoudre, analytiquement ou via une méthode itérative de projection sur les contraintes des sous-problèmes.

Le caractère distribué de l'algorithme permet de préserver naturellement la confidentialité des acteurs du réseau et permet résoudre des problèmes de grande taille, grâce à la parallélisation de la résolution. De plus, cette approche rend possible la coordination des régions et acteurs interconnectés via une communication de proche en proche, et permet de considérer un grand nombre de contingences.

Les performances de cet algorithme sont ensuite testées sur les réseaux test IEEE 14-bus et RTS 96 à trois régions (constitué de 96 générateurs et de 120 lignes). Les résultats montrent que notre approche permet de résoudre le problème de SCOPF et de déterminer les flux de puissance et la déviation relative de la fréquence pour chacun des scénarios considérés. Ils démontrent également que considérer un grand nombre de scénarios ne détériore pas forcément les performances. Par exemple, dans le cas du réseau test RTS 96, résoudre le problème de SCOPF avec 216 scénarios demande 35 % d'itération en moins que pour résoudre le problème d'Optimal Power Flow classique (sans contraintes de sécurité). Finalement, la robustesse de l'algorithme est testée en considérant le changement le plus perturbant pour un réseau interconnecté, à savoir la déconnexion de régions du système. Pour ce faire, un réseau à deux régions est construit et un scénario de séparation des deux régions est intégré à la liste des contingences. L'algorithme a ensuite permis de résoudre le problème sans même partager l'origine de la perturbation et prouve donc la grande robustesse de l'algorithme face à tout changement de topologie du réseau.

Néanmoins, cette approche ne considère pas l'incertitude sur la production créée par les erreurs de prédiction des énergies renouvelables, et en particulier, des fermes éoliennes. Le Chapitre 5 a donc pour but d'intégrer cette incertitude et de développer une approche distribuée pour résoudre ce nouveau problème de " Chance Constrained Optimal Power Flow " (CCOPF). Ce problème d'optimisation inclut des contraintes probabilistes qui permettent de garantir que les contraintes statiques de sécurité du réseau seront respectées avec une grande probabilité, connaissant la densité de probabilité de production des fermes éoliennes. Les erreurs de prédiction des fermes éoliennes sont modélisées par des lois normales indépendantes pour pouvoir résoudre le problème plus facilement, et les écarts par rapport aux plannings de production sont considérés compensés par le réglage primaire en fréquence. Dans ce cas, les variables du réseau deviennent des lois normales et les contraintes déterministes, telles que $x \leqslant x^{max}$, sont remplacées par des contraintes sur la probabilité de respecter la contrainte : $\mathbb{P}(x \leqslant x^{max}) > 1 - \epsilon$ avec $\epsilon \in [0, 1]$ proche de 0.

La formulation de ce problème d'optimisation nécessite l'emploi de paramètres de sensibilité du réseau, à savoir les "Generalized Generation Distribution Factors" (GGDF) qui permettent de déterminer les changements des flux de puissance liés à une modification de la puissance injectée sur le réseau, et l'énergie réglante primaire du réseau. La première étape de l'algorithme a donc pour but de déterminer ces paramètres de sensibilité nécessaires pour formuler le problème. L'algorithme Push-Sum [KDG03], qui permet de calculer une somme de manière distribuée, est utilisé pour déterminer l'énergie réglante primaire. Puis, différentes répartitions des flux

de puissance (déterministes) sont déterminées, et dans chaque scénario la production d'une ferme éolienne est modifiée. Les facteurs GGDF peuvent ensuite être calculés. Les résultats de cette étape sont des paramètres d'entrée de la seconde étape qui, elle, résout le problème de CCOPF, à l'aide de l'ADMM, en resserrant les contraintes des générateurs et des lignes.

Cet algorithme à deux étapes est testé sur un réseau test à 2 bus et sur le IEEE 14-bus, démontrant sa capacité à résoudre ce problème d'optimisation d'une manière distribuée qui garantit la coordination et la confidentialité des acteurs. Cependant, le problème de CCOPF ne peut pas considérer les contraintes de rampes des générateurs et, lorsque l'incertitude est élevée, peut devenir infaisable.

Une extension de cette formulation est donc développée pour rendre possible l'ajout de flexibilité au problème en permettant la réduction de la production éolienne. La réduction de la production est linéaire et a lieu quelle que soit la production réelle des fermes éoliennes. En d'autres termes, que la prévision de production d'une ferme soit surévaluée ou sous-évaluée la réduction d'une fraction de la production sera effectuée. L'algorithme permettant de résoudre ce nouveau problème est basé sur la même décomposition fine que précédemment et les agents sont également coordonnés par l'ADMM et grâce à un problème de consensus. Le problème de consensus porte ici sur l'écart type de la production de chacune des fermes éoliennes, et permet donc de résoudre les problèmes de CCOPF insolubles. Ces nouveaux sous-problèmes sont non-linéaires non-convexes et ne peuvent donc pas être résolus facilement sans solveur externe.

Cette extension a été testée sur les réseaux test 2-bus et IEEE 14-bus, et ont permis de déterminer le niveau de réduction optimal nécessaire pour rendre les problèmes faisables, tout en intégrant les contraintes de rampes des générateurs. En conclusion, cet algorithme en deux étapes permet de résoudre le problème de CCOPF, avec possibilité d'optimiser la réduction de la production éolienne, garantit la confidentialité et l'autonomie des différents acteurs, et est parallèle et adaptée aux plateformes hautes performances.

En conclusion, les méthodes développées permettent de répondre à certains des besoins énoncés en introduction, et réaffirmé dans le Chapitre 3, et particulièrement aux besoins de coordination, d'autonomie et de confidentialité entre acteurs dans un contexte de réseaux interconnectés de grandes tailles. Le Chapitre 4 répond au besoin de sécurité vis-à-vis des incidents pouvant perturber le réseau et le Chapitre 5 répond lui au besoin de sécurité vis-à-vis de l'incertitude de production des fermes éoliennes.

Différentes pistes de recherches peuvent finalement être dressées suite à cette thèse. Tout d'abord, la complexité des modèles de flux de puissance (considéré linéarisé dans cette thèse) et la complexité des appareils peuvent être améliorées. Notamment, les charges, considérées constantes dans ce manuscrit, peuvent être remplacées par des problèmes de Smart-Grid résolus également par l'ADMM qui est souvent employé dans ce cadre. Il est également possible de formuler et résoudre un problème d'optimisation considérant tous les besoins de sécurité énoncés en introduction.

Finalement, les dernières pistes de recherche concernent les améliorations algorithmiques nécessaires à un déploiement réel.

CONTENTS

NOMENCLATURE

D	is the set of devices;
N	is the set of nets;
G	is the set of generators that are all considered involved in the primary frequency control;
L	is the set of lines, we use the DC power flow equations;
F_l	is the set of loads, considered fixed loads;
W	is the set of wind farms;
$\mathcal{L}$	is the number of possible contingency scenarios. The superscript in parenthesis, (s), refers to the number of the scenario and the base case is designated by the superscript (0);
$D^{(s)}$	represents the set of devices disconnected in the scenario $(s) \in [(1), \mathcal{L}]$;
p_d	is the active power entering device d;
$\dot{p}_n$	is the active power leaving net n;
θ_a or $\dot{\theta}_a$	is the voltage phase angle of agent a;
α_a or $\dot{\alpha}_a$	is the relative steady-state frequency deviation of agent a;
σ_a or $\dot{\sigma}_a$	is the standard deviation related to the active power of agent a;
$\mathbf{\Sigma}$ or $\dot{\mathbf{\Sigma}}$	is the vector of standard deviation of the wind farms of the system;
u_a	is the dual variable associated with the active power of agent a;
v_a	is dual variable associated with the voltage phase angle of agent a;
w_a	is the dual variable associated with the relative steady-state frequency deviation of agent a;
$\mathcal{W}_a$	is the vector dual variables, of agent a, associated with the standard deviation of the wind farms of the system;
β_g	is the quadratic cost coefficient of generator $g \in G$;
γ_g	is the linear cost coefficient of generator $g \in G$;

P_g^{max} is the maximum power output of generator $g \in G$;

P_g^{min} is the minimum power output of generator $g \in G$;

R_g^{max} is the maximum ramp up of generator $g \in G$;

R_g^{min} is the maximum ramp down of generator $g \in G$;

$\Delta p_g^{(s)}$ is the power compensation of generator $g \in G$, for the scenario (s);

P_l^{max} is the maximum capacity of line $l \in L$;

ξ_w is the curtailment factor of wind farm $w \in W$;

GF_l^w is the Generalised Generation Distribution Factor (GGDF) associated with line $l \in L$ and the wind farm $w \in W$;

GF_l is the GGDF matrix of line $l \in L$ that is diagonal, and each of the diagonal terms corresponds to the GGDF related to a wind farm;

p_w^i is the expected power forecast of wind farm $w \in W$ without curtailment;

σ_w^i is the forecast error standard deviation of wind farm $w \in W$ without curtailment;

K_g is the primary frequency control compensation factor of generator $g \in G$;

$\sum_{g \in G} K_g$ is the primary frequency response characteristic of the system;

ρ is the scaling parameter of the ADMM;

ϵ^{abs} is the absolute tolerance;

LIST OF FIGURES

LIST OF TABLES

1

INTRODUCTION

Over the coming years, transmission system operators (TSOs) will face the challenge of incorporating a large number of renewable energy sources (RES) [DBT17, JWW+17] into their already highly stressed networks. In addition, as the use of power systems interconnections is increasingly important, mainly for cost and security reasons, the traditional centralised techniques to manage these interconnected networks raise scalability, privacy and interoperability issues. Hence, TSOs should coordinate with each other to ensure the security of the whole interconnected system at the best price and, in the meantime, this coordination should scale to the systems size and enforce the privacy of the different power system actors. This presents an interesting multi-actor coordination problem which could be solved by using distributed optimisation techniques. However, in order to fully understand this coordination problem, we first need to elaborate on these new challenges faced by TSOs.

Our societies are more dependent on electricity than ever, thus any disturbance in the power transmission and delivery has major economic and social impact. The reliability and security of power systems are then crucial to keep, for power system operators. Formally, the reliability of a power system is defined, in [KPA+04], as *the ability to supply adequate electric service on a nearly continuous basis, with few interruptions over an extended time period.* And to be reliable, a system must be secure most of the time, which can be defined, according to [KPA+04], as the system *ability to survive imminent disturbances (contingencies) without interruption of customer service*.

Transmission system operators, whose main mission is to ensure this reliability and security, play a vital role in the supply and the delivery of electric power. On one side, electricity is a commodity that cannot be easily stored, so TSOs need to keep the balance between generation and consumption while minimising the system operating cost and enforcing the network's operational constraints (e.g. the capacity of the transmission lines, voltages, etc.) during each operating period. On the other side, TSOs shall operate to protect against instability, guaranteeing not only that no operational constraint is durably violated during the normal operating conditions, but also after any credible contingency occurs. The set of considered contingencies depends on the selected reliability criterion but most of the TSOs must operate at least in compliance with the N-1 criterion so that any *single* major element contingency (i.e. involving the

failure of at most one system component) can be handled, leading to a stable operating point, i.e., with no propagation of the disturbance [PMDL10].

Component failures are not the only aspects that TSOs must consider in preventing grid instability. The growing integration of RES, such as wind and solar energy sources, can also cause serious stability problems to classical grid operation due to the unpredictable, uncontrollable and highly variable nature of this kind of sources. Traditionally, power grids were designed to handle energy flows from predictable, controllable and centralised power generation units to final consumers. Thus, as RES penetration rates continue to grow, coping with their unexpected fluctuations and their consequences when operating transmission grids becomes an increasingly important and complex task [EB05, BGL10, HZ15].

Moreover, transmission systems are interconnected to decrease the cost of operation and improve the security of the system. For example, 36 countries are interconnected in Europe, forming the pan-European power system. These advantages are, yet, subject to have an effective cooperation and coordination among the interconnected TSOs and hence, not surprisingly, regional cooperation through the development of regional security coordinators is at the core of the regional strategy of European TSOs for the decades to come [EE15]. Despite this fact, European regional coordination initiatives are in their early stages and most TSOs are still solving their power optimisation problems with limited coordination with their neighbours. Inefficient coordination can lead to suboptimal or dangerous operations, especially when outages occur. For example, one of the main causes of the 2006 power incident in Europe that affected more than 15 million people through Europe, was an inappropriate coordination of the TSOs [Eur07].

One of the main challenges to realise such inter-regional coordination is that the implementation of centralised approaches is undesirable, if not impossible, due to the technical difficulties for building (i.e. communication requirements for gathering data for the whole system) and solving (i.e. the high computational complexity) such interconnected problems of unprecedented scale. In addition to this, the centralization of inter-regional data is unlikely to be practical because TSOs may not be willing to disclose actual sensitive data (e.g. financial information, system topology and/or control regulations) to other TSOs. Also, interoperability issues can arise from the use of different modelling and optimisation tools by the different TSOs.

Hence, this thesis focuses on how TSOs can operate their networks in a decentralised way but coordinating their operations with other neighbouring TSOs to find a cost-effective scheduling that is globally secure (i.e. against component failures in the high presence of RES).

The following section is dedicated to the formalisation of the requirements that we aim to address in this thesis, regarding the power systems operations and their security. The main challenges, related to the requirements listed in Section 1.1, are discussed in more detail in Section 1.2. The contributions of this thesis are then provided in Section 1.3, and the structure of this manuscript in Section 1.4.

1.1 RESEARCH REQUIREMENTS

The operation of power systems is one of the more challenging problems faced by transmission system operators (TSOs) given the complex interplay of the multiple economic and reliability objectives to be achieved. Optimisation tools are employed on a daily basis by TSOs to solve these problems efficiently, relying on predictions of the electrical consumption and renewable energy production. These optimisation tools must fulfil several major requirements, among which:

1. *Power balance*: the electricity generation (supply) and the consumption (demand) should be balanced at all times because electricity is a commodity that cannot be easily stored in large quantities and power imbalances can rapidly escalate into a cascading system failure (i.e. blackout).

2. *Minimise the cost of (normal) operation*: the total operational cost of dispatchable elements under normal system conditions should be minimised.

3. *Network constraints*: optimisation tools should return schedules that satisfy the network's operational constraints (e.g. the maximum capacity of the transmission lines, voltages, power flow equations) during each operating period. Not respecting these constraints can lead to the triggering of protection devices and/or to severe system disturbances.

4. *Secure operation with respect to (transmission lines/transformers and generators) outages*: optimisation tools should return schedules that can securely handle outages on major elements of the system, leading to a stable operating point, i.e., with no propagation of the disturbance. The set of considered outages depends on the selected reliability criterion but most of the TSOs must operate at least in compliance with the N-1 criterion so that any single major element contingency is considered.

5. *Secure operation with respect to forecast uncertainty*: optimisation tools should return schedules that are robust with respect to deviations from forecasts and their consequences (e.g. potential violations of network constraints and eventually line tripping).

6. *Multi-area coordination and interoperability*: in an interconnected power system, different actors (e.g. different TSOs) need to coordinate for the joint operation of interconnection lines and for the security related to outages and uncertainties that have an impact on the operations of neighbouring systems. In addition to this, the algorithms proposed should be able to handle the potential interoperability issues arising from the use of different modelling and optimisation tools by the different operators.

7. *Privacy and autonomy*: the privacy and autonomy of interconnected power system actors should be enforced because, as they represent different entities, they

may not be willing, in a competitive context, to disclose actual sensitive data (e.g. financial information, system topology and/or control regulations) to other participants or even to a central coordinator.

8. *Scalability*: finally, the expansion of power systems due to its high level of interconnection require optimisation tools that scale well with the size of the network.

The following sections discusses the remaining challenges of the secure generation dispatch for electrical transmission networks, and the gap in the literature that this thesis addresses.

1.2 DISCUSSION ON THE OPEN CHALLENGES

From the problems and requirements identified in the previous section, there are some key challenges that must be addressed for the secure operation of interconnected systems:

1. When scheduling generators production in an electrical transmission network, the first key challenge is to ensure that the algorithms minimise the cost of normal operations of the network (Requirement 2) whilst respecting the power balance and network constraints (Requirement 1, 3). This problem that is solved in a daily basis by transmission system operators is known in the literature as Optimal Power Flow (OPF). Due to the quadratic and sinusoidal relations between voltage magnitude and phase angle, and, between active and reactive powers, the OPF problem is non-linear and non-convex. To simplify the calculation, the AC power flow equations are often relaxed or approximated. In particular, the linearised (DC) power flow approximation is often employed and consists in neglecting the losses on power lines and in assuming constant voltage and small voltage phase angles.

2. The second key challenge is to find schedules that secure operations with respect to the outage of any major power system device (i.e. major transmission lines, transformers and generators) (Requirement 4). This problem is known in the literature as Security Constrained OPF (SCOPF), an extension of the OPF problem that ensures that the operating limits would also be satisfied in the post-contingency steady-states of a set of pre-defined contingencies. The number of contingencies considered being large, especially when considering interconnected power systems, solving SCOPF problem can lead to computational difficulties if the optimisation tools are not scalable (Requirement 8).

3. The third key challenge is to find schedules that are robust to forecast errors (i.e. to the potential deviation between the forecast and the actual values). In the literature, this problem is usually modelled under the so-called Chance-Constrained

OPF (CCOPF) framework, an extension to the OPF in which the system security constraints can be violated with a small predefined level of probability to capture the uncertainty. The main difficulty being that, in general, chance-constrained optimisation problems are computationally intractable since they require the computation of multi-dimensional probability integrals.

In addition to the three challenging optimisation problems cited above, Requirements 6 and 7 imply that different actors of the system need to coordinate their operations whilst maintaining their autonomy and privacy, suggesting the use of distributed optimisation. Under distributed optimisation approaches, the large-scale power system problem is divided into smaller sub-problems in a way that sub-problems can be efficiently solved and effectively coordinated to obtain a final solution to the original problem. Given that actors can adopt distinct models and algorithms to solve their individual sub-systems, such approaches inherently deal with the interoperability requirement of interconnected power systems. Furthermore, the fact that local sub-problems can be solved in parallel (i.e. in individual processing units) and that typically the complexity of solving these smaller problems is significantly reduced with respect to solving the global problem leads to a good scalability of these approaches.

Based on the type of information being exchanged among sub-problems, distributed optimisation approaches applied to power system optimisation problems are typically divided in two categories [WWW17a]: (i) generator-based decomposition with cost information exchange; and (ii) geography-based decomposition with physical information exchange. However, generator-based decomposition approaches [ZC12, EES15] may lead to the exposure of the actors' strategy (through price/cost information) and hence they do not satisfy Requirement 7. Moreover, these methods have only proven to be efficient when neglecting global constraints of the system such as power flow equations and capacity limits of transmission lines, imposing an undesirable trade-off between power balance and security issues, and scalability requirements (Requirements 1 and 8).

Conversely, under geography-based decomposition methods, the large-scale power system is decomposed following its physical topology into smaller sub-regions of lower complexity that can be effectively solved. Since only limited physical information (i.e. voltage, power flows) needs to be exchanged among adjacent sub-regions (or between a central controller and sub-regions if not fully distributed) such approaches inherently respect the privacy of the different actors.

Under this category, Augmented Lagrangian methods and in particular the Alternating Direction Method of Multipliers (ADMM) have attracted increasing attention in recent years[1] due to its full distributivity and its improved convergence compared to other state-of-the-art distributed optimisation algorithms. In this line, Kraning et al. developed in [KCLB14] a message passing method, based on ADMM, to solve a dynamic network energy management problem that relies on DC (linearised) power flow

1 See Section 2.3 for reviews on the different distributed algorithms that have been applied to power system related optimisation problems and for a discussion on the suitability of the ADMM.

equations, in a fully distributed manner. The non-convex AC power flow equations were included in [ST15] to solve, with the same approach, an OPF problem applied to micro-grids, proving the efficiency of the ADMM to solve non-convex power system problems.

In the context of security constrained problems, Chakrabarti et al. [CKC+14], building on the work of [KCLB14], applied the ADMM to solve the SCOPF problem with DC power flow equations, ensuring that the operating limits would be satisfied after each transmission line contingency. However, the paper lacks any empirical evaluation in real circuits (e.g. the distributed algorithm is only evaluated in a single two bus system). A more extensive experimental validation is performed in [PK12] with the application of the ADMM as a heuristic method to solve the same SCOPF problem with AC non-convex equations, in the large-scale Polish 3012-bus system. But, the decomposition they employ (scenario-based) does not respect requirements 6 and 7, regarding the coordination and the privacy of the actors.

Nevertheless, despite showing the scalability and efficiency of the ADMM, all these above-cited works cannot integrate any contingency that results in the loss of the power balance between production and consumption. Hence, none of these works can secure operation with respect to the loss of a generator (i.e. as part of Requirement 4) or with respect to forecast deviations (i.e. Requirement 5). It turns out that modelling such contingency states requires taking into account the automatic schemes implemented on power systems to keep the power balance, and in particular, the primary frequency control (PFC) scheme that is the first and fastest of such automatic schemes.[2] As mentioned in [CD17], among the different reserve schemes, the ability to provide sufficient primary frequency control is less studied in the literature than optimised responses of the system. Also, when studied, it is usually modelled by means of centralised approaches, as in [KCP10, DHKP16]. It is important to note that since the generators participating in the primary frequency control automatically adapt their production with respect to the frequency deviation that, in turn, is a global variable of the system in steady-state, modelling it in a distributed manner is not a trivial task.

Last but not least, all these above references do not account for any source of forecast error and hence they do not satisfy Requirement 5. The main challenge when dealing with forecast uncertainty is the computational complexity of computing the multi-dimensional probability integrals in the resulting CCOPF problem. To overcome this difficulty some works [VML12, MHH+12] have opted for a scenario-based approach that transforms probabilistic constraints into hard constraints corresponding to a specific number of uncertainty scenarios. However, ensuring a-priori guarantees on the solution accuracy, requires to sample a very large number of scenarios, leading to large computational times and memory requirements [LM15]. Instead, an alternative approach is followed in the works of [BCH14, ROKA13, LM15], where the forecast error of wind farms are assumed to be following (previously known) mutually independent Gaussian probability distributions. The Gaussianity assumption

2 See Section 2.1.3 for a review of the frequency schemes in power systems.

allows for an analytical reformulation of the problem, leading to a deterministic problem with lower computational complexity than scenario based approaches [MGL14]. However, these works propose centralised approaches to solve the CCOPF problem which are very well suited for single regional area systems, but not for the multi-area interconnected systems tackled in this thesis.

Against this background, there is a clear need for a scalable distributed optimisation algorithm that coordinates different operators in a large scale interconnected system to find a joint optimal generation schedule secure with respect to the outage of any major power system component and with respect to possible forecast errors. To do that, the algorithm will need to be able to model contingencies that lead to power imbalance and hence, the primary frequency response of the system.

This thesis fulfils this need taking as starting point some existing approaches in the literature. More precisely, this thesis provides new decentralised algorithms that are built on:

- The fully decentralised power network decomposition of Kraning et al. [KCLB14] solved via ADMM, extended in [CKC$^+$14] to be secure with respect to the contingencies of transmission lines.
- The analytical reformulation from [ROKA13, BCH14] of the CCOPF problem based on the assumption that the forecast errors are Gaussian which allows to take into account the uncertainty with lower computational complexity.

The following section discusses the research contributions of this thesis to tackle the open challenges identified in this section.

1.3 CONTRIBUTIONS OF THE THESIS

One of the main focus of the presented requirements is the security of power systems (Requirements 3, 4, 5). As power systems continuously evolve with new customs, technologies and regulations, a permanent analysis of large power security failures is crucial for identifying new trends as well as for drawing recommendations to improve the system security. For this reason, Chapter 3 of this thesis analyses 9 major blackouts that happened in the period between 2005 and 2016, among them some of the largest blackouts of all times. We classify these blackouts depending on the conditions and events before and during the cascades and identify their main characteristics. When comparing our findings with those of blackouts of previous periods, our analysis reveals that blackouts of the last decade tend to present different features than their precedents. These characteristics reinforce the requirements of Section 1.1 and lead to new ones, such as the necessity to include the separation into different areas of an interconnected system. These should be taken into account in the development of decentralised optimal power flow algorithms in the chapters to follow.

In Chapter 4, we extend the framework of [CKC$^+$14] in order to take into account the automatic primary frequency control of generators. By doing so, we are able to

model DC power flow steady-states corresponding to different scenarios that represent different outages involving a modification of the active power balance. The frequency deviation is computed by distributed consensus via ADMM and used to coordinate the power reallocation process after an incident, without even knowing the origin of the disturbance. Our distributed approach is scalable and enables the coordination of the different actors of the system whilst respecting their necessary privacy and autonomy.

Then, to account for the uncertainty of production, we developed a two-step distributed approach to solve the CCOPF considering the primary frequency response of generators in a fully distributed manner in Chapter 5. The first step aims at determining the sensitivity factors of the system, needed to formulate the problem. The so-called Generalised Generation Distribution Factors measure the line flow changes due to deviations from generation schedule and the frequency response characteristic of the system. The results of this first step are inputs of the second step that is the CCOPF. Both steps are solved in a distributed way by the ADMM algorithm. The uncertainty is integrated through a forecast error probability distribution and we employ Gaussian distributions for its simplicity to compute the distribution of the sum of random variables. The simulation results show that, under low penetration of uncertain sources with low uncertainties, the algorithm is able to find the optimal solution of the CCOPF problem. However, when the problem is unfeasible due to an important uncertainty, the algorithm should integrate flexibilities. We then propose a formulation of the CCOPF with curtailment capabilities for the RES through a consensus problem on the standard deviation of the RES probability density function. This extension allows the integration of more uncertain devices in the system as the flexibility introduces a way to mitigate the impact on the fulfilment of the network constraints. In conclusion, this two-step algorithm ensures the privacy and autonomy of the different system actors and it is de facto parallel and adapted to high performance platforms.

The following section details the structure of this thesis.

1.4 THESIS STRUCTURE

The remainder of this thesis is structured as follows:

Chapter 2 presents the relevant state-of-the-art literature that is necessary to tackle the requirements of Section 1.1. Because this thesis lies at the intersection of two research fields, namely power systems and distributed optimisation, this chapter aims at providing the necessary background for both communities.

Chapter 3 analyses nine large power blackouts that happened between 2005 and 2016. This study aims at characterising the main common features of recent blackouts in order to determine the important parameters to take into account in the distributed optimisation algorithms developed in Chapters 4 and 5. These characteristics are compared to those found in previous blackouts studies and used to justify the requirements

from Section 1.1
The material contained in this chapter has been published in:

- Maxime Velay, Meritxell Vinyals, Yvon Besanger and Nicolas Retière. *An analysis of large-scale transmission power blackouts from 2005 to 2016*. In the 53rd International Universities Power Engineering Conference, September 4-7, 2018, Glasgow, Scotland

Chapter 4 presents a novel distributed algorithm based on ADMM for solving the Security Constrained Optimal Power Flow problem, including the primary frequency control of generators. This chapter also provides a discussion on the simulation results obtained by testing the algorithm on several standard IEEE systems.
The material contained in this chapter has been published in:

- Maxime Velay, Meritxell Vinyals, Yvon Besanger and Nicolas Retière. *Agent-based Security Constrained Optimal Power Flow with primary frequency control*. In EUMAS 2017 Proceedings of the 15th European Conference on Multi-Agent Systems, December 14-15, 2017, Évry, France

Chapter 5 formulates a Change Constrained Optimal Power Flow problem that accounts for the uncertainty on RES production and the consequent automatic frequency response of generators to power deviations. Then, it proposes a novel algorithm based on ADMM to solve this problem in a completely distributed way as well as an extension of this algorithm that accounts for the possibility of control the curtailment of the wind farm production to limit the risks of constraints violations. This chapter also discusses the performance of both algorithms in different simulations.
The material contained in this chapter has been published in:

- Maxime Velay, Meritxell Vinyals, Yvon Besanger and Nicolas Retière. *Distributed chance-constrained optimal power flow based on primary frequency control*. In the ninth ACM International Conference on Future Energy Systems (ACM e-Energy), June 12-15, 2018, Karlsruhe, Germany.

Chapter 6 finally concludes regarding the achievement of the thesis. A discussion about the improvement of this work is then conducted and future works are proposed.

2

RELATED WORK AND BACKGROUND

This chapter aims at introducing the necessary background on power system operations and optimisation, as well as the relevant related works on distributed optimisation to follow the thesis. In more detail, Section 2.1 describes the power systems structure, the frequency control schemes and the physics and modelling of power flows. In Section 2.2, the principal optimisation problems solved by power system operators are introduced and the main challenges are discussed. The main state-of-the-art of the distributed approaches that can be implemented under the multi-agent system paradigm and applied to optimal power flow problems are reviewed and compared in Section 2.3. Section 2.4 reviews in detail the literature that employed the Alternating Direction Method of Multipliers (ADMM) to the different optimal power flow problems. This section also details the different power network decompositions that have been used with ADMM, and discusses the advantages and drawbacks of each decomposition. Section 2.5 formalises the network decomposition used in this thesis and the ADMM algorithm. Finally, Section 2.6 concludes by summarising the main challenges addressed in this thesis.

2.1 POWER SYSTEM OPERATIONS

Power system operations are at the core of the requirements developed in Section 1.1 and depend on major aspects of power systems. First, the power system structure is an essential input parameter since it defines most of the interconnections, inter-operations and coordination aspects of the power system. Then, the most important constraints on power system operations are the power balance of the system (Requirement 1) that is realised by the frequency control schemes and the physics of the power flows (included in Requirement 3). Next sections describe in details these three aspects of the power system operations.

2.1.1 *Power systems structure*

Power systems were historically developed around large and centralised generating units that supply the power that needs to be transmitted to loads that are spread in space. Power systems have been dedicated to making the link between those large

producers and the customers. Because loads are not necessarily located close to the generating units, long distance transmission of power is needed. Furthermore, the voltage is elevated by step up transformers in order to reduce the power losses and to save conductors. This high voltage part of the power system is called *transmission system*.

The reliability of a transmission system is crucial and hence, the system topology is meshed to provide alternative paths in case of outages of some components. The transmission system also interconnects different grids, managed by different actors, through interconnection lines. These interconnections provide emergency support and help reducing the cost of operations by exchanging power among the different areas.

Transmission systems are operated by *transmission system operators (TSO)* (also known as *independent system operators (ISO)*). The role of these operators is to manage the power flows, including interconnection lines, and to ensure the power balance between generation and consumption on the system and more generally, the reliable and secure operation of the transmission. Figure 2.1 illustrates the structure of a generic interconnected power system where generation units are connected through step up transformers to the transmission system. Observe that the lines of interconnection between different transmission systems, represented by black bold lines, link the different transmissions systems, designated by the blue circles.

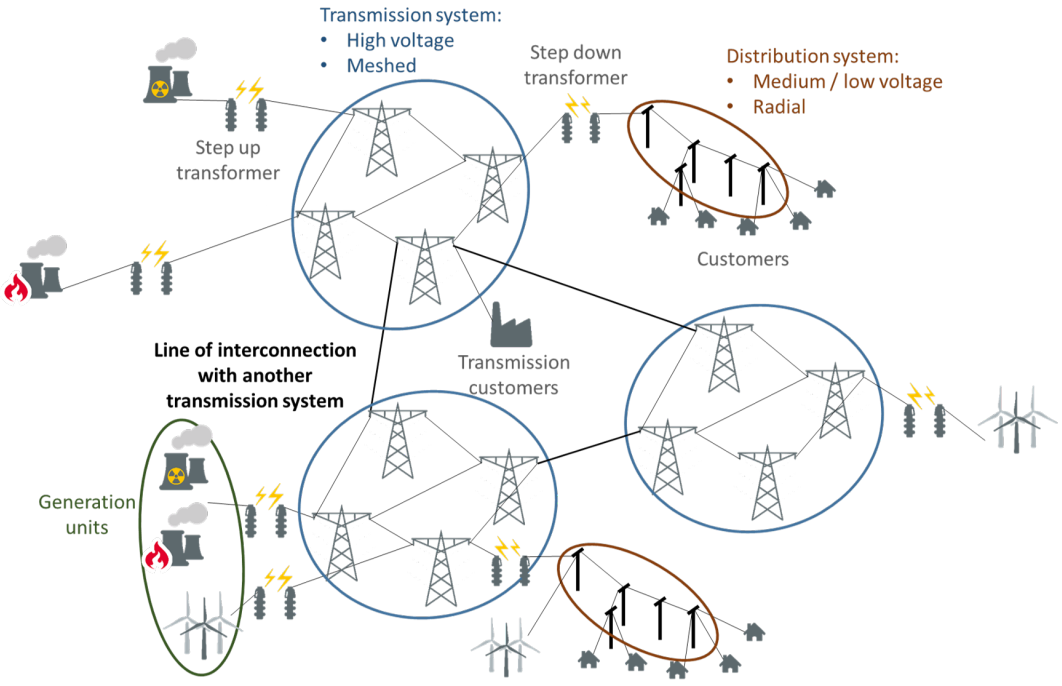

Figure 2.1: Power system structure.

As shown in Figure 2.1, step down transformers are connecting the transmission system with the *distribution system*. These distribution systems are managed by *distribution system operators (DSO)* that are responsible for the continuity and quality of

the power delivered.
From the first transformer that is the main substation of the distribution system, different substations and transformers distribute and adapt the voltage to the loads. Small (renewable) generating units can also be connected to distribution systems. Another characteristic of distribution systems is that, because loads are spread, the length of conductor needed to connect them is much larger than transmission system. This is one of the reasons why distribution systems have less redundant structure (i.e. radial, except sometimes in big cities) and are less instrumented than transmission systems. Distribution systems thus, offer little alternative path, if any, especially when the system is exploited radially because the loss of a power delivery device disconnects all downstream devices.

Note that the security of the system (Requirements 4 and 5) is mainly ensured at the transmission level, as well as the optimisation of the cost of operations (Requirement 2). The privacy and autonomy (Requirement 7) of the actors can be an issue at different borders and the main one is at the interconnections among transmission systems, because interconnected transmission systems can be operated by different operators. In addition, the connections of any actor (generating units and customers) might also bring privacy and autonomy issues and especially, the connection between transmission systems and distribution systems, because of the increasing role the distribution systems play in the balancing of the system.

In this thesis, we focus on transmission systems and we include the interconnections between transmission systems because most important security and coordination issues take place at this level.

2.1.2 *Power flow models*

Power flows are at the centre of the power system operations and it involves complex electromagnetic phenomenon. The level of complexity of the modelling of those phenomenon is then critical for the accuracy and the computational complexity of the model. A widely used trade-off is the quasi-static power flow model that depends on two complex variables: the power S and the voltage E (phase-to neutral). The real variables taken into account in the so called AC (for Alternating Current) power flow equations, include the active and reactive power which are respectively the real and imaginary parts of the power S, denoted as P and Q. Analogously, they include the voltage magnitude (V) and voltage phase angle (θ) that are respectively the magnitude of E and the phase angle of E. With j so that $j^2 = -1$, we have $S = P + j \cdot Q$ and $E = V \cdot e^{j \cdot \theta}$.

Power systems models are composed of buses and devices, where buses are lossless connection points for the devices of the power system. Active and reactive power are injected or consumed at each bus by different devices, such as generators, loads, shunt capacitors, etc. The power (active and reactive) can be transmitted from one bus to another through a power delivery device (e.g. a transmission line or a transformer).

AC power flow equations

A power delivery device, like a transmission line or transformer, is governed by the so-called *AC* power flow equations.

The AC power flow equations are in what follows expressed from the device point of view (despite a nodal formulation also exists and is usually employed to formulate the equations in a matrix form). [And08], among others, provides a general formulation of power delivery elements, or branches that accounts for the series admittance of a device from bus k to m:

$$y_{km} = g_{km} + j \cdot b_{km} \tag{2.1}$$

where g_{km} is the conductance and b_{km} is the susceptance of the device. This general modelling also includes the shunt susceptance b_{km}^{sh} divided in two: half on each side of the series admittance, to form the so-called π-*model* represented in Figure 2.2a. When representing a whole network, the lines are represented as in Figure 2.2b, simply with a line connecting the two buses. The voltage magnitude ratio a_{km} and the phase shift φ_{km} are transformers parameters.
A transformer is said to be in-phase if $\varphi_{km} = 0$ and $a_{km} \neq 1$, and is said to be phase-shifting, if $\varphi_{km} \neq 0$ and $a_{km} = 1$. If $a_{km} = 1$ and $\varphi_{km} = 0$, the device is in-phase and has no voltage magnitude modification, this is the transmission line case.

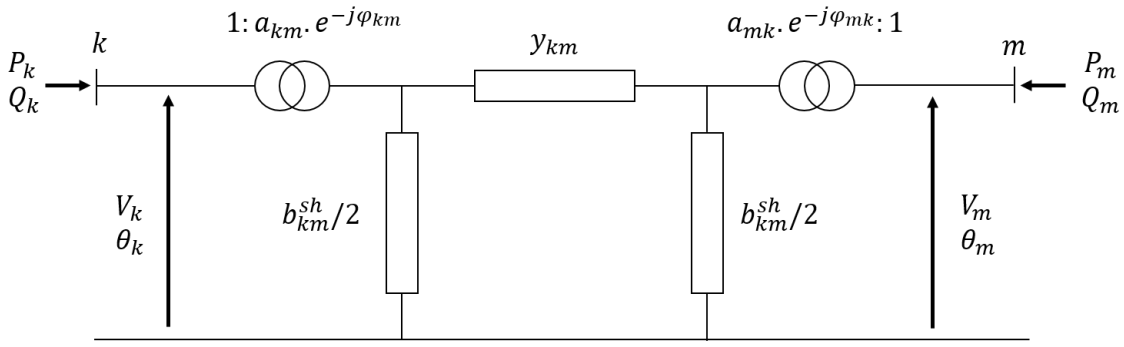

(a) π-line representation.

(b) Network representation

Figure 2.2: Line representations from bus k to bus m.

Let's introduce the following notation before presenting these power flow equations. We note P_k and Q_k, respectively, the active and reactive power flows from bus k to bus m. The voltage magnitude and phase angle at bus k are noted: V_k and θ_k.

$$\begin{aligned} P_k &= g_{km} \cdot a_{km}^2 \cdot V_k^2 \\ &\quad - a_{km} \cdot V_k \cdot V_m \cdot \Big(g_{km} \cdot \cos(\theta_k - \theta_m + \varphi_{km}) + b_{km} \cdot \sin(\theta_k - \theta_m + \varphi_{km}) \Big), \\ Q_k &= -(b_{km} + b_{km}^{sh}) \cdot a_{km}^2 \cdot V_k^2 \\ &\quad + a_{km} \cdot V_k \cdot V_m \cdot \Big(b_{km} \cdot \cos(\theta_k - \theta_m + \varphi_{km}) - g_{km} \cdot \sin(\theta_k - \theta_m + \varphi_{km}) \Big) \end{aligned} \tag{2.2}$$

The active and reactive power losses are defined as the difference between the power entering the line and the power flowing out of the line so that the active and reactive power losses are: $P_{loss} = P_k + P_m$ and $Q_{loss} = Q_k + Q_m$.
Note that a nodal formulation of the power also exists and can be computed by applying the Kirchhoff's law on each bus, i.e. the sum of power flowing to the bus from lines and transformers should be equal to the injected power at the bus.

To enforce a safe functioning of those branches, manufacturers define a limit in current noted I_{km}^{max}. If this limit is crossed for too long, lines start sagging and can be damaged in addition to be dangerous for people or equipment around. We use the formulation from [RRRSR10] expressed depending on the square of the maximum current. Moreover, the voltage magnitude needs to stay within a range around the nominal voltage of the device, i.e. between V_k^{min} and V_k^{max} that are determined by network studies [COC12]. These constraints can be expressed as:

$$\begin{aligned} &(g_{km}^2 + b_{km}^2)(V_k^2 + V_m^2 - 2 \cdot V_k \cdot V_m \cdot cos(\theta_k - \theta_m + \varphi_{km})) \\ &+ ((b_{km}^{sh})^2 + 2 \cdot b_{km} \cdot b_{km}^{sh}) \cdot V_k^2 - (2 \cdot b_{km} \cdot b_{km}^{sh}) \cdot V_k \cdot V_m \cdot cos(\theta_k - \theta_m + \varphi_{km}) \\ &+ 2 \cdot b_{km} \cdot g_{km}^{sh} \cdot V_k \cdot V_m \cdot sin(\theta_k - \theta_m + \varphi_{km}) \leqslant (I_{km}^{max})^2, \\ &V_k^{min} \leqslant V_k \leqslant V_k^{max}, \quad V_m^{min} \leqslant V_m \leqslant V_m^{max} \end{aligned} \tag{2.3}$$

These AC power flow equations are non-convex and differentiable which makes the use of Newton-Raphson method very efficient and the most widely used method to solve power flow equations. In that case, the power injections at each load bus are known and the voltage magnitude and phase angle at each load bus are thus determined iteratively by the method. To do that, the Jacobian of the active and reactive power mismatches from the known injections, with respect to the voltage magnitudes and phase angles, is calculated and allows to update the previous solution. One can note that a strong coupling between the active power and the voltage phase angles, and between the reactive power and the voltage magnitudes exists in this Jacobian. It is especially true for transmission systems, where it is possible to approximate the power flow equations by decoupling the variables, i.e. On one side, a set of equations involving the active power and the voltage phase angles, and on the other side, a set of equations involving the reactive power and the voltage magnitude.

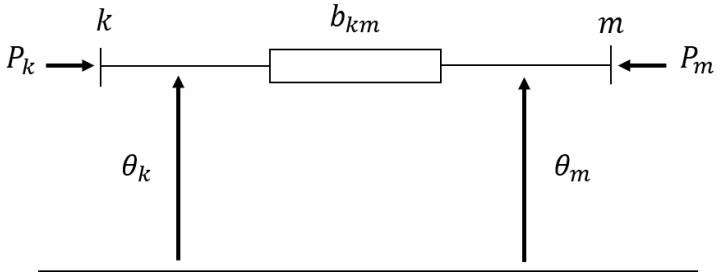

Figure 2.3: DC power flow analogy.

DC power flow approximation

The power flow can be even further simplified, leading to the linearised (DC) power flow approximation. This approximation is sometimes used for N-1 calculations in today's power system industry due to its computational speed and simplicity [ODK11, WMZL13] with respect to the full AC power flow model. The term *DC* is employed because an analogy can be made between the linearised power flow equations and the electric equations in Direct Current, as illustrated in Figure 2.3.

This approximation relies on the assumption that, under normal operation: (i) the voltage magnitude is at its nominal value; (ii) the voltage phase angle differences are close to 0; and (iii) there is no active power losses in the line, i.e. the conductance g=0. These assumptions are particularly true in transmission systems, where $g_{km} << b_{km}$ and the voltage is high so that the active power losses are low, and because these systems are meshed and the voltage is particularly controlled [And08].

Locally, a line from bus k to bus m is ruled by the power flow equation:

$$P_k = -P_m = b_{km} \cdot (\theta_m - \theta_k) \tag{2.4}$$

The constraint on the current flow is translated to a constraint on the power flow in the line. The maximum active power capacity of the line is noted P_{km}^{max} and the constraint is thus:

$$-P_{km}^{max} \leqslant P_k \leqslant P_{km}^{max} \tag{2.5}$$

A nodal formulation of the DC power flow equation can be formed in a compact way:

$$P^{inj} = B \cdot \theta \tag{2.6}$$

where P^{inj} is the vector of power injection (or consumption) at the different buses, θ is the vector of voltage phase angles and B is the susceptance matrix.

For the rest of this thesis, we use the prefix *AC* to refer to the non-convex power flow equations described in Section 2.1.2 and the prefix *DC* to refer to the linearised power flow equations of Section 2.1.2. Now that the classical power flow models that constitute an important part of the network constraints of the Requirement 3 have been introduced, the following section focuses on the control mechanisms of power systems that aims at enforcing Requirement 1, namely the power balance of the system.

2.1.3 *Frequency controls*

Transmission system operators must keep the power balance of the system, meaning the power injected must be equal to the consumption and the losses at any time. To control the power balance of power systems, measures of the frequency are utilised as inputs because frequency variations reflect the power balance of the system and have the same value in steady-state in the entire power system. In more detail, if the frequency is decreasing, it means that the demand (including the losses) is greater than the production; otherwise if the frequency increases, it means that there is more generation than demand. The frequency is then controlled at three different levels [ES13]. Most generators on transmission systems participate in the frequency controls that can be decentralised (control that only relies on local measurements and do not include communication) or distributed (rely on coordination with or without a central coordinator). Figure 2.4 illustrates the three controls of the system frequency that are described next.

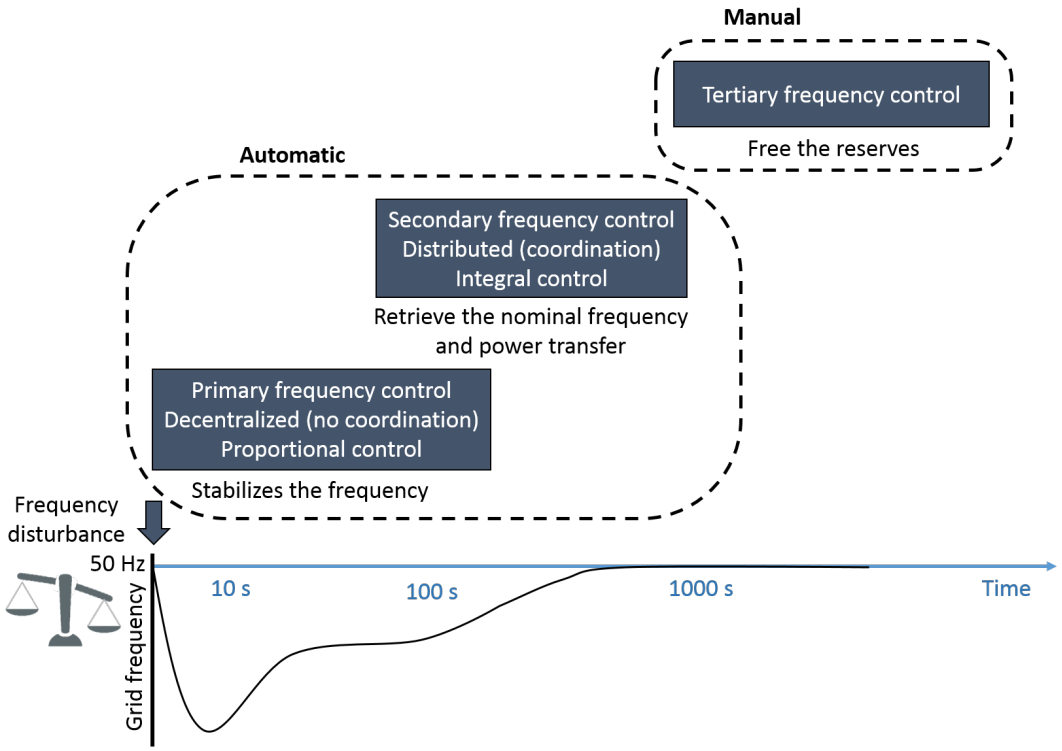

Figure 2.4: Power system frequency regulations.

The *primary frequency control* (PFC) aims at stabilising the frequency by balancing the active power of the system. This is a decentralised, meaning that there is no communication among components, droop control, proportional to existing frequency error: the generating units measure and stabilise the frequency locally and automatically. Therefore, after this first control, the frequency is just stabilised but does not go

back to the nominal value. The response of generators is governed by the speed droop that is adapted to the characteristics of the different machines, and by the capacity of the generator. The reaction of the primary frequency control is the first layer of control and is the fastest one (the speed of reaction is of the order of a few seconds and the generators need to be able to react within some seconds to 1 minute). The basic static equation to model the primary frequency response, ΔP, of the generators of the system links the frequency deviation Δf after the PFC from the nominal frequency f_0, the total active power scheduled P_0 and the equivalent speed droop of the system s, so that:

$$\frac{\Delta P}{P_0} = -\frac{1}{s} \cdot \frac{\Delta f}{f_0} \tag{2.7}$$

The *secondary frequency control* is an integral control, i.e. the control is not only proportional to the existing error but it also depends the time for which it has persisted, that has two goals. The first one is to get back the system frequency within the dead band around the nominal frequency of the system. The second goal is to recover the power transfer between the different areas of the system. This centralised control thus necessitates communication and coordination to get the transfer mismatch of the areas. It is automatic and the typical response time of the secondary frequency control is a minute [NER11].

Finally, the *tertiary frequency control* is triggered manually by transmission system operators. In that case, the tertiary control restores the primary and secondary reserves that are available power dedicated to the primary and secondary frequency control, within tens of minutes.

The reserves of the frequency controls must be sufficient to handle most disturbing events happening on the system. Moreover, unlike the secondary and tertiary frequency controls that are the results of optimisation problems, the primary frequency control is a decentralised control (i.e. no communication is involved). Thus, it is crucial that, in addition to having sufficient reserves, the primary frequency control does not lead to further disturbances, e.g. congestion of lines or transformers of the system.

2.2 OPTIMAL POWER FLOW PROBLEMS

Now that the structure and the main constraints of power systems have been identified, the major quasi static optimisation problems solved by TSOs for managing the operations can be introduced. These problems are generically referred to as *optimal power flow problems*.

Due to the importance and the complexity of the OPF problems, a rich literature have been developed during the past 60 years to improve the performance of the methods that solve these problems. We review the literature on three different optimisation problems: Section 2.2.1 focuses on the original Optimal Power Flow problem, Section 2.2.2 deals with the Security Constrained Optimal Power Flow problem and finally, Section 2.2.3 introduces the main references on the Chance Constrained Optimal Power Flow problem.

2.2.1 *Optimal Power Flow*

The classic *Optimal Power Flow* (OPF) problem was first formulated in 1962 by [Car62]. It aims at finding the optimal schedule of production (Requirement 2) according to forecast demand on the system that also respect the system constraints. This is the basic optimisation problem, solved on a daily basis by transmission system operators, and it mainly includes operational constraints of the system (Requirement 3), and the power flow equations described in Section 2.1.2.

Since the first OPF formulation by [Car62], a large variety of formulations and methods have been developed to efficiently solve the OPF problems. A number of surveys and reviews have classified the existing references in the OPF field [HG91, MAEH99, MEHA99, PJ08, FSR12, COC12] and the history of the development of this problem can be found in more detail in [COC12].
Several important parameters that allow a comparison of different OPF approaches, are listed in [FSR12], and are represented in the following standard form of the OPF:

$$\begin{aligned} \min \quad & f(u,x) \\ \text{subject to :} \quad & g(u,x) = 0 \\ & h(u,x) \leqslant 0 \end{aligned} \tag{2.8}$$

The first one is the type of control (variable u in Eq. 2.8, e.g. active or reactive power injection, transformers tap ratio, etc..) and state (variable x in Eq. 2.8, e.g. power flows, voltage magnitude, etc.) variables, especially if there are discrete variables. The objective function (function f in Eq. 2.8) of the OPF also varies depending on the aim of the problem (Requirement 2), e.g. minimise the power injection schedule cost or the losses in the system. The type of equality constraints (defined by the function g in Eq. 2.8) determines the network and flow constraints (Requirement 1), when the inequality constraints (defined by the function h in Eq. 2.8) refine the model of the devices and of the security of the system (Requirement 3).
The methods employed depend on the modelling of the OPF problem, the main ones are the non-linear, quadratic programming, the Newton Raphson method, linear programming and interior point methods reviewed in [MAEH99, MEHA99, FSR12, PJ08]. Motivated by the rise of bio-inspired optimisation techniques, [PJ08] presented progress in this category and reviewed techniques, such as artificial neural networks, fuzzy logic methods or genetic algorithms, to solve the OPF. The main advantages of these techniques rely in the ability to consider more qualitative (more complex and less regular) constraints and objective functions, and in the ability to find global optimum when other techniques can be stuck at local optimum.

More recently, [Cap16] reviewed the evolution of the AC-OPF problem, stating that there is no difference to be made between OPF and SCOPF because, in the real world, only SCOPF are employed. The authors encouraged researchers to investigate problems closer to real operators' problems that account for accurate modelling of power system functioning and for security issues related to outages and to uncertainty.

2.2.2 *Security Constrained Optimal Power Flow*

In the Security Constrained Optimal Power Flow problem, contingency scenarios that model potential outages, are considered, and security constraints (Requirements 1-3 and 4) related to those scenarios are integrated to the classic OPF problem. The main challenges and techniques to be addressed for solving SCOPF problems are reviewed in [CRP+11]. This analysis is justified by changes that appeared since the 1990s, such as an increased stress, uncertainty, control devices complexity on power systems and the impact of control actions taken in one of the regions on neighbouring systems. In more detail, SCOPF formulation complexity especially arises from the size of the problem, the numerous potential control actions and their sequence used after an outage occurs on the system. The high dimensionality of SCOPF [CW08, CRP+11, WMZL16], in comparison with the classic OPF due to the number of scenarios to consider, is then the major challenge for methods solving SCOPF problems. Several approaches have been implemented to deal with this issue, such as reducing the number of scenarios to consider [CW08] or the dimension itself by simplifying or omitting less affected regions of the system as in [KSM18]. It is also possible to employ parallelisation techniques that can speed up the solutions like the Benders decomposition scheme in [MPG87].

In the literature, SCOPF models are classified into two types: the *preventive* SCOPF (PSCOPF) and the *corrective* SCOPF (CSCOPF).

One one hand, the *preventive* model considers automatic response of the system due to a disturbance without considering the possibility to re-schedule the control variables. [AS74] define the PSCOPF as the ability of the system to ensure its safety during the period after the fast and automatic control acted, but before slow (corrective) control actions, such as human decisions, have been applied. They formulate the PSCOPF problem using AC power flow equations, and solve it with a centralised iterative method that is tested considering line outages only. In fact, most references in PSCOPF only consider transmission line outages and do not consider generators failures, although it should be accounted [KCP10]. When the disturbance modifies the power generation schedule of the system, the first automatic control response is the primary frequency control of generators. The response is governed by the speed droop of generators and it automatically changes the active power production of generators to balance the system, see Section 2.1.3. And yet, the new operating point can create violations in post-contingency scenarios. The aim of PSCOPF is then to prevent these violations from happening in any case. For instance, [KCP10] presented a PSCOPF problem formulation that integrated the primary frequency control of generators. The speed droops of generators are usually input parameters of the problem, as it depends on the technology of the generator. Nevertheless, this parameter can be tuned within a certain range of values. These speed droops of generator were optimised in [DHKP16] to provide the most effective response of the generators participating in the primary frequency control. The authors demonstrated that the cost of operation can be reduced for an equivalent security.

On the other hand, *corrective* models find an optimal response of the system regarding the incident that happened [MPG87]. In that case, it is assumed that the system can handle short-term violations and that optimal corrective actions can be determined and performed before triggering any power system protections against violations [CW08]. Corrective SCOPF can provide the optimal solution of the secondary frequency control and a list of corrective actions to the operator that then decide and apply the counteractions. The CSCOPF was formulated in [MPG87] for an economic dispatch with security constraints, where generation rescheduling is used to relieve the violation created by the outages considered. [CW08] tackled the CSCOPF considering corrective actions such as generators power or voltage rescheduling, transformer tap ratio control and other discrete control variables that can switch apparatus to remove the violation of a constraint. Line switching creates a reconfiguration of the power flow in the system, if the action is correctly defined, the switching can relieve overload violations, or voltage violations as in [SV05]. Some references included in the objective function the aim of minimising the number of control actions [CW11, PS15], because it impacts the cost and the complexity of performing the actions.

In summary, the security constrained optimal power flow can be tackled considering the automatic reaction of the system and / or the optimised response of controllable devices. The main challenge in solving SCOPF problems is the handling of the size of the problem (Requirement 8) that is much larger than the OPF problem, especially in the context of interconnected power systems.

2.2.3 *Chance-constrained Optimal Power Flow*

The classical SCOPF reviewed in the previous section does not consider any uncertainty on the generation or demand side, which is, according to [Cap16], a key challenge to comply with the development of future power system operations. Alternatively, the so-called Chance-Constrained Optimal Power Flow (CCOPF) problem [BCH14] accounts for this uncertainty, obtaining a schedule that respects network constraints with a high probability. Broadly speaking, chance-constrained optimisation is a methodology in which the system security constraints can be violated with a small predefined level of probability. As an example, if we consider the constraint $x \leqslant x^{max}$ on variable x, the chance constraint is the constraint on the probability $\mathbb{P}[x \leqslant x^{max}] \leqslant 1-\epsilon$, with $\epsilon \in [0,1]$. In general, chance-constrained optimisation problems are computationally intractable since they require the computation of multidimensional probability integrals. To overcome this difficulty, some works have opted for a scenario-based approach that transforms probability constraints into hard constraints corresponding to a specific number of uncertainty scenarios, as in [VML12]. However, to ensure a-priori guarantees on the performance of solutions, a large number of scenarios need to be sampled, leading to large computational times and memory requirements [LM15].

Instead, references [BCH14, ROKA13, LM15, CD17] took an alternative approach and assumed that the forecast error of each wind farm was following a (previously known) probability density functions (PDFs) and that they were mutually independent. All above mentioned references proposed centralised approaches to solve the CCOPF problems which are very well suited for single regional area systems (i.e. managed by a single system operator). They assumed that the forecast error can be modelled by a Gaussian distribution to allow an analytical reformulation of the chance constraints, leading to a deterministic problem with lower computational complexity than scenario based approaches [MGL14]. Roald et al. proposed in [ROKA13] an exact reformulation of the security constrained OPF with chance constraints related to the uncertainty on the wind power forecast, and under the assumption of independent Gaussian distributions. Similarly, Bienstock et al. [BCH14] formulated the CCOPF and proposed an efficient cutting-plane algorithm that proved to be able to solve large problems. The same cutting-plane algorithm was used in [LM15] to solve a CCOPF formulation that modelled the uncertainty of load reserves in addition to generators reserves considering secondary frequency response schemes. Chertkov et al. highlighted, in [CD17] that among the different reserve schemes, the ability to provide sufficient primary frequency control was less studied in the literature than optimised responses of the system, and thus they enhanced the CCOPF formulation by including a refined model of the primary frequency control.

When details on the uncertainty are not available or inaccurate, other techniques can be employed as in [LDB16] where the CCOPF was considered with Gaussian distributions for modelling wind farms generation. The Gaussian distributions were however considered imprecise and thus, a robust chance constrained problem was built by introducing an uncertainty set on the Gaussian distributions parameters.
Other optimisation problems considering uncertainties that are not CCOPF, also exists but are not considered in this thesis. As an example, it is also possible to consider the uncertainty without any distribution as in [Jab13] where renewable energy sources uncertainty was modelled by an uncertainty set using robust optimisation techniques. The primary frequency control of controllable generators was considered in response of the wind farms deviations from forecast. Load uncertainty was however supposed known and was modelled by Gaussian distributions. Chance constraints were then included to account for the demand side uncertainty.
Information gap decision theory can also be employed and consists in maximising the robustness of the system due to under estimation of wind forecast and in minimising the opportunity function if the forecast is overestimated. [MSK16] applied this technique on an AC OPF formulation where the objective was to reduce the power flows in lines by controlling the reactive power injection from the distributed generation and exploiting demand response.

Finally, when the uncertainty is large, the margins and reserves needed to cover most deviations from forecast can easily exceed the system capabilities. In that case, the schedule, that satisfy the chance constraints of lines and generators, may not exist (i.e. the CCOPF problem does not have a feasible solution). As mentioned in [AES10],

a way to mitigate the impact of the forecast errors and return to feasibility is to curtail RES production. The possibility to curtail RES in case of congestion increases the flexibility of the system and can reduce the reserves and margins needed, allowing the secure integration of more RES. For example, [RMC+16, RAM+16] propose two different curtailment strategies to provide flexibility in a CCOPF problem. The first strategy consists in curtailing the maximum production of the wind farm in order to mitigate issues coming from an under-estimation of its generation. The second strategy consists in curtailing a percentage of the wind farm production, regardless of their actual production, and use the curtailed power as primary frequency control reserves.

In summary, the Chance-Constrained OPF problem is the most used formulation of the OPF under uncertainty, and, for tractability of the solution, the probability distributions are usually considered Gaussian. In this thesis, we will use similar techniques to integrate the risk arising from the uncertainty of wind farms (with and without curtailment).

Having reviewed the main power system operation optimisation problems, the following section discusses the main distributed approaches to solve them as well as the disadvantages of the centralised ones.

2.3 DISTRIBUTED APPROACHES FOR OPTIMAL POWER FLOW PROBLEMS

To achieve better overall reliability and economic efficiency, power systems are interconnected. However, TSOs managing different regions need to cooperate and coordinate efficiently to make the most of these interconnections and to ensure that the interconnected system is secure. Hence, it is important to develop power system optimisation models that ensure a secure and economically efficient operation not only of each regional system, but also of the interconnected system as a whole under and in spite of uncertainties. Unfortunately, the application of centralised approaches in such large-scale interconnected networks is undesirable if not impossible due to [WWW17a]: the *computational and communication burden* of gathering data and taking decisions for the whole system at a central controller; and the *privacy issues* of having TSOs and generation companies disclosing potentially sensitive information and/or strategic models. The computational burden is especially worsen by the fact that the larger a system, the larger and sparser its admittance matrix, which causes problems for the inversion of this matrix.

Distributed methods bring a solution to both problems by parallelising it, and by limiting the sensitivity and the spreading of the data exchanged. An overview of the main distributed methods that have been applied to OPF-like problems is provided in Section 2.3.1, as well as a survey of comparisons of those methods in Section 2.3.2. These comparisons drive our justifications for the method employed in this thesis. The

implementation of those methods as multi-agent systems is finally motivated in Section 2.3.3, after introducing the main characteristics of multi-agent systems (MAS).

2.3.1 *Overview of main distributed methods*

Distributed methods for the OPF problem are first studied in [KB97], where a coarse-grained decomposition of interconnected power systems is proposed. This section provides a brief overview of the main optimisation methods applied to OPF problems since then, namely, the Auxiliary Problem Principle (APP), the Optimality Condition Decomposition (OCD), the Analytical Target Cascading (ATC), the Consensus + Innovation (C+I) and lastly, the Alternating Direction Method of Multipliers (ADMM).

Auxiliary problem principle - APP

The *Auxiliary Problem Principle* was first applied to optimal power flow problems in [KB97], with a decomposition of the problem that follows the existing regions boundaries of transmission systems. The APP applied to multi-area OPF consists in replacing interconnection lines by duplicated dummy buses, i.e. two dummy buses are created per interconnection line, one for each of the connected areas. Coupling constraints enforce the consistency of the duplicated dummy buses, in order to keep the equivalence with the initial problem. Figure 2.5b represents the decomposition of the 3-area system with one interconnection line between each region, depicted in 2.5a, and provides the coupling constraints. The augmented Lagrangian is then formed on these coupling constraints and cross-terms of the Lagrangian are linearised.
The APP algorithm then consists in solving, in parallel, each area sub-problem and in determining the duplicated variables at the borders. These variables are exchanged and allow the update of the multipliers. This can be implemented in a fully distributed manner: no central coordinator is needed. Parametrization of the APP can also be enhanced to improve the convergence properties as investigated in [HPK02]. Further information about the APP can be found in [Coh80].

Optimality condition decomposition - OCD

The *Optimality Condition Decomposition* method relies on a regional decomposition of the system. The first order optimality (or Karush-Kuhn-Tucker - KKT) conditions are decomposed according to the regional decomposition, similarly to Figure 2.5b. Each sub-problem, i.e. regional optimality conditions, is solved in parallel by a Newton-Raphson step and the tie line variables are exchanged with the neighbouring regions. The neighbouring variables are included in the objective function and constraints of each sub-problem, and are considered constant for the next iteration. An application of the OCD method on the DC-OPF problem can be found in [BB03], where the method is tested on multi-area test systems.
A correction term can be added to account for errors in the searching direction that arises from the fact that the coupling between regions are ignored in the sub-problems.

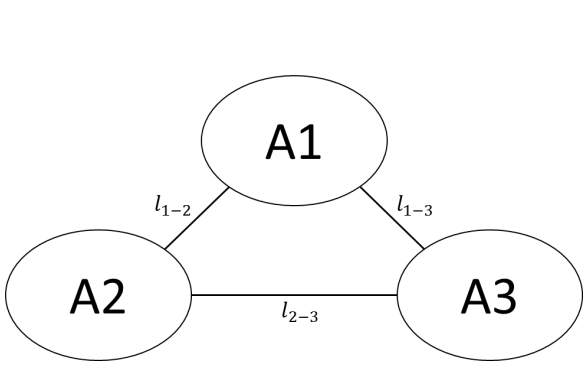

(a) 3-area problem

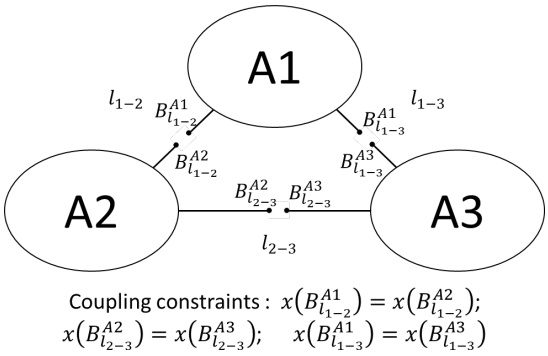

(b) Decomposition without a central coordinator

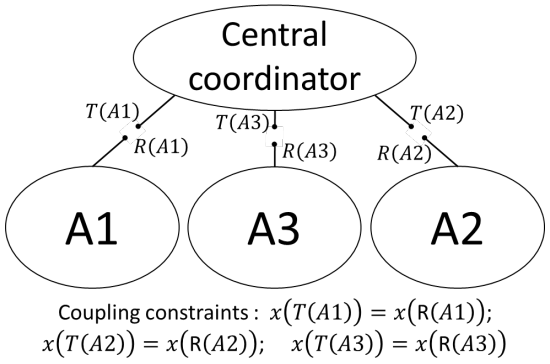

(c) Decomposition with a central coordinator. T is the target, i.e. the dummy bus on the coordinator side, R is the response, i.e. the dummy bus on the area side.

Figure 2.5: Decomposition without and with a central coordinator and coupling constraints that are relaxed. $x(B)$ represents the variables at bus B.

This improvement of the classic OCD method can significantly reduce the number of iterations and convergence time, as shown on large test systems in [GHT16b].

Analytical target cascading - ATC

The *Analytical Target Cascading* method is a hierarchical method that consists in coordinating the target values of the *parents problems* with the response values of the *children problems* through the inclusion of penalty functions. The application of ATC to power system optimisation problems is done through a two level hierarchy (master-slave problems) where the upper level is a central coordinator that coordinates the different regions. Figure 2.5c depicts this decomposition and the associated coupling constraints.
The children or slaves that are the areas to be coordinated, solve, in parallel, sub-problems that are independent from each other, and rely on the target values provided by the parent via the addition of the penalty function. Once the sub-regions have

solved their local problem, they send their response to the central coordinator. The convergence is achieved once the target and the response values of the regions reach a sufficient consistency.
The ATC method, based on [TEPR06], was employed to solve a security constrained unit commitment in [KF14, KFL15]. The effectiveness of the method was proven by the application of the method on large test systems, up to a 4672-bus system.

Consensus + Innovation - C+I

Consensus-based algorithms were first used to solve the DC-OPF problem by reaching a consensus on the individual marginal cost of generation, represented by the Lagrange multiplier. For this reason, unlike APP, OCD and ATC, the decomposition of the problem is made at the nodal level to be able to define these individual marginal costs, e.g. [ZC12].
However, these methods are only suitable when neglecting line capacity constraints, because such constraints make the marginal cost unequal. To overcome this drawback, *Consensus + Innovation* approaches that add first order optimality conditions as innovation updates are employed. Only communications with physical neighbours are needed but extra communications can be added to reduce the number of iterations needed.
Applications of C+I methods have been proposed by Mohammadi et al.. In [MKH14, MHK15] the DC-OPF problem is solved using respectively a synchronous and asynchronous innovation-based approach, whereas the role and impact of the communication is studied in [MHK14]. The SCOPF problem is tackled and solved with a C+I method in [MKH17].

Alternating Direction Method of Multipliers - ADMM

The *Alternating Direction Method of Multipliers* is formed from a problem artificially separated into two subproblems, by duplicating variables at the border of the chosen separations. A coupling constraint enforces the equivalence with the initial problem, i.e. the equality of the duplicated variables. The augmented Lagrangian is then formed on this coupling constraint and the ADMM consists in, alternatively, minimising the augmented Lagrangian sequentially on the two duplicated variables and finally updating the dual variables. The ADMM can be implemented with (Figure 2.5c) or without a central coordinator (Figure 2.5b). The central controller is then dedicated to solving the second minimisation step of the method. The decomposition can be made at different levels from the nodal level similarly to the C+I method, to the decompositions following the APP, OCD and ATC methods. The ADMM can also be accelerated through a Nesterov-like step inside the dual variable update step, as shown in [WWW17b].

2.3.2 *Comparison of the main approaches*

A number of authors have compared and reviewed these distributed methods, and have classified those depending on different characteristics.

The first characteristic is whether the method uses a central coordinator or a peer-to-peer communication protocol, as discussed in [KMG+16]. The ATC and the ADMM with central controller have a hierarchical structure i.e. the different entities only communicate with the central coordinator: the master level. The other methods mentioned have peer-to-peer communications, i.e. there is no central coordination and only local communication, and have the advantage of enabling the parallelisation of each of the step of the different methods.

The type of information exchanged is another interesting characteristic as it determines how well the privacy (requirement 7) is respected. [WWW17a] distinguish: (i) generator-based decompositions that rely on the exchange of cost information through Lagrangian Multipliers; and (ii) the geography-based decompositions that rely on the exchange of physical information. The physical information can only contain voltage phase angles, as for ATC and APP, or mismatch with constraints of the system, as in ADMM, OCD and C+I. It also depends on the basic tools that are used to form the methods, for example, the OCD and C+I methods are Karush-Kuhn-Tucker (KKT) based methods, when the other mentioned methods rely on the Augmented Lagrangian relaxation.

More importantly, the quantity of information exchanged at each iteration and the difficulty to solve the problems at each iteration are mentioned in [KMG+16, WWW17a], as important parameters for the performances. The methods with low computational effort per iteration take full advantage of the parallelisation of the problem, as it breaks down the problem to small and easy to solve sub-problems. However, these advantages may come at the cost of a higher amount of data exchanged per iteration that is the case of C+I method and for the peer-to-peer version of the ADMM. On the contrary, the methods that exchange less information per iteration have higher computational effort per iteration.

The number of iterations to converge is then crucial either to reduce the computational effort or the amount of data exchanged. The number of iterations is highly dependent on some tuning parameters for the ADMM, the APP and the C+I methods and should be thus chosen carefully to improve the performances. For the ADMM, the scaling parameter governs the speed of convergence of the primal and the dual residuals, and allow to focus either on the feasibility or on the optimality of the solution. The experiments conducted in [KMG+16] enlighten the importance of this tuning on the performances of the ADMM.

The gain in popularity of those distributed methods leads to a number of applications of the presented methods on power system problems that are reviewed in [WWW17a] and classified into DC-OPF, AC-OPF, Unit Commitment[1] (UC) or other

1 Problem in which the decisions variables are whether a generator is producing or not (commitment of the generators, binary variable), and how much power is produced by each generator.

applications such as co-optimisation. It appears that the method applied to the wider variety of problems and with the larger number of applications to power system optimisation problems is the ADMM. The C+I was merely applied to DC-OPF problems, the OCD was applied to DC-OPF and AC-OPF problems, when the ATC was only applied to UC problems. The APP was applied to the DC-OPF, AC-OPF and UC problems.

[MDS+17] focuses on research tracks related to online implementation of those methods and [KMG+16] on the application of more complex or accurate OPF problems to these algorithms, such as applying AC-OPF and SCOPF problems. The improvement of the performances of these algorithms by improving the convergence rate or studying the best problem decomposition is also identified as a crucial problem. For improving the performances, the ADMM, the APP and the C+I methods have the advantage of allowing the tuning of parameters, impacting greatly the convergence.

With these descriptions and comparisons, we motivate the choice of the method that we employ in this thesis. The ADMM was chosen for :

(a) Its proven convergence properties for convex problems, its observed ability to solve non-convex problems, and its potential in term of scalability (Requirement 8);

(b) Its applicability to a wide variety of power system optimisation problems under different decompositions and especially following a physical decomposition at different scales (Requirements 6 and 8);

(c) The ADMM method can be implemented in a peer-to-peer fashion that necessitates no coordinator, as in Figure 2.5b, and the type of information exchanged ensures the actors privacy and autonomy (Requirements 6 and 7);

(d) Finally, the ADMM is increasingly studied in the literature for smart-grids or micro-grids applications, so that using the ADMM at the transmission level have the advantage of being easily connectible to DSO and smart-grids or micro-grids future optimisation tools, allowing a great interoperability (Requirements 6 and 7);

2.3.3 *Implementation under the Multi-Agent System paradigm*

The main mathematical methods were presented and compared, however, the implementation of those methods, and in particular of the ADMM, is crucial for the good functioning and performances of the algorithms. The Multi-Agent System (MAS) paradigm is particularly appealing for solving power system problems, due to the characteristics of agents that are presented next, and especially for distributed optimisation.

There are two key concepts that can define agents in the general case, according to [Woo01]. The agents that are software entities, evolve in an *environment*, and these

agents can *autonomously* interact with this environment. An agent then perceives its environment through sensors, and it can perform actions that have an impact on its environment. The autonomy means that the agents do not need a human intervention to take the decision of performing the action [Woo01], and so, agents take the decision through an internal reasoning.

MAS are studied for many different applications in power systems, some reviews of those applications can be found in [MRM16, MDC+07a, MDC+07b, RKF16]. Agent-based modelling and simulation allow to analyse complex and large power systems aspects through individual behaviours [RKF16]. Simulations main interests are identified in [MRM16] for long time horizon such as planning, electricity market or network management.
Online applications that perform the actions on real physical systems can also be accomplished by agents for network operation, control and protection.

When dealing with distributed optimisation problems, the agents are entrusted with the different sub-problems described in Section 2.3.1. The agents represent actors of the system, and the MAS framework inherently satisfy some of the requirements developed in Section 1.1. In this context, the environment is composed of a network of communicating agents. The agents are provided with communication protocols that allow interoperations between agents as well as a coordination (Requirement 6). Moreover, the autonomy of the agents respond to the Requirement 7, because it lets the agents keep their privacy and autonomy. The agents sense their environment (the network of agents) through the reception of messages from their neighbouring agents or of messages received from a central coordinator. The interaction is accomplished by sending messages, again, either to the neighbouring agents or to the central coordinator.

In summary, the multi-agent system technology can answer the requirements regarding the coordination and interoperation between actors, as well as the autonomy and privacy needs. The implementation of the mentioned methods in a MAS framework, and especially those without a central coordinator, should then be favoured as it suits well the decomposition of the optimisation problems.

2.4 ADMM FOR OPTIMAL POWER FLOW PROBLEMS

After describing and comparing the different distributed methods available, the ADMM was selected in this thesis and should be implemented in a multi-agent system framework. However, the ADMM can be employed in various ways, e.g. different decompositions, and it was also chosen for this reason. This is why, we describe and choose, in Section 2.4.1, the most suited decomposition to match the requirements of Section 1.1. We then review the applications of the ADMM to the power system optimisation problems described in Section 2.2: Section 2.4.2 focuses on the applications of the ADMM to the original OPF problems, Section 2.4.3 on applications to the SCOPF problems and Section 2.4.4 on applications to OPF problems including uncertainty.

2.4.1 *Decompositions*

As mentioned, the Alternating Direction Method of Multipliers allows a variety of decompositions of the power system problems considered. The main decomposition is a physical decomposition that follows the physical boundaries of the system, as illustrated in Figure 2.6. On these boundaries coupling constraints are built and form the foundation of the physical coordination of the zones or areas of the problem. These

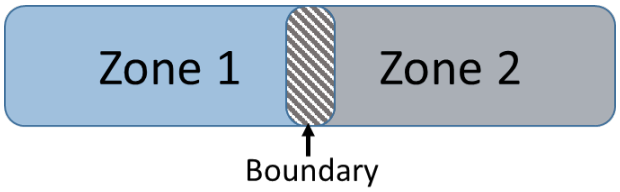

Figure 2.6: Principle of the decomposition

zones can be coordinated in a fully decentralised way such that they communicate directly with their neighbours (peer-to-peer scheme depicted in Figure 2.5b) or through a central coordinator (i.e. master-slave scheme depicted in Figure 2.5c).

In the literature, we can also find decompositions that do not follow the physical structure of the power system. For example, the ADMM has also been applied using a so-called scenario-based decomposition in which each sub-problem represents a contingency case and the duplication of variables is then only done on the base case variables that are related to the different scenarios [PK14, PS15]. However, such non-physical decompositions do not ensure the requirements 6 and 7 related to the coordination and to the privacy of the different actors.

In this section, we discuss the different levels of physical decomposition that have been applied using the ADMM in the literature, as well as the impact on the efficiency of the algorithm. We distinguish the advantages of both the coarse-grained and the fine-grained decompositions and finally, we motivate the choice of the level of decomposition.

Coarse-grained decomposition

The term *coarse-grained decomposition* was proposed in [KB97] with the idea to define areas that match the transmission system operators or countries borders, so that the interconnected areas have limited connections, as schematised in Figure 2.7a.
This decomposition is used in [KB00], to solve the AC optimal power flow problem of large scale inter-connected power systems. The ADMM proved its efficiency especially when considering a small number of interconnected systems. This type of decomposition leads to high computational efforts per iteration but does not exchange large amount of data. Several previous works have employed such a decomposition with the ADMM framework [DZG13, Ers14, Ers15, WWW17b] and proved its appli-

cability and effectiveness.

The impact of the power systems decompositions has been investigated for the ADMM methods in [GHT16a]. The authors proposed to use a spectral clustering method that is based on an affinity matrix that aims at capturing the coupling between buses of the system for the decomposition. This spectral clustering proved its efficiency in improving the performance of the ADMM method when solving the AC-OPF problem. The number of regions and their size are critical parameters for the performance of the algorithm: a larger number of regions decrease the computation time with the drawback of increasing the communications [GHT16a].

Another research study was carried out in [LBD15], where three levels of decomposition are applied to the ADMM for solving the AC and the non-linear DC [2] OPF problems on large scale test systems. The first decomposition is at the TSO level: each TSO area is considered as one sub-problem as proposed in [KB97]. The second decomposition considers the network (the lines of the system) and the individual users (devices with a non-zero cost function) as different sub-problems. In other words, two types of problems are defined: one specifically dedicated to enforce network constraints and another composed of blocks of users. The last decomposition considers the blocks of users as aggregators of distribution systems and the individual users are explicitly integrated. The three types of decompositions are conducted using a spectral clustering algorithm, similarly to [GHT16a]. The results provide information on the convergence of these decompositions and show that it has more impact than the number of constraints involved in the problem. However, the particularity of the network and case study also have an important effect on the convergence properties of the method.

All these above-cited works emphasise the importance of the strategy of decomposition of the problem but also of the level of decomposition and the number of regions. An alternative strategy is to break the problem into fine-grained sub-problems to make the most of the parallelisation.

Fine-grained decomposition

Fine-grained decompositions are defined here in opposition to coarse-grained decomposition and consist in separating the problem into minimal entities, as shown in Figure 2.7b. The decomposition can be performed at the buses, where each bus becomes a sub-problem that include parts of the constraints and objective functions of the neighbouring devices (potentially different actors). In this case, buses communicate with other neighbouring buses. This is the case of the references [SPG13, PL14, MWF15] that applied this decomposition with the ADMM on AC OPF problems.

It is also possible to decompose the problem at the bus/device boundaries, where there are two categories of sub-problems: the devices and the buses. Each of these

2 Linearised power flow equations with inclusion of a model of power losses.

categories is solved in a different optimisation step of the ADMM whereas within each step the sub-problems are solved in parallel. [KCLB14] and [ST15] rely on this decomposition and have applied this decomposition on (DC/AC)-OPF problems. Under this decomposition, the sub-problems are particularly simple to solve, e.g. the bus problems are solved analytically.

Those decompositions involves more data exchanged per iteration than coarse-grained decompositions, but the advantage comes from the simplicity of the sub-problems to solve and from the increased level of parallelisation.

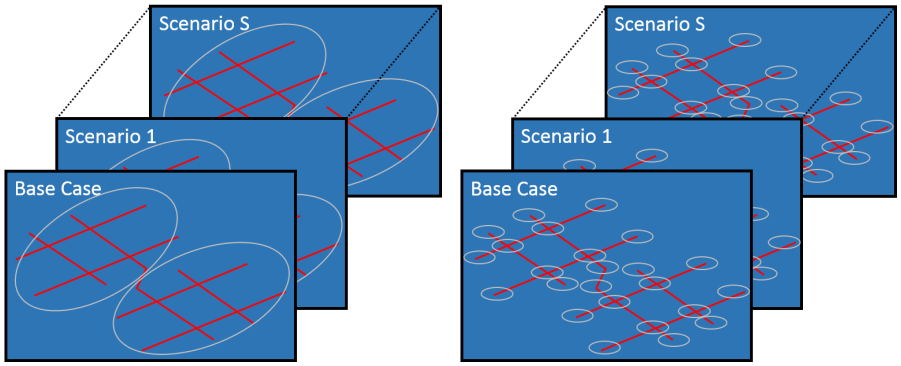

(a) Coarse-grained decomposition (b) Fine-grained decomposition

Figure 2.7: Different decompositions of the SCOPF problem; sub-problems separations are represented by the grey circles and are the same in each scenario.

Conclusion on the decomposition

For the physical decompositions, the two levels of decomposition have their advantages and drawbacks. On the one hand, the coarse-grained decomposition implies lower quantity of information exchanged compared to fine-grained decomposition but at the cost of larger and more complex problems to solve at each iteration. It is consistent with the requirement 6 that enforces a coordination and the autonomy of the actors, when only considering actors as TSOs. The requirement 7 on the privacy can also be respected but only between regions and the requirement 8 on the scalability is enforced with respect to the number of areas coordinated. On the other hand, the fine-grained decomposition that is the one chosen in this thesis, takes full advantage of the parallelisation, as it breaks the initial problem into very simple sub-problems. It results into a highly scalable (Requirement 8) method, although, it requires the exchange of more information. Finally, the autonomy and privacy of any actor can be enforced (Requirements 6 and 8), especially for the bus/device decomposition chosen here. It is particularly interesting on systems that are growingly integrating distributed actors and because the ADMM is increasingly studied in the literature for smart-grids or micro-grids applications.

In summary, a bus/device fine-grained decomposition is selected because it provides the greatest autonomy and privacy of all potential actors of the system. The ADMM in conjunction with a fine-grained decomposition provides a great potential in term of scalability and of coordination of the different entities involved in power systems optimisation problems.

2.4.2 *ADMM applied to the Optimal Power Flow problem*

Due to the non-convex nature of AC power flow equations, ADMM is only assured to converge to the optimal solution of OPF problems under specific contexts, e.g., radial distribution networks [SPG13]. Nonetheless, several works have reported good results when applying ADMM directly to non-convex AC-OPF problems. For example, [ST15] showed how, in an application to AC-OPF with demand response in (meshed) micro-grids, it converges to near-optimal solutions in a timely fashion relative to other models. Also, [GHT16a] reports convergence to a locally optimal solution on a large-scale Polish 2383-bus transmission system. The analysis of the convergence speed and accuracy of the ADMM method was carried out in [Ers14, Ers15], when solving the AC OPF problem. In addition to the inclusion of a control of the penalty parameters that aims at ensuring better convergence properties of the ADMM method, a proposition of decomposition where each sub-system only contains one generator is introduced in [Ers15], to create compact regions.

To get rid of the non-convexity of the OPF problem, other works have opted for relaxing or approximating the AC power flow model, ensuring in this way the convergence of the ADMM to the global solution. For instance, several approaches proposed convexifying the OPF problem before applying the ADMM algorithm. Such convex relaxations include a semi-definite programming (SDP) relaxation [DZG13], sequential convex (SC) approximations [MWF15] and second-order cone program (SOCP) relaxations [PL14]. Other works focused on the linearised approximation of the problem, leading to the DC OPF problem [KCLB14, WWW17b].

Table 2.1 summarises the mentioned references and provides the type of decompositions applied to the OPF problem, as well as the power flow model used. Half of the references applied a coarse-grained decomposition and half applied a fine-grained decomposition, showing that both approaches can be efficiently employed. Most applications consider the AC power flow equation, which proves the ability of the ADMM algorithm to solve the AC-OPF problem.

However, despite of testing the scalability, the respect of privacy and the coordination allowed by the ADMM for large-scale power systems, all the above references address the OPF problem, i.e. without security constraints. Thus, we explore the literature about SCOPF applied to the ADMM algorithm in the following section.

References	Type of decomposition	Power flow modelling
[KB00]	Coarse-grained	DC
[WWW17b]	Coarse-grained	DC
[Ers14]	Coarse-grained	AC
[Ers15]	Coarse-grained	AC
[DZG13]	Coarse-grained	AC unbalanced (SDP)
[GHT16a]	Coarse-grained	AC
[LBD15]	Coarse-grained	AC & DC
[SPG13]	Fine-grained (bus)	AC
[PL14]	Fine-grained (bus)	AC (SOCP)
[MWF15]	Fine-grained (bus)	AC (SC)
[KCLB14]	Fine-grained (bus/device)	DC
[ST15]	Fine-grained (bus/device)	AC

Table 2.1: OPF applied to ADMM

2.4.3 *ADMM applied to the Security Constrained Optimal Power Flow Problem*

A few references of the literature employed the ADMM to solve the SCOPF problem in a decentralised way. [CKC+14], building on the work of [KCLB14], were the first to apply the ADMM to solve the preventive DC-SCOPF problem, handling different reliability constraints across multiple scenarios. Yet, this work lacks empirical evaluation on real circuits because the distributed algorithm is only evaluated in a single two bus system. In [PS15], authors employ the ADMM, with convergence acceleration strategies, to solve a corrective DC-SCOPF problem (without primary frequency control) that minimises the number of post-contingency corrections and power rescheduled. [PK14] apply the ADMM as a heuristic method to solve the AC-SCOPF problem (i.e. with the original AC power flow equations) and test it in the large-scale Polish 3012-bus system. Results show how the ADMM algorithm is capable of yielding a robust solution, which is numerically proved to be the global optimum. Li *et al.* tackled, in [LWZ+16], a corrective contingency-constrained tie-line scheduling problem, in the context of multi-area system, using a robust optimisation formulation and the ADMM algorithm.
Although all these cited studies solve SCOPF problems via the ADMM algorithm, most are tackling corrective SCOPF and the action of the primary frequency control is neglected. Hence, these works do not integrate the real automatic reaction of the system to the loss of power balance.

In the view of requirements 6 and 7, related to the coordination and the privacy of the different actors of the system, the decompositions employed are also important for SCOPF problems. The fine-grained bus / device decomposition (see Section 2.4.1) from [KCLB14], is applied in [CKC+14] whereas a two-stage robust optimisation

scheme is decomposed at a coarse-grained scale in [LWZ+16].
Still, most of the references, [PK12, PK14, PS15, LKYH13], employ a scenario-based decomposition, described in Section 2.4.1. This decomposition allows a high scalability regarding the number of scenarios (requirement 8), nevertheless, the privacy and coordination issues (requirements 6 and 7) cannot be handled with this decomposition, as each scenario contains the entire power system model.

Lastly, the types of contingencies integrated in the experiments of these references are mainly restricted to line outages, which means that the contingencies do not disturb the power balance of the system. One exception is [LWZ+16], in which contingencies on lines and generators are considered. The contingencies are, however, intra-area only, i.e. a contingency can only impact devices in its own region and the contingencies on transmission lines are not considered, while it can be very harmful.

References	Type of decomposition	Power flow modelling	SCOPF type	Contingencies considered
[CKC+14]	Fine-grained (bus/device)	DC	Preventive	Lines only
[LWZ+16]	Coarse-grained	DC	Corrective	Intra-region lines and generators
[PS15]	Scenario	DC	Corrective	Lines only
[LKYH13]	Scenario	DC	Corrective	Lines only
[PK12]	Scenario	AC	Corrective	Lines only
[PK14]	Scenario	AC	Corrective	Lines only

Table 2.2: SCOPF applied to ADMM.

Table 2.2 outlines the main characteristics of the existing work on the SCOPF problem based on the ADMM. The type of decomposition, the power flow modelling employed, the type of SCOPF problem solved and the contingencies considered in the experiments are reviewed.

In summary, while, as we have seen in Section 2.2.2, some centralised approaches deal with preventive SCOPF problems that account for automatic control of power systems, it is not the case for the mentioned ADMM-based approaches. Moreover, outages on generators are not considered in these works, except from [LWZ+16] that, yet, do not consider outages on transmission lines or separation of the system. This is the reason why Chapter 4 tackles this problem that has not been addressed with the ADMM and the bus / device decomposition strategy.

2.4.4 *ADMM applied to the Optimal Power Flow problem under uncertainty*

The literature on CCOPF problem solved by the ADMM method is more limited than OPF and SCOPF. The multi-area tie line scheduling problem, with DC power flow equations, was formulated in [LSW+15], and accounts for wind uncertainty through a

robust optimisation scheme. The problem is partitioned with a coarse-grained decomposition, similar to [KB97] and allows the use of the ADMM method to solve it in a distributed manner. However, as the problem is discontinuous and non-convex, a decentralised alternating optimisation heuristic procedure is developed and integrated to the ADMM algorithm. This heuristic consists in, alternatively, solving the unit commitment problem (with binary variables) considering fixed boundary variables, and solve the problem over the boundary variables with fixed commitment. Hassan et al. also proposed, in [HDDC17], a decentralised chance-constrained OPF-based control policy that minimises power losses and regulate the voltage magnitude. The active and reactive power injections of inverter-based distributed energy resources were optimally controlled in a distributed manner using an ADMM-based approach.

Very few references are available on this topic, although the uncertainty is a growing issue in power scheduling (requirement 5). Chapter 5 of this thesis models probabilistic uncertainty in a fully distributed manner using an ADMM-based approach.

2.5 NETWORK DECOMPOSITION AND ALGORITHM: FORMAL DEFINITION AND NOTATION

As detailed in sections 2.3.2 and 2.4.1, the ADMM is employed in this thesis based on a bus / device decomposition that was first introduced by [KCLB14]. In this section, we present the decomposition and the notations used in the next chapters. The application of the ADMM on the DC-SCOPF problem is detailed and constitute the necessary background for the understanding chapters 4 and 5.

2.5.1 *Network decomposition*

Following the decomposition proposed by [KCLB14], we divide the set of power system network components into two groups:

(i) the set of *nets* (N), that, similarly to the electrical bus concept, connect devices;

(ii) the set of *devices* (D) that is composed of all power components that are not buses (i.e. in this thesis, transmission lines, generators and loads, whose sets are respectively noted L, G and F_l).

Those two sets are then defined as two different classes of agents, and each of these agents $a \in N \cup D$ is associated to:

(i) a local objective function that represents the component operating cost ($f_a(\cdot)$);

(ii) a set of constraints that the operation should satisfy in order to be feasible (C_a).

We consider here the linearised, or DC, power flow equations, for the sake of simplicity and thus consider two types of variables: the active power and the voltage phase

angle. In this context, the objective function is set to zero for all agents except for generators for which the objective function encodes the cost of generation.

Now, we create an edge for every pair of agents whose objective function or constraints have some variables in common (i.e. the cost and/or the feasibility of both agents depend on at least some shared variables). We refer to this set of edges as *terminals* ($\mathcal{T}$).
The terminals constitute the communication framework between agents.

For each agents $a \in N \cup D$, we use a to refer to both the agent itself as well as to the set of terminals associated with it, i.e., we say $t \in a$ if terminal t is associated with agent a. As shown in [KCLB14], for a power network, this leads to a bipartite graph between nets and devices in which each terminal t connects a device and a net. In other words, the sets of devices D and the set of nets N are both partitions of $\mathcal{T}$, or, the other way round, the set of terminals $\mathcal{T}$ can be partitioned by either the devices or the nets.
For example, Figure 2.8a shows a simple 3-bus circuit whereas Figure 2.8b shows its network model where net agents are represented by rectangles, device agents by circles and the terminals by lines.

This decomposition is extended in [CKC$^+$14] to solve a (preventive) SCOPF problem in which the optimisation is performed over a number of possible contingency scenarios, $\mathcal{L} \in \mathbb{N}^+$, each related to a contingency. We note that the first scenario, (0), is the one that stands for the base case (with no contingency). Given a contingency $\tau \in [0, \mathcal{L}]$, we define $D^{(\tau)}$ as the set of devices that are disconnected in that scenario (τ). The scenarios are noted with parenthesis to distinguish scenarios numbers from other superscripts like the iteration number.

Thus, in a SCOPF problem, each terminal $t \in T$ has associated one (active) power schedule over the set of contingencies $\mathcal{L}$: $p_t = (p_t^{(0)}, \ldots, p_t^{(\mathcal{L})}) \in \mathbb{R}^{\mathcal{L}}$.

Henceforth, we apply the following sign convention: power coming out of a terminal to the device is positive and going into a terminal from the device is negative. To be consistent, from a net point of view, signs are inverted. Then, for all $\tau \in [0, \mathcal{L}]$, $p_t^{(\tau)}$ is the (real) power consumed (if positive, otherwise produced) by device d through terminal t, for the contingency scenario (τ). We provide, in Figure 2.8c, the nets and the devices partitions of the active power schedule of $\mathcal{T}$ to illustrate the partitioning of the set of terminals. Similarly, we use an analogous notation for voltage phase angle schedule over the set of contingencies $\theta_t = (\theta_t^{(0)}, \ldots, \theta_t^{(\mathcal{L})}) \in \mathbb{R}^{\mathcal{L}}$.

The set of all power schedules associated with an agent $a \in N \cup D$ (being a either a device or a net) is denoted by $p_a = \{p_t | t \in a\}$, which we can associate with a $|a| \times \mathcal{L}$ matrix.
For example, in Figure 2.8c, the set of active power schedules of the device agent l_{12} and of the net agent n_2 are defined as $p_{l_{12}} = \{p_{t_2}, p_{t_3}\}$ and $p_{n_2} = \{p_{t_1}, p_{t_2}\}$ respectively. For voltage phase angle schedules, we use an identical notation to power schedules, i.e. $\theta_a = \{\theta_t | t \in a\}$. Similarly, the set of all power schedules of the network is denoted by $p = \{p_t | t \in \mathcal{T}\}$ and the set of all voltage phase angle schedules of the network by $\theta = \{\theta_t | t \in \mathcal{T}\}$, each of which can be associated with a $|\mathcal{T}| \times \mathcal{L}$ matrix.

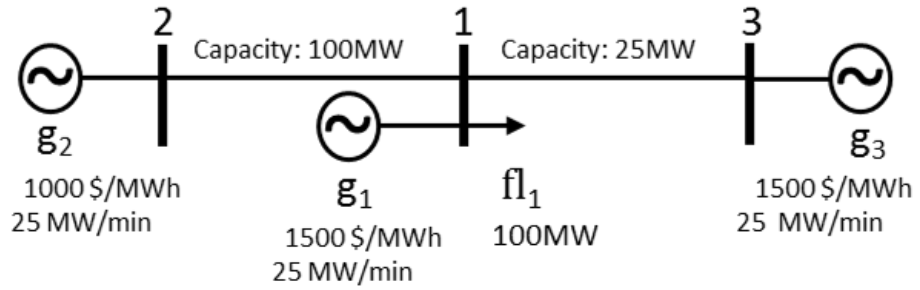

(a) 3-bus circuit

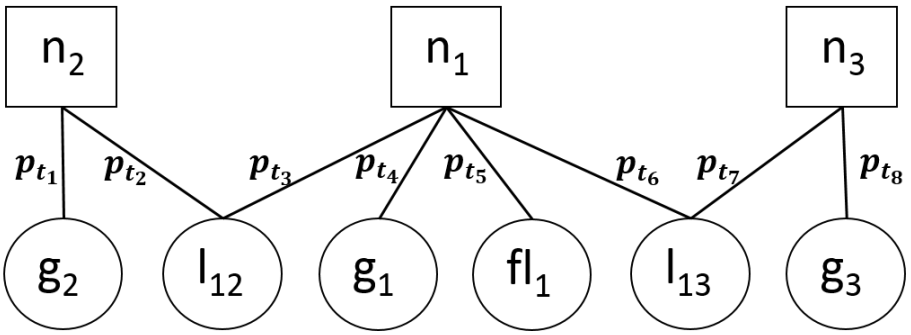

(b) Bus/device decomposition model

$$p = \begin{bmatrix} p_{t_1} \\ p_{t_2} \\ p_{t_3} \\ p_{t_4} \\ p_{t_5} \\ p_{t_6} \\ p_{t_7} \\ p_{t_8} \end{bmatrix} = \begin{bmatrix} p_{n_2} = \begin{bmatrix} p_{t_1} \\ p_{t_2} \end{bmatrix} \\ p_{n_1} = \begin{bmatrix} p_{t_3} \\ p_{t_4} \\ p_{t_5} \\ p_{t_6} \end{bmatrix} \\ p_{n_3} = \begin{bmatrix} p_{t_7} \\ p_{t_8} \end{bmatrix} \end{bmatrix} = \begin{bmatrix} p_{g_2} = [p_{t_1}] \\ p_{l_{12}} = \begin{bmatrix} p_{t_2} \\ p_{t_3} \end{bmatrix} \\ p_{g_1} = [p_{t_4}] \\ p_{fl_1} = [p_{t_5}] \\ p_{l_{13}} = \begin{bmatrix} p_{t_6} \\ p_{t_7} \end{bmatrix} \\ p_{g_3} = [p_{t_8}] \end{bmatrix}$$

(c) Partitioning of the set of active power schedules.

Figure 2.8: A simple bus test circuit ; its graphical representation in the network model from [KCLB14] and the partitions of the active power schedule.

Under these notations, the global objective function of any preventive SCOPF problem can be written as:

$$\begin{aligned} \min_{p,\theta \in \mathbb{R}^{|\mathcal{T}|\times\mathcal{L}}} & \sum_{d\in D} f_d(p_d,\theta_d) + \sum_{n\in N} f_n(p_n,\theta_n) \\ \text{subject to : } & \forall d \in D : p_d,\theta_d \in C_d, \\ & \forall n \in N : \ p_n,\theta_n \in C_n \end{aligned} \tag{2.9}$$

where (p_d,θ_d) and (p_n,θ_n) are the variables of p and θ respectively involved in f_d and in f_n.

The global objective function is intended to find the active power and voltage phase angle schedules that minimise the overall operating cost while satisfying the power flow equations and being feasible for all specified contingency scenarios.

2.5.2 *Alternating Direction Method of Multipliers*

Following [KCLB14, CKC+14], this optimisation problem from Equation 2.9 can be solved by a distributed coordination protocol based on the Alternating Direction Method of Multipliers (ADMM) [BPC+11].

Derivation

Under ADMM formulation, first, the net agents objective functions are defined over a duplicated copy of the original variables, denoted as $\dot{p}$, $\dot{\theta}$. Then equality coupling constraints ($p = \dot{p}$, and $\theta = \dot{\theta}$) are added to keep the equivalence with Eq. 2.9.

$$\begin{aligned} \min_{p,\theta \in \mathbb{R}^{|\mathcal{T}|\times\mathcal{L}}} & \sum_{d\in D} f_d(p_d,\theta_d) + \sum_{n\in N} f_n(\dot{p}_n,\dot{\theta}_n) \\ \text{subject to : } & \forall d \in D : p_d,\theta_d \in C_d, \\ & \forall n \in N : \ \dot{p}_n,\dot{\theta}_n \in C_n, \\ & p = \dot{p}, \ \ \theta = \dot{\theta} \end{aligned} \tag{2.10}$$

The scaled form of the augmented Lagrangian is then formed by relaxing the equality coupling constraints:

$$\begin{aligned} L(p,\dot{p},\theta,\dot{\theta},u,v) = & \sum_{d\in D} f_d(p_d,\theta_d) + \sum_{n\in N} f_n(\dot{p}_n,\dot{\theta}_n) \\ & + \frac{\rho}{2}(||p-\dot{p}+u||_2^2 + ||\theta-\dot{\theta}+v||_2^2) \end{aligned} \tag{2.11}$$

where ρ is the *scaling* (or *penalty* or *tuning*) parameter, u and v are the dual variables associated, respectively, with the active power schedule p and the voltage phase angle schedule θ.

The problems then become separable using the fact that the set of devices D and the set of nets N are both partitions of the set of terminals $\mathcal{T}$, and that imply the two later equalities:

$$||p - \dot{p} + u||_2^2 = \sum_{t \in T} ||p_t - \dot{p}_t + u_t||_2^2 = \sum_{d \in D} ||p_d - \dot{p}_d + u_d||_2^2 = \sum_{n \in N} ||p_n - \dot{p}_n + u_n||_2^2$$
$$||\theta - \dot{\theta} + v||_2^2 = \sum_{t \in T} ||\theta_t - \dot{\theta}_t + v_t||_2^2 = \sum_{d \in D} ||\theta_d - \dot{\theta}_d + v_d||_2^2 = \sum_{n \in N} ||\theta_n - \dot{\theta}_n + v_n||_2^2$$

The ADMM algorithm eventually consists in, alternatively, minimising the Lagrangian of Eq. 2.11, using previous equalities, with constant nets variables ($\dot{p}$, $\dot{\theta}$) then, with constant devices variables (p, θ), and finally in updating of the scaled dual variables (u and v). In that way, ADMM can be viewed as a version of the method of multipliers in which separable minimisations over different primal variables are performed in successive steps.

In a nutshell, the ADMM algorithm consists in iteratively applying the following three steps at a given iteration $k+1$ and for some scaling parameter $\rho > 0$:
The *device-minimisation* step (i.e. parallelised among device agents): $\forall d \in D$

$$\begin{aligned}(p_d^{k+1}, \theta_d^{k+1}) = \arg \min_{p_d, \theta_d \in C_d} (f_d(p_d, \theta_d) + \frac{\rho}{2} ||p_d - \dot{p}_d^k + u_d^k||_2^2 \\ + \frac{\rho}{2} ||\theta_d - \dot{\theta}_d^k + v_d^k||_2^2)\end{aligned} \tag{2.12}$$

The *net-minimisation* step (i.e. parallelised among net agents): $\forall n \in N$

$$\begin{aligned}(\dot{p}_n^{k+1}, \dot{\theta}_n^{k+1}) = \arg \min_{\dot{p}_n, \dot{\theta}_n \in C_n} (f_n(\dot{p}_n, \dot{\theta}_n) + \frac{\rho}{2} ||p_n^{k+1} - \dot{p}_n + u_n^k||_2^2 \\ + \frac{\rho}{2} ||\theta_n^{k+1} - \dot{\theta}_n + v_n^k||_2^2)\end{aligned} \tag{2.13}$$

The (price) *scaled dual variables* update (i.e. parallelised among net agents): $\forall n \in N$

$$u_n^{k+1} = u_n^k + (p_n^{k+1} - \dot{p}_n^{k+1}) \tag{2.14a}$$
$$v_n^{k+1} = v_n^k + (\theta_n^{k+1} - \dot{\theta}_n^{k+1}) \tag{2.14b}$$

The problem is, by construction, already separated in local sub-problems which allows each agent (either net or device) to solve its sub-problem in parallel and to coordinate via message-passing through terminals with neighbouring agents.

At each iteration, each device agent computes a minimisation step for its local objective function (Eq. 2.12) that minimises the operating cost of the device (i.e. encoded by f_d and C_d), and a penalty that depends on messages passed to it through its terminals by its neighbouring nets in the previous iteration ($\dot{p}_n^k$, $\dot{\theta}_n^k$, u_n^k and v_n^k).
Similarly, each net agent computes its minimisation (Eq. 2.13) and scaled dual variables steps (Eq. 2.14a,2.14b) with an argument that depends on messages passed to it

through its terminals by its neighbouring devices in the previous iteration $(p_d^{k+1}, \theta_d^{k+1})$. In more detail, nets are loss-less energy carriers (i.e. buses) with zero cost function (e.g. $f_n(\cdot) = 0$), but with constraints on the power and phase schedules of their terminals that enforce Kirchhoff's physical laws. Following [KCLB14, CKC+14], each net $n \in N$ requires *power balance* and *phase consistency*, which is represented by the constraints:

$$\sum_{t \in n} \dot{p}_t = 0, \tag{2.15}$$

$$\dot{\theta}_t = \dot{\theta}_{t'}, \ \ \forall t, t' \in n^2 \tag{2.16}$$

For the constraints specified above, the computation of the *net-minimisation* step (Eq. 2.13) can be solved analytically as in [KCLB14] [3]as follows, $\forall t \in n$:

$$\dot{p}_t^{k+1(s)} = p_t^{k+1(s)} - \frac{1}{|n|} \sum_{t \in n} p_t^{k+1(s)}, \tag{2.17}$$

$$\dot{\theta}_t^{k+1(s)} = \frac{1}{|n|} \sum_{t \in n} \theta_t^{k+1(s)}, \tag{2.18}$$

with $|n|$ the number of terminals (connections) of net n, i.e. the size of vectors $\dot{p}_n$ and $\dot{\theta}_n$.Note that for AC-OPF problems, the nets agents problems are solved analytically: the nets agents reactive power solution is computed similarly to Eq. 2.17, and the nets agents voltage magnitude is computed similarly to Eq. 2.18.

Convergence

The three steps of the ADMM are carried out iteratively until a sufficient consistency is reached at each net. The consistency is characterised by two residuals: the primal residual, and the dual residual. The primal residual, noted r, captures the consistency between the nets and the devices variables. Considering Eq. 2.17 and 2.18, the primal residual measures the power imbalance and the phase consistency at each net. The vectors of primal residual at iteration $k+1$, for scenario (s), and for each bus $n \in N$ can be then expressed as:

$$\begin{aligned} r_n^{k+1(s)} &= \begin{bmatrix} p^{k+1(s)} - \dot{p}^{k+1(s)} \\ \theta^{k+1(s)} - \dot{\theta}^{k+1(s)} \end{bmatrix} \\ &= \begin{bmatrix} \frac{1}{|n|} \sum_{t \in n} p_t^{k+1(s)} \cdot \mathbb{1}_{|n|} \\ \theta^{k+1(s)} - \frac{1}{|n|} \sum_{t \in n} \theta_t^{k+1(s)} \cdot \mathbb{1}_{|n|} \end{bmatrix} \end{aligned} \tag{2.19}$$

with $\mathbb{1}_{|n|}$ the vector of 1 of size $|n|$ (number of terminals of net n).

3 Eq. 2.17 and 2.18 are the results of a projection on a hyperplane defined by the constraints of Eq. 2.15 and 2.16.

The dual residual, noted s, measures the change of the nets variables between two consecutive iterations, and with Eq. 2.17 and 2.18, it can be computed as the difference between two consecutive iterations of

(i) the difference of the active power scheduled and the average power at the bus, and

(ii) the average phase angle.

The vectors of dual residual at iteration $k+1$, for scenario (s), and for each bus $n \in N$ can be expressed as:

$$\begin{aligned} s_n^{k+1(s)} &= \begin{bmatrix} \rho \cdot (\dot{p}^{k+1(s)} - \dot{p}^{k(s)}) \\ \rho \cdot (\dot{\theta}^{k+1(s)} - \dot{\theta}^{k(s)}) \end{bmatrix} \\ &= \rho \cdot \begin{bmatrix} p^{k+1(s)} - \frac{1}{|n|} \sum_{t \in n} p_t^{k+1(s)} \cdot \mathbb{1}_{|n|} - p^{k(s)} + \frac{1}{|n|} \sum_{t \in n} p_t^{k(s)} \cdot \mathbb{1}_{|n|} \\ \frac{1}{|n|} \sum_{t \in n} \theta_t^{k+1(s)} \cdot \mathbb{1}_{|n|} - \frac{1}{|n|} \sum_{t \in n} \theta_t^{k(s)} \cdot \mathbb{1}_{|n|} \end{bmatrix} \end{aligned} \tag{2.20}$$

The vectors primal and dual residuals of net n at iteration $k+1$ are finally:

$$r_n^{k+1} = \begin{bmatrix} r_n^{k+1(0)} \\ \cdots \\ r_n^{k+1(\mathcal{L})} \end{bmatrix} \qquad s_n^{k+1} = \begin{bmatrix} s_n^{k+1(0)} \\ \cdots \\ s_n^{k+1(\mathcal{L})} \end{bmatrix} \tag{2.21}$$

As shown in [BPC+11], the algorithm convergence can be determined when the primal and dual residuals are small compared to primal ϵ^{prim} and dual ϵ^{dual} tolerances. The convergence criterion are then:

$$||r_n^{k+1}||_2 \leqslant \epsilon^{prim} \tag{2.22a}$$

$$||s_n^{k+1}||_2 \leqslant \epsilon^{dual} \tag{2.22b}$$

[KCLB14] propose to normalise these tolerances based on an absolute tolerance ϵ^{abs} and on the size of the network. We apply this normalisation at the bus level, such that, for any net $n \in N$:

$$\epsilon_n^{prim} = \epsilon_n^{dual} = \epsilon^{abs} \cdot \sqrt{|n|} \tag{2.23}$$

This convergence implies the global convergence of the system with an absolute tolerance of ϵ^{abs} because, with the triangle inequality we have:

$$||r||_2 \leqslant \sum_{n \in N} ||r_n||_2 \leqslant \sum_{n \in N} \sqrt{|n|} \cdot \epsilon^{abs} \leqslant \sqrt{\sum_{n \in N} |n|} \cdot \epsilon^{abs} \tag{2.24}$$

This procedure is summarised in Algorithm 1 with a flat start that means that all variables (from devices and nets) and all dual variables are initially set to 0.

The ADMM is guaranteed to converge to the optimal solution when the objective functions and constraints of the problem are convex, closed, proper, see Appendix A in [BPC+11] for one of the proofs. Thus, when all devices have convex, closed, proper objective functions and a feasible solution to the SCOPF exists, the ADMM-based algorithm converges to the optimal solution of the problem.

Algorithm 1 ADMM on OPF

1: Flat start (all variables set to 0)
2: **while** $\forall n \in N,\ \left(||r_n||_2 < \epsilon^{prim} \text{ and } ||s_n||_2 < \epsilon^{dual}\right)$ **do**
3: Solve devices-minimisation (Eq. 2.12)
4: Send schedules to neighbouring nets
5: Solve nets-minimisation (Eq. 2.13)
6: Update dual variables (Eq. 2.14a and 2.14b)
7: Calculate the primal and dual residuals (Eq. 2.19 and 2.20)
8: Send results to neighbouring devices
Iteration ++

2.6 CONCLUSION

A large literature exists on power systems optimisation problems, however, considering the interconnections of transmission systems, the problems are very large and the computational and communication burdens necessitate scalable tools (Requirement 8). Interconnections are built to achieve better overall reliability and economical efficiency, and yet, they also raise interoperability (Requirement 6), privacy and autonomy (Requirement 7) issues. Widely used centralised approaches are not suited for those issues unlike distributed approaches that are gaining popularity since they can preserve the independence of regional operators and actors, while fully taking advantage of the interconnections. Several distributed methods and ways of decomposing OPF-based problems exist but the Alternating Direction Method of Multipliers has been identified as one of the most applicable and efficient methods. Its simplicity, its ability to decompose power system problems at different levels and better convergence performance compared to other state-of-the-art algorithms for distributed optimisation [BPC+11], made ADMM the most employed distributed algorithm for power system optimisation problems in the last years [WWW17a].

Several references exist on the application of the ADMM to power system optimisation problems, in particular, [KCLB14] that develop a fully distributed algorithm to solve the OPF problem, through a fine-grained decomposition. Other references have tackled the Security Constrained Optimal Power Flow, such as [CKC+14] that formulated the SCOPF problem under the same decomposition. However, the outages considered are only on lines of the system and so, the formulation does not consider the rescheduling due to the automatic reaction of the system (preventive) or optimal actions (corrective). The ADMM has been used to solve corrective SCOPF under different decompositions but the preventive SCOPF has not been correctly addressed, especially because none includes the primary frequency control of generators and so, outages on generators. This justifies the development of such a method in Chapter 4 of this thesis.

Very few references focus on the integration of uncertainties in the OPF problem using ADMM or other distributed methods, despite the increasing interest in this optimisation problem. In particular, the CCOPF problem has never been addressed using

ADMM, probably because, in the general case, the problem is intractable. Nevertheless, the centralised approaches assuming that the forecast error of each wind farm follows (previously known) mutually independent probability density functions appears to be interesting for distributed methods. Indeed, the analytical reformulations of the chance constraints, lead to deterministic problems that have lower computational complexity than other techniques such as scenario based approaches [MGL14]. Chapters 5 is thus dedicated to the inclusion of chance constraints in the ADMM approach, thus ensuring the scalability, the autonomy and cooperation of the different actors.

3

STUDY OF THE EVOLUTION OF THE MAIN BLACKOUTS FEATURES - 2005/2016

The security of power systems and, in particular the prevention of large scale catastrophic events such as power blackouts, is at the core of this thesis requirements and objectives. To this end, in this first chapter, 9 major power blackouts that happened between 2005 and 2016 are analysed in order to determine the main common characteristics that need to be taken into account in the development of algorithms in the chapters to follow.

The remainder of this chapter is organised as follows. Section 3.1 introduces the different phases of a blackout as well as the blackouts selected for this study. Section 3.2 reviews previous studies in the literature. Afterwards, the different sections follow the different blackout phases: Section 3.3 analyses the most relevant preconditions that enabled these blackouts to happen, Section 3.4 describes the initiating events and Section 3.5 analyses the cascades of events that followed. Section 3.6 finally concludes on the main findings from this analysis and discusses the parameters that are important to take into account in the rest of the thesis.

3.1 INTRODUCTION

The actual path to a blackout involves a complex, interdependent sequence of events. As depicted in Figure 3.1, following [MRSV05, IEE07, LBZR06], the progression of the cascade of events can be divided into 4 phases. The first phase is called (I) *preconditions* and it includes the period before any major disturbance, when the power system is in a *stable* state (i.e. all technical and operational constraints are respected). The blackout in itself starts by one or a few decorrelated *initiating events* that disturbs the power system and starts an instability which strength may be variable at the first steps. This initial disturbance propagates in the form of a *cascade of events* that can last from a few seconds to several hours. The cascade can usually be separated into two phases: (II) *steady-state* (also known as *slow*) and (III) *fast* (also known as *high-speed*). When the blackout reaches its *final state* (i.e. when the cascade ends), unserved loads, power generation tripped and the number of people impacted can be evaluated (i.e. to be considered a blackout either part or the entire system should have collapsed). The (IV) *restoration* of the system starts from this point and takes from tens of minutes to several days to achieve full recovery.

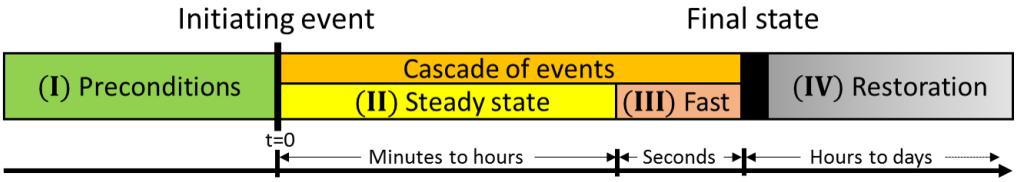

Figure 3.1: Division of the progression of a blackout into phases as proposed in [LBZR06].

Continuous data analysis of previous blackouts is crucial for controlling their perpetual evolution as well as for drawing effective recommendations for their prevention [BCD+08, VBC+12, CND16]. Consequently, the vulnerability of power systems and, in particular previous blackouts have been widely studied to improve power systems reliability [AS09, YLZL09, ADF+05, BSJ+15]. This period during which the power electricity grid experienced significant evolutions (e.g., energetic transition, instrumentation and control automation and demand increase, among others [ADF+05]) includes some of the largest blackouts in history.

This chapter aims at determining what the main characteristics of the major power cascading failures of the past 10 years are in order to identify what aspects should be taken into account by the algorithms to mitigate the risk of incidents. With this aim, we have studied the evolution of the recent blackouts characteristics, in turn consequence of the deep developments undergone by power systems during these last years. We have first selected 9 blackouts according to different criterion. We need blackout reports that exist and that are publicly available to have access to it. The reports need to contain a detailed description and analysis of what happened, and the context in which it happened to be able to compare the blackouts between each other and with the blackouts from previous studies. Table 3.1 provides details for each of these blackouts: the abbreviation used in the rest of the chapter, the date, the location and the main references on which we based our analysis.
Note that the 2006 European outage is not included in this study because, despite the large disturbance that triggered automatic load shedding schemes, the European system did not collapse. The 2006 blackout in Pakistan is also not analysed due to the lack of accurate data available to us. Moreover, notice that the development of these power systems was not done at the same time nor with the same technologies in all countries; in particular, the analysis contains only two long-time developed power system, i.e. Usa11 and Austr16.

We have classified the blackouts depending on the context, on the initiating events and on the characteristics of the cascades because these describe the proceeding of blackouts and thus are widely used to analyse blackouts in the literature. We have studied the evolution based on this period and have compared the characteristics of the blackouts before and after 2005. Finally, we analyse what should be integrated in

the algorithms developed in the next chapters.

This chapter first provides the related literature in Section 3.2. Afterwards, the different sections follow the different blackout phases: Section 3.3 analyses the most relevant preconditions that enabled these blackouts to happen, Section 3.4 describes the initiating events and Section 3.5 analyses the cascades of events that followed. Section 3.6 finally concludes on the main findings from this analysis and discusses the parameters that are important to take into account in the rest of the thesis.

Abbreviation	Date	Location	References
Indo05	2005/08/18	Indonesia	[oEotRoI05]
Colom07	2007/04/26	Colombia	[ROG08, P. 07] [Gut09]
Braz09	2009/11/10	Brazil	[ONS09, Ilh10] [AGG+12]
Braz11	2011/02/04	Brazil	[ONS11, AGG+12]
Usa11	2011/09/08	USA/Mexico	[FN12]
Chile11	2011/09/24	Chile	[CDE11]
India12	2012/07/30-1[1]	India	[Cer12]
Turk15	2015/03/31	Turkey	[Pro15]
Austr16	2016/09/28	Australia	[AEM16]

Table 3.1: Details of the 9 blackout analysed.

3.2 RELATED WORK

Given the large economic and social impact of blackouts, a variety of methods have been proposed in the power system literature to study this challenging topic. Baldick *et al.* [BCD+08] and Vaiman *et al.* [VBC+12] provide comprehensive reviews on this area and discuss the main methods for cascading failure analysis and simulations. Of particular interest here, both works highlight the importance of previous blackout data analysis for the progress of the field towards effective methods for blackout risk assessment. Consequently, several studies have been published on the analysis of the cascading failures, each covering a specific time period. For instance, in [AS09], Atputharajah *et al.* describe the causes and the development of 9 blackouts that happened between 1965 and 2007, highlighting the role of reactive power reserves, which ensure voltage stability, and of the voltage phase angle differences, which keep regions synchronized. In a similar line of work, Yamashita *et al.* [YLZL09] analyse the causes and the sequence of events that led to 4 blackouts within the period from 1996

1 Two blackouts happened on two consecutive days. Operators had time to restore the system before the second blackout happened. Since pre-conditions and initiating events are of same nature, we will only develop the differences in the description of the cascade.

to 2006 to find patterns of sequences. They discuss the control actions that could prevent cascade of events, either system operation or emergency control, and emphasise the importance of overload cascades mitigation since it often leads to system splitting. Further, Andersson *et al.* summarises in [ADF+05] three power blackouts that happened in 2003: in North America, in Sweden & Denmark and in Italy. The paper draws recommendations and details how new technologies, like flexible alternating current transmission system (FACTS) or high-voltage direct current (HVDC), can improve power systems security and stability.

Blackouts have been the focus of discussion of two panel sessions [20004, 20006] and of a series of invited papers [PK06, PKT06, Dag06, PBJW06, WM06, HP06] in the IEEE Power & Energy Magazine September / October 2006, both sponsored by the IEEE Power System Dynamic Performance Committee and Blackout task force. In its final report [IEE07], the task force summarises the causes and lessons learnt from documented blackouts in the period 1965-2006 as well as the best practices and tools that may be used to reduce the risk of future blackouts. The report also provides some high-level policy recommendations.

Lu *et al.* also focused on the blackouts that happened between 1965 and 2005 in [LBZR06]. They study 37 blackouts, and propose a classification of each phase of the blackouts, which we use in our analysis. The main suggestion brought by this analysis is to develop actions that can avoid to enter the fast cascade that cannot be stopped by operators.

More recently, Bo *et al.* [BSJ+15] analyse 23 representative blackouts of the period 1965-2012 with the objective of providing suggestions on the expansion and improvement of the Chinese power grid. The main recommendation resulting from this article is to put the safety of power system operation first by managing the planning, construction, scheduling and emergency in a more unified way to prevent large-scale blackouts.

Finally, [VS16] analyse 14 blackouts of the period 2003-2015 and classify the blackouts according to 5 indices: the number of people impacted, the lost load in MW, the duration, the affected population and the severity[2]. This study focuses mainly on the comparison of the way reliability regulations are enforced: either legally binding (that is the case of the North American system) or not (that is the case of the European system). It concludes that a non-legally binding enforcement of the operational rules is inadequate to power system's needs.

In conclusion, the analysis of previous blackouts is essential to mitigate the risk of future catastrophic events by providing recommendations for the planning, operation or regulation of power systems. Several previous studies emphasise the crucial role of prevention in avoiding blackouts, and studying previous blackouts through the prism of prevention can help identifying important features to consider. This chapter then

2 The severity is defined, in [VS16], as the ratio of the energy not served by the base of power, and is expressed in System.minute. For example, a severity of 1 System.minute can represent a loss of the entire system for 1 minute, or the loss of half of the system for 2 minutes.

differs from the mentioned analysis in its objectives because it aims at highlighting what characteristics of power systems should be integrated in the modelling of prevention problems.

3.3 PRE-CONDITIONS

The pre-conditions are the set of state variables of the power system before the disturbance happens, when the system is in a stable state. In other words, pre-conditions define the context in which incidents happen. In our analysis, we used the main pre-conditions described in [LBZR06] and [YLZL09], namely: peak demand, important equipment out of service, inadequate reactive power reserves and natural reasons. The ageing of equipment did not appear in the reports analysed and hence, it is not mentioned below, although this pre-condition played a significant role in some previous blackouts.

In addition, we extend this list to include three pre-conditions identified as significant in our analysis, namely: dependency among regions, mismatch between scheduled and actual power flow and the N-k reliability operating criteria (i.e. a metric of the reliability of the system). Figure 3.2 summarises the pre-conditions that preceded each of the nine[3,4] analysed blackouts, where pre-conditions are depicted within the square boxes below the blackouts abbreviations. We describe each of these pre-conditions in the following sections.

3.3.1 *Peak demand*

In previous periods, blackouts were often happening during peak demand periods (usually winter and/or summer), when the system, being under stress due to the high loading, operates close to the operating and stability limits. However, as summarised in Figure 3.2, 8 out of 9 blackouts of the period 2005-2016 happened under normal loading conditions. The only exception is the blackout in India12, in which the loading of the system reached respectively 99.7 GW and 100.5 GW load served prior to disturbance whereas the peak demand met at the time was around 110 GW.
Hence, this result contrast with those of previous blackouts (i.e. Of the period 1965-2005) for which peak demand was identified as the main pre-condition. As an example, around 65 % of the 37 blackouts analysed in [LBZR06] happened during peak conditions.

3 For Colom07 the list of pre-conditions is not exhaustive, given the lack of information in the available reports.

4 India12 encountered two very similar blackouts on two consecutive days, we thus treat the pre-conditions and initiating events as one blackout.

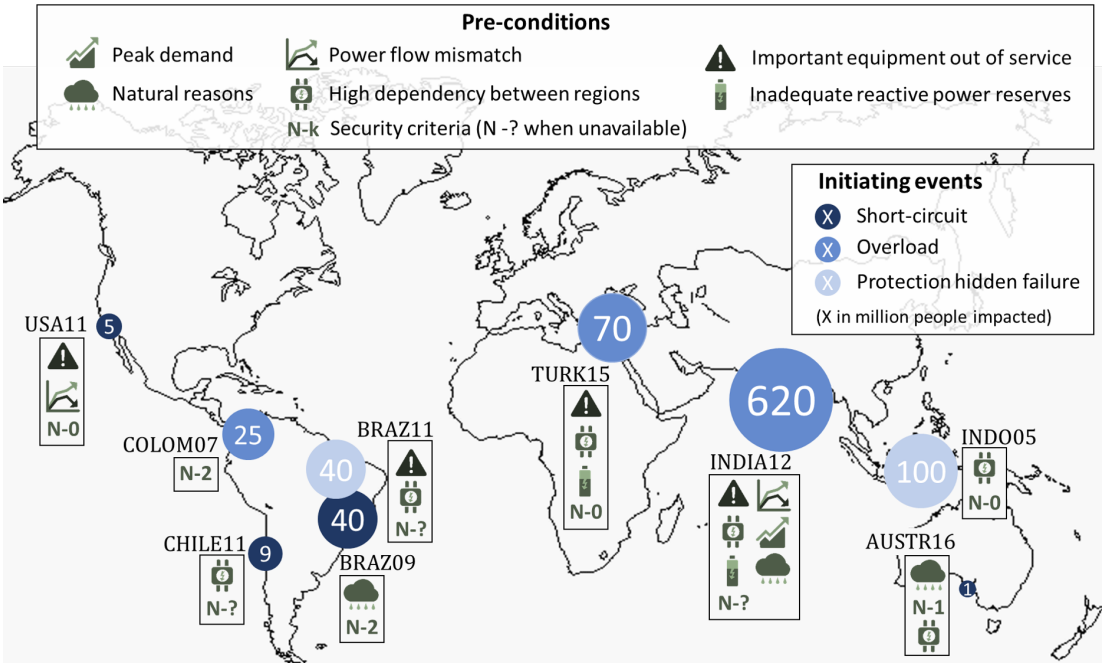

Figure 3.2: Location, million people impacted, pre-conditions and initiating events that triggered each blackout.

3.3.2 *Important equipment out of service*

Equipment can be out of service due to unexpected technical or supply problems (i.e. *forced* outage) or due to upgrading and maintenance works (i.e. *planned* outage). As highlighted in [BCD+08], one particularity of planned outages is that they are usually performed during normal or low loading periods (i.e. spring and autumn).

The absence of important equipment, as a result of (mainly planned) outages, played a key role in the development of many of the analysed blackouts, as we discuss next. In Turk15, the backbone of 400 kV transmission lines corridor between the Eastern and Western parts of the country was weakened due to planned outages of lines and series capacitors. In Braz11, a 500 kV line was disconnected for maintenance purposes. In Usa11, 600 MW generation in Baja California and two 230 kV lines were under maintenance prior to the blackout. Five transmission lines were unavailable due to maintenance in Chile11. In India12, several generating units and transmission elements (between the Northern, Western and Eastern regions) were under maintenance or under forced outage due to technical issues.

3.3.3 *Dependency among regions*

Dependencies on supply between regions of an interconnected network can have a great impact on the size and the speed of the blackout. In more detail, when an im-

portant disturbance happens, regions are often disconnected to avoid its propagation. However, in presence of strong dependencies on power supply, the deficit or excess of power generation can provoke a rapid collapse, leaving regions in an irrecoverable situation. We consider that one region is highly dependent, and consequently at risk, if the power imported is greater than 20 % of its total consumption, or close to the limit of import capability with power reserves issues. This metric is in line with previous blackouts; for example before 2003 Italian blackout, Italy was importing 25 % of its consumption, of which 21 % were from Switzerland and France. Notice that although the dependency among regions was not explicitly listed as a pre-condition in previous reports, it was frequently mentioned in the description of the blackouts contexts (e.g. [ADF+05] revealed that Southern Sweden/Eastern Denmark and Italy power systems were highly dependent on their neighbours previously to the two blackouts that followed). We explicitly mention it as a pre-condition to highlight the risk of operating tie lines close to their limits especially when the loss of those could trigger very fast blackout.

As we can observe in Figure 3.2, the dependency among regions turns out to be one of the main pre-conditions in our study since, as detailed next, 6 out of 9 blackouts faced this situation. In more detail, the Jakarta-Banten region of JAMALI system in Indo05 and the South Australia region in Austr16 were importing respectively 21 % and 32 % of their consumption from neighbouring regions. In Chile11, the North Central region of the central interconnected system (SIC)[5] was importing power mainly from only two areas, the South/East Ancoa and the Southern SIC. These dependencies created a deficit/excess of power after SIC separation.

In some blackouts, these high dependencies between regions can be explained by the heterogeneous distribution of resources, for example hydroelectricity is not available everywhere. For instance, in Turk15, the Eastern region was exporting a lot of hydroelectricity (42 % of its production), most of it to the Western region that, without this potential, was importing 21 % of its load demand. Similarly, in Braz11 (a country in which 70 % of its production is from hydroelectricity) the North Eastern region was importing up to 36 % of its load power demand, mostly from the hydroelectric resources in the South and Central regions of the country. Indeed the Braz11 blackout was initiated by a protection hidden failure at a hydro plant substation.

Finally, before both blackouts in India12, the Northern region was importing from the Western region between 12 % and 15 % from its load demand due to the unavailability of few thermal units that were under forced outage. Although this percentage of import is lower than the one from the 2003 Italian blackout that we took as reference, the fact that the Northern region was short in power reserves and that the import created congestion on the interconnection lines on the path across Western-Eastern-Northern regions justifies this classification. The lack of active power reserves is due to planned and forced outages of thermal units and the outages on interconnection lines exacerbated the congestion, see 3.3.2.

5 In Chile there are four electrical interconnected systems operating independently of each other.

3.3.4 *Inadequate reactive power reserves*

The lack of reactive power reserves prevents the system from stabilising the voltage and thus could lead to voltage instability or even collapse. In particular, when transmission lines are highly loaded, reactive power is consumed and reactive power support can be needed to avoid power losses and low voltage. This support can be provided by generators or by Static Var Compensators (SVC).

In India12, the reactive power support needed for highly loaded transmission line was not available where needed, especially on the corridor between the western and northern regions. The series capacitors[6] under maintenance during the blackout Turk15 reduced the transfer capacity of the corridor East-West and increased the voltage drop of the transmission lines.

3.3.5 *Natural reasons*

Natural reasons can be an important factor in blackouts, especially extreme weather conditions like heavy rains, wind, or thunderstorms that can harm elements of the system or lead to short-circuits. For instance, Braz09 blackout happened during heavy rain and wind due to a thunderstorm. Both India12 blackouts happened during the monsoon in the south of the country and created forced outages of some transmission devices. The Austr16 blackout happened during a lightning storm.

Power system operators are aware of this risk and can take exceptional measures to mitigate the risk of propagation of the disturbances. In Braz09, the 765 kV part of the system was operated to be N-2 secure, i.e. the loss of any pair of 765 kV devices should not trigger a cascade, because of the risk of lightnings. Nevertheless, in South Australia region, even with the high lightning risk, the operator assessed that there were no transmission line classified as vulnerable to lightning and hence, did not take more preventive measures than usual.

3.3.6 *Mismatch between scheduled and actual power flow*

The mismatch between the scheduled and actual power flows along interconnection lines is very risky because operators might not take the most suitable counter-measures in such emergency cases (i.e. there may be no contingency plan to handle such unexpected situation). Thus, before both India12 blackouts, significant mismatch between scheduled and actual power flows on interconnection lines were noticed. In Usa11, the Western Electricity Coordination Council also observed unscheduled flows on major paths.

6 Series capacitors are designed to compensate the reactive power consumption of lines and so increase the transfer capacity of the lines.

3.3.7 *N-k operating reliability criteria*

Security of power systems has been traditionally determined by the (deterministic) N-k security criteria. Formally, a power system is *N-k secure* if the simultaneous loss of any set of k elements does not trigger a cascade. Figure 3.2 depicts the N-k criteria at which power networks were operated prior to the blackout, and so provides an idea of the security of the system at the time of the initiating event[7].
Most of transmission system operators (TSOs) must operate at least in compliance with the N-1 criteria [PMDL10] so that the system can lose any of its major devices and stay stable, i.e. with no propagation of the disturbance. However, because of unpredictable conditions or errors, the system sometimes cannot be kept within the N-1 limits. This was the case in the Indo05, Usa11 and Turk15 blackouts, all triggered while the corresponding systems were not N-1 secure. Interestingly, the Turkish transmission system was not N-1 compliant, even though both TSO (Eastern and Western) regions were individually N-1 secure, which highlights the necessity of a close coordination between operators of interconnected networks.

Finally, it is worth pointing out that in Colom07 and Braz09 blackouts, the systems were respectively totally and partly N-2 before the incident, which was nevertheless not sufficient to deal with the disturbance that followed.

3.3.8 *Pre-conditions conclusion*

The main pre-conditions identified in our analysis are, first, the high dependency among transmission regions and second, the equipment out of service. The combination of these two conditions is particularly dangerous when interconnection lines are missing. Then any disturbance can overload the remaining lines and trigger the separation of the system which is at risk when regions are dependent on neighbours supply. The interconnections of power systems are at the centre of the pre-conditions identified in this section, due to the dependencies between regions but also because as mentioned for Turk15, the security of each of the regions of the system do not imply the security of the whole. It highlights the importance of considering all regions and their interactions when considering the security of an interconnected system.
We have noticed an evolution during the last decades concerning the pre-conditions: for the period pre-2005, 65 % of blackouts happened in peak period [LBZR06] whereas we observed the opposite tendency today. It seems that a high loading of the interconnection lines and the lack of regional reserves are more likely to lead to a blackout than peak demand conditions.
Nevertheless, all blackouts considered in [LBZR06] happened in USA, Europe or Australia, whereas blackouts analysed here mainly took place in South America or Asia (i.e. all except Usa11, Turk15 and Austr16). Hence, these systems have been de-

7 When the security criteria is not known at the time of the event, it is depicted as *N-?*.

veloped at different times and on different continents, using different constraints and technologies, which makes the comparison difficult.

Finally, it is also important to note that the notion of vulnerable devices to an incident and of credible contingencies, is decisive for the secure operations of power systems, particularly because the number of contingencies considered impacts the complexity of the problem to be solved and the cost of operations.

3.4 INITIATING EVENTS

Initiating events are disturbances that trigger the cascade of events on the power systems, as illustrated in Figure 3.1. The main initiating events[8] are short-circuits, overloads and protection hidden failures. Figure 3.2 shows the initiating events that triggered each of the nine blackouts, marked as the colours of the circles. We describe the occurrence of each of these events in the analysed blackouts, according to available data, in the following sections.

3.4.1 *Short-circuits*

Short-circuits can happen due to natural reasons or errors, such as flash-overs caused by birds or wire insulation break downs. For instance, during Braz09, as a prevention from an ongoing thunderstorm, the Brazilian TSO decided to operate its 765 kV network as N-2 secure. Nevertheless, three short-circuits happened (on two main 765 kV lines and on a 765 kV busbar) almost simultaneously (within an electrical period). Additionally, the Austr16 blackout was initiated by the combination of four single and one double phase-to-ground short-circuit faults that happened within 88 seconds and led to up to six voltage disturbances. Finally, the Chile11 blackout was triggered by a single-phase short-circuit on a switch. The short-circuit that triggered the Usa11 blackout was due to a wrong manoeuvre of a technician while disconnecting a capacitor bank (i.e. it created an arc on a 500 kV line that could not reconnect afterwards because the voltage phase angle difference was too large).

3.4.2 *Overloads*

When a power delivery device is loaded above its limits (i.e. Overloaded), its protections can disconnect it to avoid the lagging of line or damaging the device. The India12 and Turk15 blackouts were triggered by overloads. In India12, the short-circuits that happened due to the monsoon weakened the circuit; then the initiating events were overloads in the heavily loaded North region for both blackouts.
In Turk15, the disconnection of a line on the main corridor between the Eastern and Western regions due to overloading triggered a very fast separation of the two transmis-

8 Although the loss of power plants is usually identified as a main initiating event in previous studies, here it is not included because it does not apply to any of the analysed blackouts.

sion systems. The Colom07 blackout was initially triggered by a human error during a maintenance (i.e. an operator did not follow the sequence of manoeuvres), which in turn led to the overload of a breaker that disconnected a substation that supplied the city of Bogota.

3.4.3 *Protection hidden failures*

Protection hidden failure is a malfunction of a protection device that trips whereas it should not have according to the settings of the system; or the opposite that it does not trip whereas it should have.

The Braz11 blackout was triggered by the accidental opening of circuit breakers and the malfunction of a breaker failure protection, which in turn led to the disconnection of several 500 kV lines. Indo05 blackout was triggered by the false signals from a protection device sent to Suralaya Power Plant.

3.4.4 *Initiating events conclusion*

We did not notice any major difference with the findings from studies of previous blackouts periods (e.g. [LBZR06]), as short-circuits, overloads and protection hidden failures were also the main initiating events.

3.5 CASCADES OF EVENTS

In a blackout, the disturbance created by the initiating events propagates step by step and creates a sequence of events related to each other [MRSV05, IEE07]. In this section, first, we classify the studied blackouts according to their speed. Then, we provide a discussion about the relationship between the presence of certain pre-conditions and the high speed of the blackout.

3.5.1 *Speed of the cascade propagation*

Figure 3.3 illustrates in more detail the mechanisms of the blackouts development, especially the phases *II* and *III* of Figure 3.1 that correspond to the cascades. It shows that the cascade that follows the initiating events can often be divided into two successive phases, namely: (II) steady-state progression and (III) fast cascades. Unlike the fast cascade, the time between two events in the steady-state progression typically ranges from several minutes to several hours. Temporary steady-states are reached after each of the events, but long term operational constraints are violated and eventually lead to the triggering of further protections. The time between the beginning of a violation and the triggering of the protection is long enough to allow system operators to take countermeasures. As an example, lines protections against overloading trigger depending on the loading and on the duration of the overload. Typically, in France,

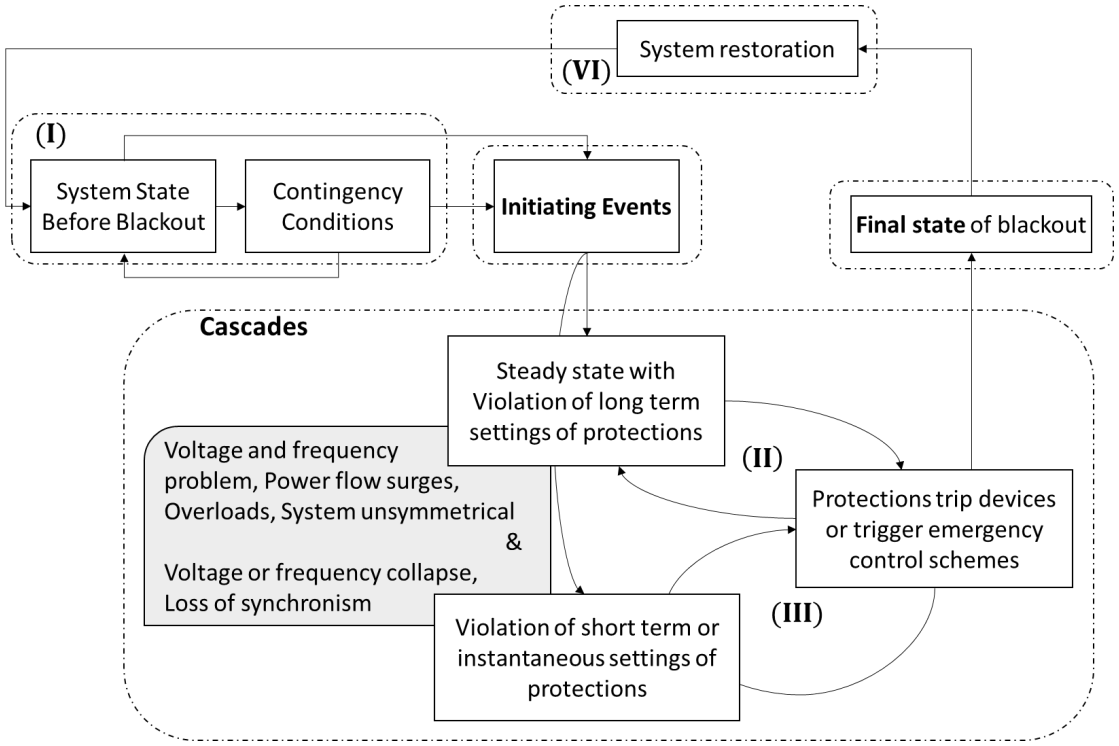

Figure 3.3: Mechanism of blackouts inspired from [MRSV05, LBZR06].

lines protections trigger after around 20 minutes if the overloading is above 130 % of the maximum capacity of the line [CVL00].

Clearly, the smaller violations are, the slower a cascade propagates and the more time operators have to decide which the most suitable decisions to take are. But when the cascade accelerates and enters the fast cascade, the defence plan of the system (automatic actions) is the only barrier that can stop the propagation because operators do not have time to react. Indeed, this fast cascade is composed of transient phenomenon that trigger the short term or instantaneous operational limits of protection devices, as illustrated in Figure 3.3, leading to a cascade lasting between a few seconds to minutes. Following the example about typical lines protections, if the loading is above 170 % of the line capacity, the overload protection triggers within a few seconds [CVL00]. The problems faced during the cascades are, however, not restricted to overloads. Voltage and frequency issues or even collapse, power flow surges, unsymmetrical systems and loss of synchronism also occur and can eventually trigger emergency control scheme such the system separation or automatic load shedding.

The speed of those two phases is illustrated in Figure 3.4 that depicts the duration of each cascade phase and the severity of the blackouts and allows a comparison with previous blackouts. The horizontal axis shows the duration of the steady-state progression, whereas the vertical axis shows the duration of the fast cascade. The size of the circles represents the severity of the blackout computed as the maximum loss of power consumption times the duration of the total restoration. This definition differs

from the one from [VS16] as, here, the severity is simply a rough approximation of the energy unserved and thus do not scale to the system normal loading. The lack of information for Chile11 and Colom07 prevented us to apply the definition from [VS16]. The dark circles correspond to the nine blackouts whereas the pale circles correspond to seven blackouts that happened before 2005. For blackouts prior to 2005, we use mainly data from [LBZR06] that selected those 7 blackouts for being the ones with better documented cascades. We clearly see in Figure 3.4 that most of the cascades of blackouts after 2005 (i.e. 7 out of 9) directly started with the fast cascade, skipping the steady-state propagation (i.e. most of the blackouts are concentrated on the left side of the graph). This high speed propagation can be caused by the large magnitude of the disturbance or by the proximity of the system state to the stability limits. The clearest case is Turk15, where the point of no return was reached after only 1.6 seconds and thus operators could not do anything to stop the blackout. Nevertheless, in Indo05 and in Usa11 the steady-state progression lasts 25 and 11 minutes respectively before the cascades accelerate.

These findings contrast with those obtained for blackouts prior to 2005. For example, according to [VBC$^+$12], more than half of the blackouts prior to 2012 in America and Europe were slow in progression. Likewise, the analysis in [IEE07] concluded that most major blackouts from 1965 to 2006 were triggered by a single initiating event and underwent a steady-state progression before entering the fast cascade. Figure 3.4 also supports this hypothesis by showing the presence of a steady-state cascade in 4 out of 7 blackouts prior to 2005. In conclusion, this study shows that recent blackouts exhibit greater tendency to shorten or skip the steady-state progression than their precedents. The cause for this may be that these power systems were operating too close to the stability limits, which questions the trade-off between the economic dispatch and the network security. But as mentioned in Section 3.3.8, the differences in development and characteristics of the power systems are also other potential explanations for these observations.
This high speed of the cascades implies that the only barrier that could have stopped most of those blackouts was the defence plan of the systems. The system operators did not have time to react after the initiating event happened. Those high speed cascades should then be avoided because it does not allow system operators to react to the disturbance and to mitigate the impact of those. The reasons of this speed are thus discussed in the next section, in order to take them into account in the next chapters.

3.5.2 *Discussion on the causes of the high-speed cascades*

In this section, we discuss the impact that some major pre-conditions have on the speed of the cascade that followed the initiating events. The cascade of overloads with large transfers of power and the separation of highly dependent regions were identified as the main reasons of these high speed cascades.

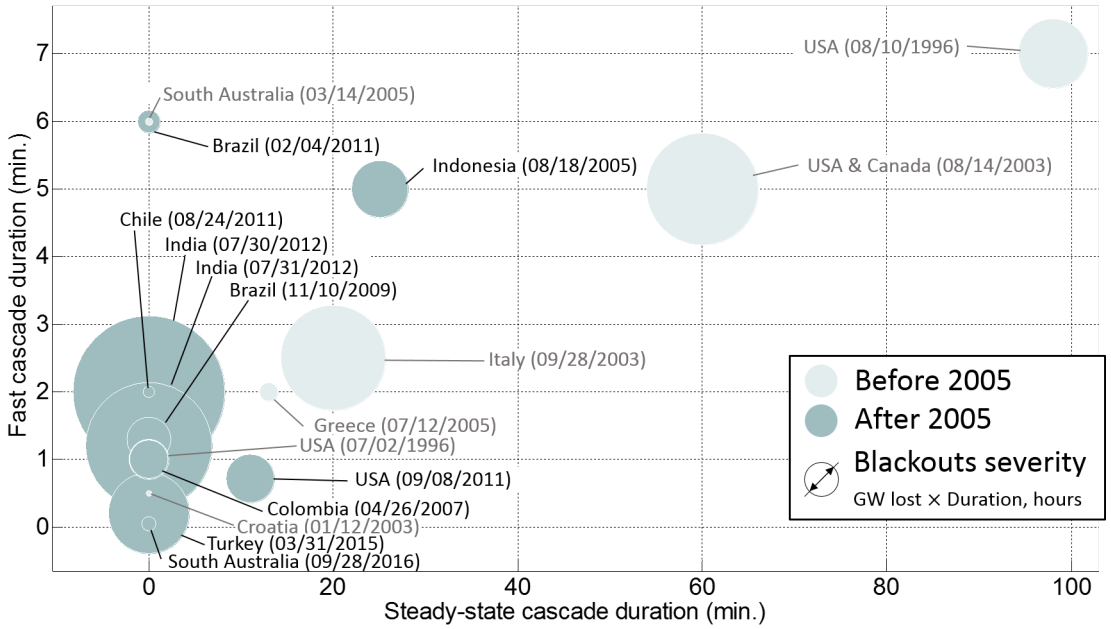

Figure 3.4: Steady-state progression duration vs fast cascade duration of blackouts prior to 2005 (pale circles) and blackouts after 2005 (dark circles). The diameter of the circles represents the severity of the blackout, computed as the maximum power lost times the duration of the total restoration.

Cascade of overloads with large transfers of power

A cascade of overloads starts with the loss of a power delivery element, i.e. a line or a transformer, which recursively leads to new overloads and disconnections as a result of the transfer of power to the remaining lines. Cascades of overloads are typically slow in progression, strongly depending on overload protections settings, and usually belong to the steady-state progression. In our analysis, Indo05 and Usa11 blackouts followed this typical trend. In more detail, in Indo05, a cascade of overloads started after the initiating event as part of the steady-state progression phase. Likewise, in Usa11, a cascade of overloads (i.e. Of transformers mainly) progressively increased the loading of a major path, making the over-current protections trip and eventually triggering the separation scheme of San Diego Gas & Electricity and Southern California Edison networks.
Nevertheless, the speed at which the overloaded devices disconnect depends on the magnitude of the overload. Thus, if the overload generates a large transfer of power, it can, in turn, trigger an extremely fast cascade of overloads.

The large transfers of power can be generated by initiating events that affect key components of the system. This was the case in Colom07 where the disturbance at the main Bogota substation triggered a quick disconnection of ten overloaded lines and transformers. The resulting transfer of power initiated a fast cascade of overloads. In Braz09, during the first 5 seconds of the cascade, 50 elements (among which lines, transformers and generators) were disconnected from the grid. Figure 3.5 shows

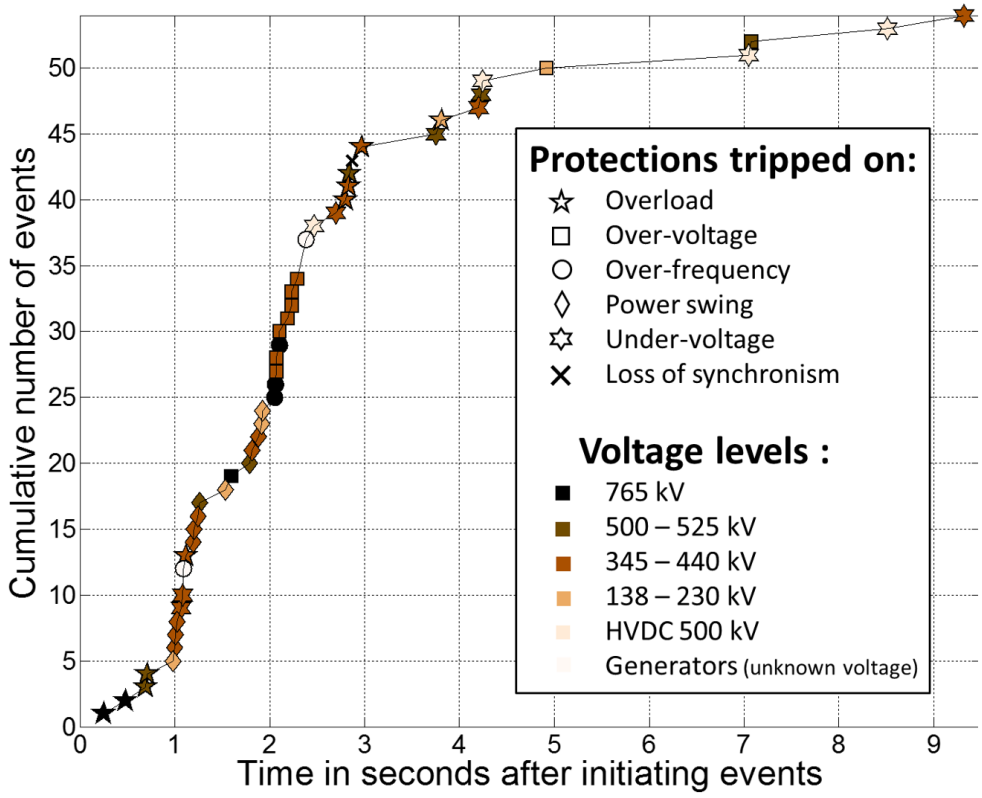

Figure 3.5: Cumulative number of elements disconnected during the first ten seconds (i.e. after the initiating event) of the Braz09 blackout. The plot symbols indicate the reason of the disconnection and the voltage level of the element.

graphically the evolution of the cascade of events of Braz09, plotting when the protections were triggered as well as the reasons for which they were triggered and their voltage level. We can observe in Figure 3.5 how the disconnection of 3 parallel 765 kV loaded lines, which were hit by quasi-simultaneous short-circuits, started a very fast and violent cascade due to the large transfer of power that followed. The consequences of such large transfer of power made protections trip not only on overload but also on over-frequency, under and over-voltage.

At other times, large transfers of power are due to the contingencies on the transmission lines that connect highly dependent regions. For example in Turk15, the transmission line corridor between the Eastern and the Western regions had some lines out of service, and the power flow between these two neighbouring regions was important because of the dependencies on supply. These conditions increased the stress on the remaining interconnection lines and after the initiating event, a very fast cascade of overload started immediately.

Forced outages of generating units created a dependency between the North and its neighbouring regions prior to India12 blackout. In addition, natural reasons created outages on interconnection lines which increased the loading of the lines to the North region and contributed to a fast cascade.

Separation of highly dependent regions

Although separation schemes are meant to mitigate the propagation of the instability by islanding healthy regions, they can also end up provoking the fast collapse of the system when regions are highly dependent on each other on supply or demand. In other words, it is highly likely that unbalanced regions collapse quickly after the separation.

Thus, in Turk15, the deficit (21 %) and excess (42 %) of production made the Western and Eastern systems collapse after their separation, which was a point of no return for the cascade. In Austr16, the South Australia region was importing 32 % of its consumption and relied for almost half on wind farms. As a result of the voltage disturbances that followed the initiating events, the wind farms reduced by two their production and thus increased the imports of the regions by 23 %. The main tie lines automatic protections of loss of synchronism tripped because of this disturbance, which quickly led to a frequency collapse of the region. In Braz11, the Northeast region was importing 36 % of its power demand and after the islanding of the region, the system ended up collapsing. In India12, the fast cascade saturated the interconnection lines connected to the North region leading to under-frequency conditions. The other regions faced an over-frequency that disconnected the remaining generators. The same situation happened in Chile11, where the North Central region was facing under-frequency and the Southern region an over-frequency after separation. Even for the two only blackouts with a steady-state progression, i.e. Indo05 and Usa11, the separation of the system indeed initiated the fast cascades.

We clearly highlight that reaching separation schemes of regions that are significantly dependent on each other often leads to a very fast and unstoppable collapse of the system. The sharp change in power production or consumption caused by the separation is too fast and too large to be handled by the defence plans.
These conditions must then be identified depending on the importance of a connection for the stability of each region as well as the mechanisms that respond to the system disturbances. Criticality analysis of these power exchanges can be carried out to help designing countermeasures that should mitigate this risk. As an example, the primary reserves or even the defence plan, could then be adapted to these special conditions. This is why the simulations in Chapter 4 focus on the separation of two regions and study the ability to model this issue as well as the impact on the power schedule.

Malfunctioning of power monitoring equipment

Monitoring systems providing wrong information (or even failing), either prior or during the cascade of events, can dramatically impact the management of the contingencies (i.e. power system operators are left unaware of the real loading situation and their actions or inaction can worsen the cascades).
In India12, respectively 25 % and 50 % of the Supervisory Control And Data Acquisition (SCADA) systems data was unavailable prior and after the initiating events. In

addition, a 400 kV line monitored value was frozen 30 % lower than reality during the event and the line ended up overloaded. In Usa11, the SCADA system of an important transformer suffered from accuracy issues which prevented operators to have a full awareness of the ongoing overload.

3.5.3 *Cascade conclusion*

The duration of the cascade of events, especially the steady-state progression, is a critical parameter as it is the time that operators have to attempt to stop the cascade. As suggested in [LBZR06], mitigation actions should be taken before the fast cascade starts, i.e. before the system becomes uncontrollable with human time-scale actions. However, among the blackouts analysed in this chapter, only two entered the steady-state phase and for a short period of time. The other blackouts directly started with the fast cascade, just after the initiating event happened, and thus they did not allow operators to take actions. The speed of the blackouts analysed here differs from those of previous studies [LBZR06, IEE07, VBC+12]. Nevertheless, the major cause of this speed was already mentioned in previous reports, e.g. [IEE07]: power systems are operating closer to stability limits, under growing stress and power transfers over long distances are increasing.

The speed and the type of the cascades of events are highly related to the pre-conditions and the initiating events. We note that dependencies between regions that are likely to separate the system under emergency, may in turn trigger a very fast cascade due to the deficit/excess of power supply. We identified two main reasons for these transfers to be large (i.e. important enough to create a fast cascade of overloads), namely initiating events that affect key system components or transmission lines that connect regions highly dependent on supply.

Finally, to mitigate the risk of power blackouts, it is crucial to limit the stress on transmission systems and operate the systems further from the stability limits. This should reduce the number of cascades, but more importantly should slow down the propagation of the disturbance in case of a beginning of blackout, and thus, provide more time to the operators to take counteractions.

3.6 CONCLUSIONS

This chapter provided a study of 9 blackouts that occurred between 2005 and 2016. The main common features of those blackouts were analysed and discussed and this conclusion aims at summarizing what elements should be integrated in priority into the algorithms developed in the next chapters.

First to integrate the possibility of unpredicted outages, it is common practice to list the credible contingencies or the vulnerable elements of the system to make it robust to their loss. Hence, the choice of those lists is critical for the security of the system

and if not well determined, the loss of one of the elements not taken into account can lead to the system collapse. Thus, it is important to consider a thorough list of vulnerable devices.

Then, unlike most blackouts of the twentieth century, the analysed blackouts did not happen under peak demand, but rather when the interconnection lines between regions were highly loaded. In other words, blackouts did not happen during system peak loading but rather when the loading of inter region transmission devices was close to the protection devices security limits. Moreover, the interactions between neighbouring systems, especially in term of security, should be integrated because, as illustrated in Turk15 blackout, the security of each individual system does not imply the security of the interconnected system. This highlights the crucial need to consider the system as a whole interconnected system, despite that different entities operate the regions of the system. The impact of major credible contingencies in one region should be taken into account by the neighbouring regions to enforce a global security of the interconnected system.

We also emphasise the role of dependencies in supply that is linked to the loading of interconnection lines, in the cascade progression and speed. The impact of triggering the separation scheme should be assessed in order to evaluate and mitigate the risk of fast collapse of the potentially separated regions.

Lastly, due to the proximity of the operational states of power systems to the stability limits, the studied blackouts are very fast in progression. The speed prevents, first, the operators to act, and second, the automatic controls to play their roles. In this context, avoiding to enter the fast cascades is a key challenge to prevent blackouts from happening.

In conclusion, the study of those 9 recent blackouts justifies that this thesis focuses on prevention rather than corrective actions (Requirements 4 and 5), and it also justifies the focus on interconnected systems and on their coordination (Requirement 6) that comes with privacy and autonomy challenges (Requirement 7). The coordination of the security also comes with large number of contingencies considered as well as their impact on the whole interconnected system. The algorithms to develop in order to mitigate the risk of blackouts should thus be highly scalable (Requirement 8). This analysis also guides some aspects of the simulations conducted in the next chapter, as the separation scheme can be a credible contingency in some context.

4

DISTRIBUTED SECURITY CONSTRAINED OPTIMAL POWER FLOW WITH PRIMARY FREQUENCY CONTROL

The previous chapter identified the separation schemes as a crucial factor leading to major incidents in nowadays power systems. Certainly, in such a separation case, the balance between production and consumption is not ensured anymore and the primary frequency control is the first action that tries to retrieve this power balance. Moreover, as also highlighted in the previous chapter, recent blackouts directly triggered the high speed cascades and thus, prevented operators or the automatic controls to apply countermeasures, which emphasises the crucial need for more prevention of those incidents.

To prevent power grids from reaching these high speed cascades, this chapter presents a fully distributed method to solve the preventive[1] DC security constrained power flow (DC-SCOPF) that takes into account the automatic primary frequency response of generators after an incident. The proposed methods extends the distributed framework for solving the preventive SCOPF problem developed in [CKC+14]. As mentioned in Section 2.4.3, this work lacks empirical results and, more importantly, it does not take into account the automatic reaction of generators, the so-called Primary Frequency Control (PFC). In fact, the contingencies considered are solely restricted to line outages that do not disturb the power balance of the system. The novelty of this chapter comes from the integration of this PFC that allows considering the loss of power generation units as contingency. By doing so, we are able to model contingency states involving a modification of the active power balance. More specifically, the main contributions of this chapter are:

- *We extend the DC-SCOPF formulation from [CKC+14] by: 1) introducing a new variable representing the steady state relative frequency deviation, computed by distributed consensus and used to coordinate the power reallocation process after an incident; 2) enhancing the local problem of each generator to consider how it adjusts its production after a contingency following its primary frequency regulation.*

1 As discussed in Section 2.2.2, SCOPF problems are called preventive when, after an incident happens in a scenario, the reaction of the system follows the automatic and fast controls, and are called corrective when optimised reaction of controllable devices of the system is allowed after the incident happened.

- *We solve this problem in a distributed fashion via ADMM, showing not only how the resulting algorithm can find a solution robust to the loss of generators, but also how it can model area separation as a contingency state (the contingency lead to the separation of the system into two or more sub-systems). In particular, our algorithm is able to find a solution that, in case of such contingency, will lead to a stable operating point in each of the disconnected areas.*

- *We evaluate our approach on several standard IEEE test systems to demonstrate its effectiveness and its capacity to deal with the disconnection of areas in interconnected systems.*

The remainder of this chapter is organised as follows: section 4.1 details the modelling of the primary frequency control mentioned in Section 2.1.3. Section 4.2 introduces the decentralised formulation of the SCOPF problem and provides a derivation of the sub-problems solved by agents. Simulation results on several standard IEEE test systems are presented in Section 4.3, and prove the ability of the proposed method to consider separations of the system areas. And finally, Section 4.4 summarises the contributions of this chapter.

4.1 PRIMARY FREQUENCY CONTROL MODELLING

The primary frequency control (PFC) aims at regulating the frequency of the power system by adapting the generation [ES13], as explained in Section 2.1.3. In this section, the local steady-state equations of the PFC are first presented, before providing the global variables and calculations of the frequency deviation across the overall system to make the link with the equation introduced in Section 2.1.3.

Since this section focuses on preventive SCOPF, the change of power schedule of the generators, following a contingency $(s) \in [1, \mathcal{L}]$, is only due to the primary frequency response of the generators (of the set G):

$$\forall g \in G, \quad p_g^{(s)} = p_g^{(0)} + \Delta p_g^{(s)} \tag{4.1}$$

where $p_g^{(s)}$ is the generation after PFC due to contingency (s) of generator g, $p_g^{(0)}$ is the generation in the base case (0), i.e. prior any contingency, and $\Delta p_g^{(s)}$ is the primary frequency response of the generator g due to contingency (s).

The primary frequency response in steady-state follows the following four principles:

Active power balance

After the primary frequency response, the system should reach a new steady-state and thus the generation should be equal to the consumption (i.e. the loads of the set F_l). The active power imbalance due to a contingency $(s) \in [1, \mathcal{L}]$ is then completely

compensated by the active production of all generation units taking part in the primary frequency control:

$$\forall(s) \in [1, \mathcal{L}], \quad \sum_{f_l \in \{F_l | f_l \notin D^{(s)}\}} p_{f_l}^{(s)} + \sum_{g \in \{G | g \notin D^{(s)}\}} p_g^{(s)} = 0 \tag{4.2}$$

In other words, the power balance of the system should be kept after the primary frequency response of generators despite loads or generators may be disconnected.

Primary frequency control coefficient of generators

The primary frequency response of a generator $g \in G$ to a disturbance of the power balance of the system is determined by its coefficient K_g. Formally:

$$\Delta p_g^{(s)} = K_g \cdot \alpha^{(s)} \tag{4.3}$$

where in turn K_g is defined as the ratio of the nominal active power and the speed droop of the generator (both constants and depending on the generators characteristics) and the relative steady-state frequency deviation $\alpha^{(s)}$ for contingency (s), is defined as:

$$\alpha^{(s)} = -\frac{\Delta f}{f_0} = \frac{\Delta P}{\sum\limits_{g \notin D^{(s)}} K_g} \tag{4.4}$$

where f_0 is the base frequency[2], Δf is the frequency deviation after PFC and ΔP is the power to supply in order to compensate the power deviation from schedule.

Although the relative frequency deviation is the same across the whole power system (i.e. it is a global value), notice that, in the case of contingencies leading to area separation, we will have a different frequency deviation for each separated area.

Generators production and ramp limits

The active production of each generator has to remain within its production limits

$$P^{min} \leqslant p_g^{(s)} \leqslant P^{max} \tag{4.5}$$

The primary response of each generator does not exceed the ramp constraints, $\Delta p_g^{(s)}$ is limited because generators cannot change their production at any speed. In a time duration of $\Delta t = 1$ min, maximum ramp up is R^{max} and the maximum ramp down is $-R^{min}$.

$$-R^{min} \cdot \Delta t \leqslant \Delta p_g^{(s)} \leqslant R^{max} \cdot \Delta t \tag{4.6}$$

2 Regulated frequency of the grid (50Hz or 60Hz depending of the country)

Non-allocated power

Once a generator reaches its limits (ramp or production), the other generators have to compensate the non-allocated power according to their own speed droop. Thus, when a generator does not change as expected because it reached some constraints, this is reflected in the frequency deviation $\Delta f^{(s)}$ and in the contribution of the other generators.

4.2 DISTRIBUTED (N-1) DC-SCOPF WITH PFC

In this section, we present our distributed algorithm to the DC-SCOPF problem. We extend the distributed (N-1) DC-SCOPF model reviewed in Section 2.5 in order to be able to take into account the automatic response of generators as part of its participation to the PFC. With this aim, we need to introduce a new variable representing the (steady-state) relative frequency deviation that will be used to coordinate the power allocation process after a contingency takes place. Since the frequency deviation for a contingency scenario is a global variable of the power system, the SCOPF problem with PFC needs to be carefully reformulated into a suitable form so that it can be solved by ADMM in a distributed manner.

To achieve that, we extend the SCOPF model in Section 2.5 by creating for each contingency scenario (s) a duplicated relative frequency deviation variable ($\alpha^{(s)}$) at each terminal. As a result, the objective function of the SCOPF problem is reformulated to include the relative frequency variables as:

$$\begin{aligned} \min_{p,\theta,\alpha \in \mathbb{R}^{|\mathcal{T}|\times(\mathcal{L}+1)}} & \sum_{d\in D} f_d(p_d,\theta_d,\alpha_d) + \sum_{n\in N} f_n(\dot{p}_n,\dot{\theta}_n,\dot{\alpha}_n) \\ \text{subject to : } & \forall d \in D : p_d,\theta_d,\alpha_d \in C_d, \\ & \forall n \in N : \ \dot{p}_n,\dot{\theta}_n,\dot{\alpha}_n \in C_n, \\ & p = \dot{p}, \ \theta = \dot{\theta}, \ \alpha = \dot{\alpha} \end{aligned} \tag{4.7}$$

Thus, by duplicating relative frequency deviation variables, the problem decomposes into sub-problems as in the original model. The correct relative frequency deviation is obtained after the set of duplicated (local) variables related to the same contingency iteratively reaches consensus via ADMM. There is no need to calculate the frequency response characteristic term $\sum_{g\notin D^{(s)}} K_g$. Moreover, the nets and devices sub-problems are modified to take into account the PFC as follows:

- *Nets:* in addition to the Kirchhoff's constraints, the net model is extended to also verify locally that, in each scenario, all the terminals have the same relative frequency deviation.

- *Devices:*

- *Transmission lines*[3]*:* the model is extended to restrict that local relative frequency deviations on both sides of the line are equal for each scenario.
- *Generators:* the model is reformulated so that its production on the different scenarios is proportional to the relative frequency deviation and to the generator coefficient, when the generator is not the device undergoing an outage. Since, as we will see, this formulation leads to a non-convex device-minimisation problem, we propose an approximation to return to convexity.

The following sections detail this reformulation of nets (Section 4.2.1) and devices (Section 4.2.2) local problems.

4.2.1 *Formulation of nets local sub-problem*

In addition to the Kirchhoff's constraints, to consider primary frequency control, each net constrains that, in each scenario, all the terminals have the same relative frequency deviation:

$$\dot{\alpha}_t^{(s)} = \dot{\alpha}_{t'}^{(s)}, \ \ \forall t, t' \in n, t \neq t', \ \forall (s) \in [1, \mathcal{L}] \tag{4.8}$$

For these constraints on the relative frequency deviation, the ADMM *net-minimisation* step (Eq. 2.13) can be solved analytically (as a projection on a hyperplane, as in [KCLB14]) as follows:

$$\dot{\alpha}_t^{k+1(s)} = \frac{1}{|n|} \sum_{t \in n} \alpha_t^{k+1(s)} \tag{4.9}$$

For the power and phase angle variables, since they are constrained as defined in Eq. 2.15 and 2.16, they are updated by the same analytical solutions as in Eq. 2.17 and 2.18.

Moreover, in addition to the *scaled dual variables* updates related to the active power and voltage phase angle (Eq. 2.14a-2.14b), each net also updates the dual variables related to the relative frequency deviation variables:

$$\omega_n^{k+1} = \omega_n^k + (\alpha_n^{k+1} - \dot{\alpha}_n^{k+1}), \ \ \forall n \in N \tag{4.10}$$

4.2.2 *Formulation of devices local sub-problems*

Each device component is responsible for defining its local cost function and constraints as well as for implementing the *device-minimisation* step. Formally, $\forall d \in D$:

$$\begin{aligned} (p_d^{k+1(s)}, \theta_d^{k+1(s)}, \alpha_d^{k+1(s)}) = \underset{p_d, \theta_d, \alpha_d \in C_d}{\arg\min} \ & (f_d(p_d, \theta_d, \alpha_d) + \tfrac{\rho}{2}(||p_d - \dot{p}_d^k + u_d^k||_2^2 \\ & + ||\theta_d - \dot{\theta}_d^k + v_d^k||_2^2 + ||\alpha_d - \dot{\alpha}_d^k + w_d^k||_2^2)), \end{aligned} \tag{4.11}$$

3 We include in the transmission lines model the transformers that can be modelled similarly to lines when considering the DC power flow equations.

The next subsections detail these local sub-problems and local optimisations steps for the three types of devices considered in this paper: generators (G), transmission lines (L) and loads (F_l).

Generator devices

A generator is a single terminal device which produces power with a local cost for operating the generator at a given power level and some operating constraints that limit this power output. Following [KCLB14, CKC+14] we consider that a generator g encodes its production cost by means of a quadratic cost function:

$$f_g(p_g^{(0)}) = \beta \cdot \left(p_g^{(0)}\right)^2 + \gamma \cdot p_g^{(0)} \tag{4.12}$$

where $\beta,\ \gamma > 0$ are respectively the quadratic and linear cost coefficients. It is observed here that, as it is common in SCOPF problems, the cost of operation of the generation only depends on its power generation in the base case scenario (i.e. contingencies are not expected to happen in a regular basis so the cost of generation to deal with a contingency is usually neglected).

Also, in the base case, the power output of the generator is bounded by its production limits:

$$P_g^{min} \leqslant p_g^{(0)} \leqslant P_g^{max} \tag{4.13}$$

Then, for contingency cases implying the outage of the generator ($g \in D^{(s)}$), the power output of the generator g should be zero:

$$p_g^{(s)} = 0, \ \ \forall (s) \in \{[1, \mathcal{L}] | g \in D^{(s)}\} \tag{4.14}$$

Finally, for the rest of contingency cases (i.e. in which the generator is operative), we need to extend the set of constraints to take into account the generator automatic frequency response. Hence, unlike [CKC+14], the power output of the generator for these contingencies will not be the same as the output in the base case scenario but, instead, it will follow the generator automatic adaptation of the generation. This adaptation is proportional to the generator coefficient and bounded by its ramp limits, $\forall (s) \in \{[1, \mathcal{L}] | g \notin D^{(s)}\}$:

$$\Delta p_g^{(s)} = \begin{cases} -R_g^{min} \cdot \Delta t & \text{if } K_g \cdot \alpha_g^{(s)} \leqslant -R_g^{min} \cdot \Delta t \\ K_g \cdot \alpha_g^{(s)} & \text{if } -R_g^{min} \cdot \Delta t \leqslant K_g \cdot \alpha_g^{(s)} \leqslant R_g^{max} \cdot \Delta t \\ R_g^{max} \cdot \Delta t & \text{if } K_g \cdot \alpha_g^{(s)} \geqslant R_g^{max} \cdot \Delta t \end{cases} \tag{4.15}$$

Moreover, in all scenarios, the power output of the generator has to remain within its production limits, $\forall (s) \in \{[1, \mathcal{L}] | g \notin D^{(s)}\}$:

$$p_g^{(s)} = \begin{cases} P_g^{min} & \text{if } p_g^{(0)} + \Delta p_g^{(s)} \leqslant P_g^{min} \\ p_g^{(0)} + \Delta p_g^{(s)} & \text{if } P_g^{min} \leqslant p_g^{(0)} + \Delta p_g^{(s)} \leqslant P_g^{max} \\ P_g^{max} & \text{if } p_g^{(0)} + \Delta p_g^{(s)} \geqslant P_g^{max} \end{cases} \tag{4.16}$$

Unfortunately, the step functions in Eq. 4.15 and Eq. 4.16 lead to a non-convex device-minimisation problem. To overcome this, we fix the primary frequency response of each generator as $p_g^{(s)} = p_g^{(0)} + K_g \cdot \alpha_g^{(s)}$ and we replace the step functions by two linear constraints that directly bound the domain of variables $\alpha_g^{(s)}$ and $p_g^{(s)}$. In particular, Eq. 4.15 is replaced by:

$$\frac{-R_g^{min} \cdot \Delta t}{K_g} \leqslant \alpha_g^{(s)} \leqslant \frac{R_g^{max} \cdot \Delta t}{K_g} \tag{4.17}$$

and Eq. 4.16 by:

$$P_g^{min} \leqslant p_g^{(s)} \leqslant P_g^{max} \tag{4.18}$$

Such modifications allow us to keep the device-minimisation problem for generators convex and thus, we can rely on off-the-shelf optimisation tools to solve it efficiently. In particular, we solve the unconstrained problem and then, project the solution on the intersection of the constraints defined by Eq. 4.17 and Eq. 4.18, using Dykstra's alternating projection algorithm [BD86].

Notice that these two constraints are more restrictive than the original ones (i.e. they reduce the feasible region of the problem). In more detail, with the original constraints, it may be the case that the automatic frequency response of a generator reaches either its ramp or power outputs limits and that the other generators have, in turn, to compensate the non-allocated power according to their coefficient. Instead, the linear constraints do not consider this case and the model is restricted to find base case configurations that are capable to deal with any single-element contingency and in which the automatic response of generators do not reach their local limits (i.e. no compensation will be needed from any generator further than the planned one). We acknowledge that this more restrictive model can end up finding less economically efficient base case solutions. However, we also highlight that in such cases, the relative frequency deviation will also be lower and hence, the solutions found under this model can be also seen as more secure.

Transmission line devices

A (transmission) line is a two-terminal device used to transfer power from one net (i.e. bus) to another. Here, we use a linear DC power flow model for lines, often used in the literature to get rid of the non-convexity of the physics of AC circuits. Under this model, the power flow equations ignore real power losses as well as reactive power, and voltage magnitude is assumed to be equal to 1 pu. For that reason and from now on, we use the line models to model the transformers of the system and we will not refer to transformers as it is included in transmission lines in our work. A line l has a zero cost function ($f_l(\cdot) = 0$) but the power flows and voltage phase angles on both sides of the line are constrained. In particular, the power flow through the line depends on: (i) the power schedules (p_{l_1} and p_{l_2}) and voltage phase angles (θ_{l_1} and θ_{l_2}) at both

sides of the line (i.e. indexes 1 and 2 refer to the two different sides of the line l); and on the susceptance of the line (b_l).

In particular, for contingency cases in which the line $l \in L$ is not involved in the outage (i.e. $\forall(s) \in \{[1,\mathcal{L}]|l \notin D^{(s)}\}$), the power and phase schedules should satisfy the relations:

$$p_{l_1}^{(s)} = -p_{l_2}^{(s)} = b_l \cdot (\theta_{l_2}^{(s)} - \theta_{l_1}^{(s)}), \tag{4.19}$$

But, if the contingency case implies the outage of the line $l \in L$ (i.e. $\forall(s) \in \{[1,\mathcal{L}]|l \notin D^{(s)}\}$), the power transmitted through the line should be zero:

$$p_{l_1}^{(s)} = p_{l_2}^{(s)} = 0, \tag{4.20}$$

Moreover, in each scenario, the power going through the line has to be lower than its maximum capacity (i.e. long-term capacity in the base case and short-term capacity in a contingency case):

$$-P_l^{max} \leqslant p_{l_1}^{(s)} \leqslant P_l^{max}, \ \ \forall(s) \in [0,\mathcal{L}] \tag{4.21}$$

Finally, the line also constrains that the relative frequency deviation on both sides of the line are equal:

$$\alpha_{l_1}^{(s)} = \alpha_{l_2}^{(s)}, \ \ \forall(s) \in \{[1,\mathcal{L}]|l \notin D^{(s)}\} \tag{4.22}$$

Notice that the problem of transmission lines is separable over the set of scenarios (i.e. there is no constraint linking the variables of different scenarios) and, hence, line sub-problems can be solved independently for each scenario. Similarly, the terms depending on the relative frequency deviation variables for a given scenario are independent from other types of variables. Thus, given a scenario $(s) \in \{[0,\mathcal{L}]|l \notin D^{(s)}\}$ the device-minimisation step of Eq. 4.11 can be split and the update of the relative frequency deviation variables reduces to:

$$\begin{aligned}(\alpha_{l_1}^{k+1(s)}, \alpha_{l_2}^{k+1(s)}) = &\underset{\alpha_{l_1},\alpha_{l_2}}{\arg\min}(\frac{\rho}{2}||\alpha_{l_1} - \dot{\alpha}_{l_1}^{k(s)} + w_{l_1}^{k(s)}||_2^2 \\ &+ \frac{\rho}{2}||\alpha_{l_2} - \dot{\alpha}_{l_2}^{k(s)} + w_{l_2}^{k(s)}||_2^2) \\ &\text{subject to : } \alpha_{l_1}^{(s)} = \alpha_{l_2}^{(s)}\end{aligned} \tag{4.23}$$

Eq. 4.23 results in a projection on a hyperplane and can be solved analytically (see [PB+14]) as follows:

$$\alpha_{l_1}^{k+1(s)} = \alpha_{l_2}^{k+1(s)} = \frac{\dot{\alpha}_{l_1}^{k(s)} - w_{l_1}^{k(s)} + \dot{\alpha}_{l_2}^{k(s)} - w_{l_2}^{k(s)}}{2} \tag{4.24}$$

The active power schedules and voltage phase angles are coupled in each contingency scenario, when, on the contrary, the variables between the different scenarios are independent. Thus, given a scenario $(s) \in \{[0,\mathcal{L}]|l \notin D^{(s)}\}$ the transmission line

sub-problem to update the active power schedules and voltage phase angles variables reduces to:

$$\begin{aligned}(p_{l_1}^{k+1(s)}, \theta_{l_1}^{k+1(s)}, p_{l_2}^{k+1(s)}, \theta_{l_2}^{k+1(s)}) = \underset{p_{l_1}, \theta_{l_1}, p_{l_2}, \theta_{l_2}}{\arg\min} \; (&\frac{\rho}{2}||p_{l_1} - \dot{p}_{l_1}^{k(s)} + u_{l_1}^{k(s)}||_2^2 \\ &+\frac{\rho}{2}||p_{l_2} - \dot{p}_{l_2}^{k(s)} + u_{l_2}^{k(s)}||_2^2 + \frac{\rho}{2}||\theta_{l_1} - \dot{\theta}_{l_1}^{k(s)} + v_{l_1}^{k(s)}||_2^2 \\ &+ \frac{\rho}{2}||\theta_{l_2} - \dot{\theta}_{l_2}^{k(s)} + v_{l_2}^{k(s)}||_2^2) \\ \text{subject to : } p_{l_1} = b_l \cdot (\theta_{l_2} - \theta_{l_1}), \;\; &p_{l_1} = -p_{l_2}, \\ -P_l^{max} \leqslant p_{l_1} &\leqslant P_l^{max}\end{aligned} \tag{4.25}$$

We solve the problem in Eq. 4.25 while ignoring the inequality constraints that model the line capacity, and by using a matrix formulation. We introduce the following vectors and matrix:
$X_{l_i}^{(s)} = \begin{bmatrix} p_{l_i}^{(s)} \\ \theta_{l_i}^{(s)} \end{bmatrix}$, $ZU_{l_i}^{k(s)} = \begin{bmatrix} \dot{p}_{l_i}^{k(s)} - u_{l_i}^{k(s)} \\ \dot{\theta}_{l_i}^{k(s)} - v_{l_i}^{k(s)} \end{bmatrix}$, and $B_l = \begin{bmatrix} -1 & 0 \\ \frac{1}{b_l} & 1 \end{bmatrix}$. With i being equal either to 1 or 2 depending on the side l_1 or l_2 of the line. The solution is then the vector:

$$X_{l_1}^{k+1(s)} = (I + B_l^T \cdot B_l)^{-1} \left(ZU_{l_1}^{k(s)} + B_l^T \cdot ZU_{l_2}^{k(s)} \right) \tag{4.26}$$

When the capacity limit of the line is reached, the optimal active power is equal to the limit reached noted p_l^{lim} and the voltage phase angles are determined using Eq. 4.19 and the preferred value from each bus. Formally:
$\theta_{l_1} = \frac{1}{2} \cdot \left(\dot{\theta}_{l_1}^{k(s)} - v_{l_1}^{k(s)} + \dot{\theta}_{l_1}^{k(s)} - v_{l_1}^{k(s)} + \frac{p_l^{lim}}{b_l} \right)$,
$\theta_{l_2} = \frac{p_l^{lim}}{b_l} + \theta_{l_1}$. The line sub-problems are eventually solved analytically.

Fixed loads

A fixed load $f_l \in F_l$ is a single terminal device with zero cost function ($f_{fl}(\cdot) = 0$) which is simply described by a desired consumption $p_{f_l} \in \mathbb{R}$. In this chapter, we assume that only generation will adapt in front of a contingency (i.e. loads will remain fixed) and hence, the solution for a fixed load remains constant across all iterations of the algorithm as $\forall (s) \in \{[0, \mathcal{L}] | f_l \notin D^{(s)}\}, p_{fl}^{(s)} = p_{f_l}$.

4.3 SIMULATION RESULTS

This section presents simulation results on three circuits: the IEEE 14-bus, the large-scale IEEE RTS 96 3-area system and a two-area system (derived from the duplication of the IEEE 9-bus). For each circuit, we compute the N-1 SCOPF with PFC solution with the new ADMM-approach proposed in the previous sections, as well as the OPF solution using the ADMM-approach from [KCLB14] for assessing the cost

of security.[4] The distributed ADMM algorithm is implemented, in both cases, as a multi-agent system using the Java Agent Development[5] (JADE) platform [BBCP05], where each agent solves its corresponding sub-problem in parallel. The two ADMM parameters (the scaling parameter and the absolute tolerance) are set to the values given in Table 4.1. The base power of the systems is 100 MVA (used for per unit calculations), so for a tolerance of 10^{-4}, it means that at most the power balance needs to be respected with a tolerance of maximum 10 kW.

	IEEE 14-bus	IEEE RTS 96 3-area	Two area system
ρ	1.0	0.1	1.0
ϵ_{abs}	10^{-4}	10^{-3}	10^{-4}

Table 4.1: ADMM parameters values.

4.3.1 *IEEE 14-bus*

In this subsection, the proposed SCOPF with PFC is tested on the IEEE-14-bus test system with the transmission data from the Power System Test Case Archive [6]. The system, represented in Figure 4.1, is composed of 11 loads, 20 lines and 5 generators. We completed the model by setting the line capacity limits to 110 MW for both, short-term and long-term settings. Table 4.2 details the parameters used for the different generators. Notice that each generator is modelled with a ramp up limit of 35 MW/min. Table 4.2 also specifies the generator coefficient K_g, computed as the ratio of the nominal active power of the generator, set to the generator maximum power output (P^{max}), and the speed droop, set to 5% for all generators.
Solving the OPF problem takes 1093 iterations, whereas the SCOPF problem taking into account N-1 failures (of all lines and generators) is solved in 3582 iterations. Regarding the cost of security, the N-1 security constraints increases the cost of generation by 6.2% (i.e. from 7835 $ for the OPF solution to 8359 $ for the N-1 solution).

The largest frequency deviation is reached in the contingency case that models the disconnection of generator g_1, which, as stated in Table 4.2, is the cheapest and largest generator of the system. Table 4.3 shows that in this case, the frequency deviation of the system corresponds to 1.25 % deviation, i.e. 625 mHz for a 50 Hz system. We propose to compare the frequency deviation calculated from Eq. 4.4 with the data obtained from the simulation in this scenario, and to detail the constraints involved in this case. It illustrates the ability of the method to enforce some global constraints, in a fully distributed manner, and the impact of the assumption taken in the generators model.

4 The cost of security is defined as the percentage cost increase between the solution of the OPF problem and that of the SCOPF.

5 jade.tilab.com

6 https://www2.ee.washington.edu/research/pstca/

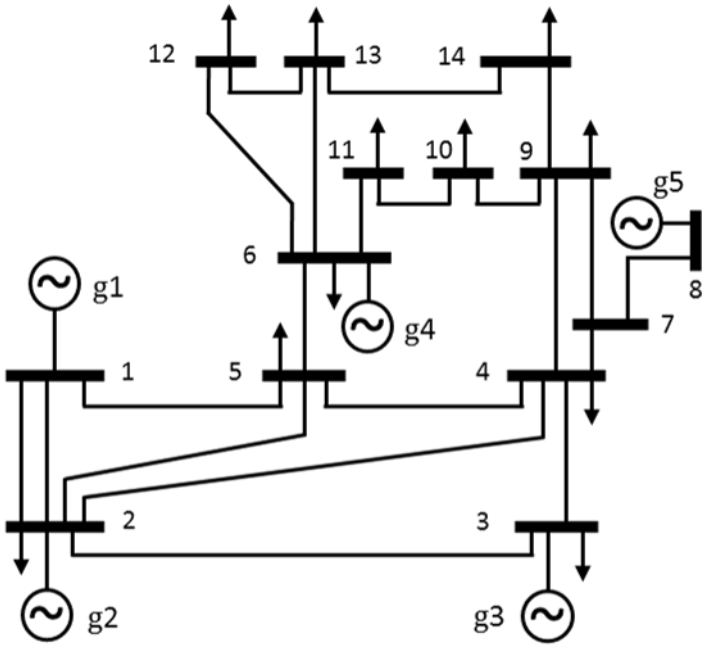

Figure 4.1: IEEE 14-bus test system.

Gen.	$-P^{min}$ MW	$-P^{max}$ MW	R^{max} MW/min	β \$/MWh^2	$-\gamma$ \$/MWh	K_g MW/%
$g1$	332.4	0	35	0.043	20	6,65
$g2$	140	0	35	0.25	20	2,80
$g3$	100	0	35	0.01	40	2,00
$g4$	100	0	35	0.01	40	2,00
$g5$	100	0	35	0.01	40	2,00

Table 4.2: Generators parameters used in the IEEE 14-bus test system.

In the base case, generator g_1 supplies 110 MW (see Table 4.3), and so, in the scenario when this generator is outaged, we have : the $p_{g1}^{(0)} = \Delta p$. Then using the coefficients of generators from Table 4.2, we obtain:

$\alpha = -\frac{\Delta f}{f_0} = \frac{p_{g1}^{(0)}}{K_{g2}+K_{g3}+K_{g4}+K_{g5}} = 1.25\%$.

This value corresponds to the maximum frequency deviation of generator g_2, as defined by the constraint characterised by Eq. 4.17. Indeed, since g_2 has the largest coefficient K_g, when g_1 is disconnected and all generators have the same ramp capacity, g_2 is the limiting generator in term of relative frequency deviation of the system. The power supply of generator g_1 in the base case ($p_{g_1}^{(0)}$) is then constrained by Eq. 4.17, so that, its disconnection does not cause a relative frequency deviation greater than $\frac{R^{max}.\Delta t}{K_{g2}} = 1.25\%$. This explains why the active power schedule of g_1, in Table

		SCOPF contingency scenarios	
Variable	OPF	base case	g1
$\alpha^{(s)}$	–	–	1.25 %
p_{g1}	-168 MW	-110 MW	0 MW
p_{g2}	-43.3 MW	-41.5 MW	-76.5 MW
p_{g3}	-42.9 MW	-36.3 MW	-61.3 MW
p_{g4}	0 MW	-36.3 MW	-61.3 MW
p_{g5}	-4.7 MW	-35 MW	-60 MW

Table 4.3: Comparison of the results between OPF and N-1 SCOPF for the IEEE 14-bus test system.

	# of scenarios	# of iterations	Cost k$
OPF	0	7627	167.3
Lines contingencies	120	6778	167.3
Generators contingencies	96	3881	179.0
All lines and generators	216	4947	179.7

Table 4.4: Results on the IEEE RTS 96 3-area test system.

4.3, shall be decreased by 35 %, from 168 MW in the OPF results, to 110 MW with SCOPF model.

4.3.2 *Application to a large-scale system: IEEE RTS 96 3-area test system*

This subsection investigates the scalability of our algorithm by testing it on a larger system with a larger number of contingencies: the IEEE RTS 96 3-area test system [For99], depicted in Figure 4.2. The problem leads to 340 different sub-problems when counting the buses, lines, loads and generators, each managed by a different agent.

In the experiments, we considered three sets of contingencies: (1) all single-line contingencies (i.e. 120 scenarios); (2) all single-generator contingencies (i.e. 96 scenarios); and (3) all single-line and single-generator contingencies (i.e. 216 scenarios). These three sets of scenarios allow a comparison of the impact of the number of scenarios on the number of iterations the algorithm needs to converge.

Table 4.4 provides a summary of the number of contingencies considered in each test, the number of iterations needed, and the costs of operation. The cost of the OPF solution is 167 k$ when the cost of the N-1 SCOPF with PFC when considering all contingencies (lines and generators) is 179 k$ which makes a 7 % increase to guarantee the security of the system. Observe that the cost of security mainly comes from the contingencies on generators as when considering only lines failures, the solution

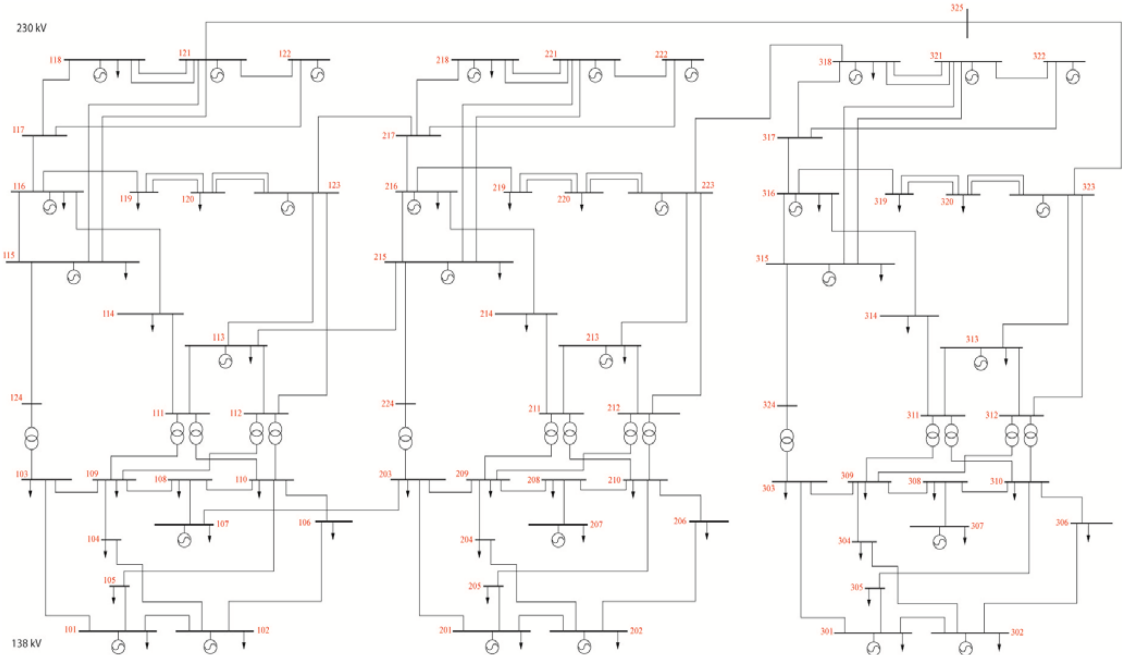

Figure 4.2: IEEE 3-area Reliability Test System.

of the SCOPF does not increase the cost of operation and so, does not modify the base case in comparison to the OPF results.

The largest relative steady-state frequency deviation is 0.18 % deviation that represents 90 mHz, and is obtained when any of the six generators producing the maximum output in the base case (385.5 MW) is disconnected.

Notice that the SCOPF solution needed 35% less iterations to converge compared to the OPF solution. A possible explanation is that by adding more constraints, the feasible space of solutions is reduced, and thus, it is easier to explore [Yok97]. Thus, as other works [LBD15] indicated, in the context of OPF that a larger circuit does not necessarily imply a worse convergence performance, here our results show, in the context of SCOPF that larger number of scenarios does not necessarily imply a worse convergence performance either.

4.3.3 *Separation of transmission system areas in a two-area system*

In this subsection, we investigate the capability of our model to consider the disconnection of two interconnected transmission areas. We built a two-area system by duplicating the IEEE 9-bus test system and adding an interconnection line (i.e. between bus 7 and bus 16), with a capacity of 250 MW, connecting both systems. The resulting two-area system is presented in Figure 4.3. We ensure power exchange between both areas by multiplying the quadratic and linear cost coefficient of generation by 10 in the second area (buses 10 to 18), see Table 4.5. All generators have the same ramp up

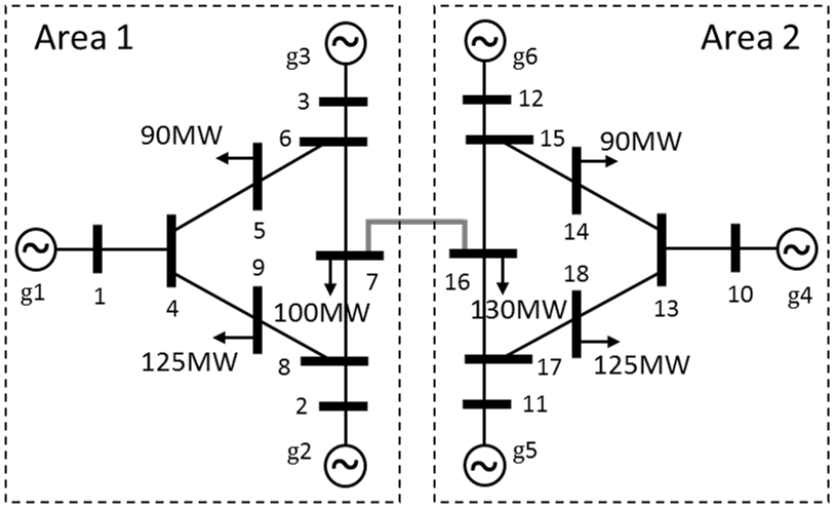

Figure 4.3: Two area test system derived from the duplication of the IEEE 9-bus test system.

Gen.	$-P^{min}$ MW	P^{max} MW	R^{max} MW/min	β \$/MWh^2	$-\gamma$ \$/MWh	$-K_g$ MW/%
$g1$	250	0	60	0.11	5	50
$g2$	300	0	60	0.085	1.2	60
$g3$	270	0	60	0.1225	1	54
$g4$	150	0	60	1.1	50	30
$g5$	200	0	60	1.0	12	40
$g6$	170	0	60	1.3	10	34

Table 4.5: Generator parameters in the IEEE 9-bus duplicated test system.

equal to 60 MW/min. The maximum power output of generators of area 2 is reduced by 100 MW and the load on bus 16 is increased by 30 MW to make the two areas consumptions different. We first solve the OPF problem on this system and, as expected, the power flow through the interconnection line 7-16 reaches its maximum, i.e. 250 MW, with a generation cost of 19921 \$. It took 1357 iterations to find the solution.

We then consider the SCOPF with only one contingency: the disconnection of line 7-16 which leads to the separation of the two areas. Note that under this contingency, the primary reserves of each area will need to recover from the lost interconnection line power transfer and hence, the maximum power transfer capacity of this line in SCOPF cannot exceed the reserve of any of the two areas. We can compute the primary reserves of each area based on the maximum value of α that is constrained as in Eq. 4.17. The most restrictive area is the second area with a maximum relative frequency deviation of $\alpha = 1.5\%$. This corresponds to the maximum primary reserves in this area, and to a maximum power transfer in the tie line of 156 MW, and to a relative frequency deviation for the first area of $\alpha = -0.95\%$. These values are the same than

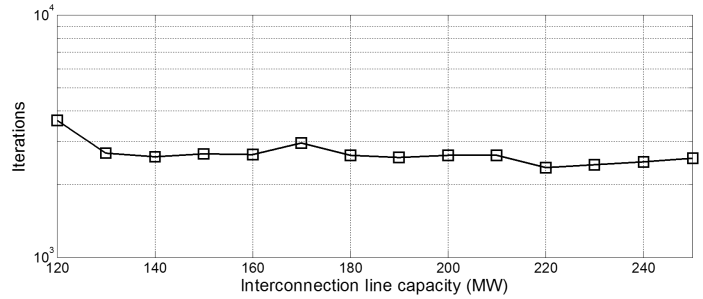

(a) Number of iterations to reach convergence.

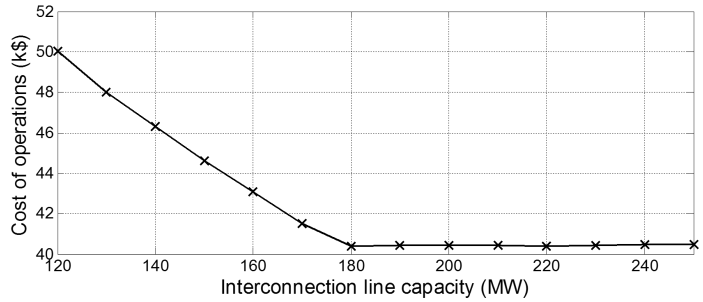

(b) Cost of operations.

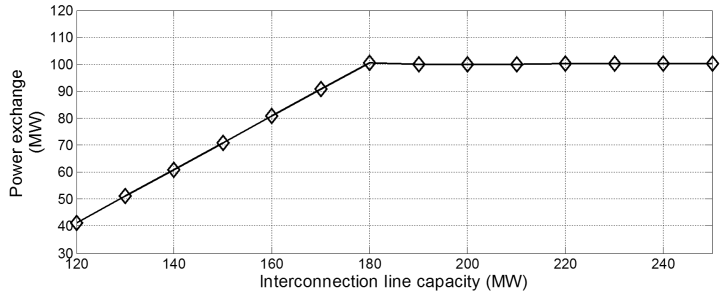

(c) Power exchanged in the tie line.

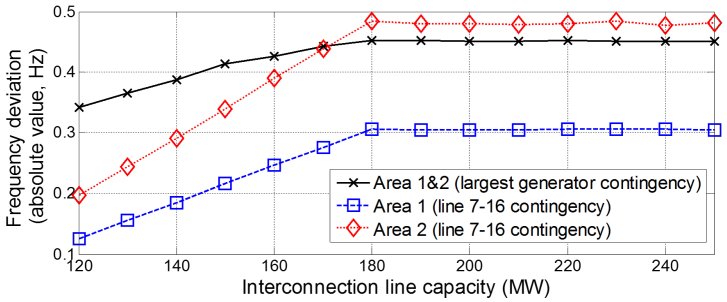

(d) Frequency deviation absolute value in each area in case of separation, and the largest frequency deviation when the areas are interconnected.

Figure 4.4: Duplicated IEEE 9-bus results.

the ones obtained by our algorithm. The SCOPF solution in this case has a 43.5 % increment in cost with respect to the OPF solution (i.e. to 28.6 k$) explained by the increment of the cost of generation parameters in the second area. The solution was found in 1913 iterations.

Most of the algorithms solving SCOPF problem do not consider the separation of a system into different areas, mainly because, to be able to consider those cases, further developments are needed, such as the detection of the separated areas. A major advantage of our approach is that there is neither need to detect the separation of the system, nor to adapt the algorithm to consider the separation scheme.

After this first test, we propose to consider all single-lines and single-generators contingencies, and to vary the capacity limit of line 7-16 to evaluate how having a less or more constrained problem affects the cost of the solution. Figure 4.4a depicts the number of iterations needed to find the N-1 solution by the SCOPF with PFC when varying the capacity of the interconnection line among the two areas. The proposed distributed algorithm is able to find the N-1 solution for all the scenarios and the security constraints do not impact significantly the number of iterations needed to reach the convergence criteria. This instantiates the good scalability of the algorithm, even when considering the separation of the system into different areas.

Figure 4.4b depicts the cost of operations when varying the capacity of the interconnection line among the two areas. Observe that as expected, when increasing the tie line capacity, the cost of operations decreases. However, after reaching a capacity of 180 MW, the cost does not vary, which means that the capacity of line 7-16 is no longer the limiting constraint. This hypothesis is confirmed in Figure 4.4c where we see that, indeed, reducing the capacity of line 7-16 decreases the power exchange and thus tends to distribute the power generation in the two areas. The maximum power exchange in these two regions is then 100 MW, regardless of the capacity of interconnection if it is greater than 180 MW. Finally, Figure 4.4d shows the largest frequency deviation that results from a generator disconnection, as well as, the absolute value of the relative frequency deviation that results from the disconnection of line 7-16, in each area. This way we are able to assess if the separation is more disturbing than the loss of any of the generators, and how it evolves when the transfer capacity of the interconnection line changes. For a capacity up to 170 MW, the worst deviation is caused by the loss of a generator, but when the capacity is greater, the event that would provoke the worst frequency deviation is the loss of the interconnection line. It results that the proposed algorithm is able to integrate the separation of an interconnected system, and to propose a schedule that allows a safe separation.

4.4 CONCLUSIONS

This chapter has presented the first totally distributed ADMM-based method to solve the preventive security constrained optimal power flow problem with primary frequency control. In more detail, we extended the distributed security constrained opti-

mal power flow framework from [CKC+14] to take into account the automatic primary frequency control of generators and we solved it in a fully distributed manner using an ADMM-based algorithm. The contribution of this chapter allows this distributed SCOPF model to find solutions that remain stable after the disconnection of a generator, a line or even after system area separation – all without requiring any form of central coordination. Moreover, the distributivity of the method naturally preserves the independence of individual region operators and achieves high scalability while fully taking advantage of their interconnection via a localized peer-to-peer communication paradigm. In summary, the method developed in this chapter integrates the coordination of interconnected regions, allow the separation of regions and allow the consideration of a large number of contingency scenarios in order to cope with the requirements of Chapters 1 and 3.

To evaluate the efficiency of our approach, we provided results first, on the IEEE 14-bus test system and on the IEEE 3-areas RTS 96 test system. Empirical results show how our method is able to find optimal SCOPF solutions for these circuits, defining for each contingency case the corresponding power flows and steady-state frequency deviation. They demonstrate not only the high scalability of our approach but also that considering a larger number of contingencies does not necessarily implies a worse convergence performance (solving the SCOPF problem in a large multi-area system, with 216 contingencies, takes 35% less iterations than solving the OPF problem). We finally tested the robustness of our distributed method to the most disturbing change in an interconnected power system that is the separation of areas of the system. The results have been obtained from a system inspired from the duplication of the IEEE 9-bus test system and eventually prove the great robustness of this method to any change of topology without even sharing the origin of the change.

5

DISTRIBUTED CHANCE-CONSTRAINED OPTIMAL POWER FLOW BASED ON PRIMARY FREQUENCY CONTROL

The ADMM-based algorithm presented in the previous chapter solves the security constrained optimal power flow problem (SCOPF) in a fully distributed manner dealing with outages on major devices of the system but without considering any uncertainty on RES production (i.e. without considering potential deviations between the forecast and the actual production value). However, with the rise of the integration of renewable energy sources, such as wind farms, an increasing share of the generation at the transmission level is highly variable, uncontrollable and with non-accurate production forecasts. Consequently, if the OPF is solved based on inaccurate forecasts and without taking into account the uncertainty on RES, the computed optimal and secure schedules can result in grid instability and, potentially, in cascading outages. Thus, the key challenge, for power system operators, is to ensure that, regardless of this growing uncertainty, the operations stay secure.

As discussed in Section 2.2.3, among the different frameworks that have been proposed in the literature to account for the RES uncertainty, the Chance-Constrained Optimal Power Flow (CCOPF) problem is of particular interest when the forecast errors can be assessed. Solving the CCOPF problem can enhance the security regarding the uncertainty of the operations of transmission systems, since under CCOPF, the forecast values are no longer considered constant, but are instead represented by probability density functions (PDF).

Against this background, we propose in this chapter to solve a DC chance constrained optimal power flow that includes the RES uncertainty, with a distributed scalable algorithm relying on the ADMM. The CCOPF problem enforces that the power system constraints (e.g. capacity limits, limits of generators, available power reserves, etc.) are respected with a high probability, given the probability density functions of the RES. As in previous research works [DO05, ROKA13, BCH14, LM15], to overcome the computational intractability of the general CCOPF framework, we model the forecast error of each RES, restricted in this chapter to wind farms, by probability density functions that are mutually independent and approximated by Gaussian distributions. Otherwise, on transmission systems, the CCOPF problems face the same challenges than the SCOPF ones, namely: the coordination between actors (Requirement 6), the scalability of the methods used (Requirement 8) and the privacy and autonomy issues (Requirement 7). The novelty of this chapter resides in the proposi-

tion of the first CCOPF distributed solution based on ADMM that relies on an exact reformulation of the chance constraints. More specifically, this chapter makes the following contributions to the state of the art:

- *We propose a two-step algorithm to solve the CCOPF problem that takes into account the uncertainty on wind farms production, and that is fully distributed. The first step aims to determine the sensitivity factors of the system, namely the Generalised Generation Distribution Factors that measure the line flow changes due to deviations from generation schedule, and the sum of the primary frequency control participation factors, i.e. the frequency response characteristic of the system. The results of this first step are inputs of the second step that is the CCOPF problem solution.*

- *We extend this first algorithm to include the possibility to curtail wind farms by the addition of a consensus problem on the wind farms standard deviations. The possibility to curtail allows to solve CCOPF problems with high wind farms penetration and high uncertainty on the production of the wind farms. Moreover, ramp constraints can be included in the CCOPF formulation whereas it cannot without curtailment capabilities.*

- *We validate both algorithms (with and without curtailment) on a two-bus test system and on the IEEE 14-bus test system. The solutions are found in a distributed way, ensure the privacy and autonomy of the different system actors, and the algorithm is de facto parallel and adapted to high performance platforms.*

The remainder of this chapter is organised as follows: Section 5.1 introduces the formulation of the CCOPF problem considered and Section 5.2 details the two-step algorithm dedicated to solving this problem in a distributed manner, and especially the problems solved by the agents of the system. Simulations results are provided in Section 5.3 and proved the ability of the method to solve the CCOPF problem, but it also emphasises the risk that, under large uncertainty, the problem can be unfeasible. Section 5.4 then presents an extension of CCOPF problem, including the possibility to curtail wind farms of the system, and simulations results highlight, in Section 5.5, the improvement of this extension compared to the initial problem formulation. Eventually, Section 5.6 concludes on this chapter contributions.

5.1 CHANCE-CONSTRAINED OPF WITH PFC FORMULATION

This section presents the modelling of the different types of devices considered in this chapter, namely: wind farms, chance-constrained dispatchable generators participating in the primary frequency control, chance-constrained lines and fixed loads. The CCOPF formulation presented is similar to that of [ROKA13], but with a focus on the OPF instead of on the SCOPF problem, and an instantiation of the chance constraints to take into account the primary frequency control schemes.

5.1.1 *Wind farms*

Let $W \subset D$ be the set of wind farms, included in the set of devices D of the system. For a wind farm $w \in W$, let p_w be its forecast expected production. Since wind farms are variable and non-dispatchable sources, there is a forecast error that models the uncertainty with respect to the expected production (i.e. mismatch are expected between the expected production and the actual production of the wind farm). Using the same reasoning as in [ROKA13], the forecast errors are represented as independent Gaussian random variables with zero mean:

$$\forall w \in W, \ \Delta p_w \sim \mathcal{N}\left(0, \sigma_w^2\right) \tag{5.1}$$

where the forecast of different wind farms are assumed to be spatially uncorrelated. Note that this assumption holds when wind farms are sufficiently far away from each other.

5.1.2 *Chance-constrained generators*

In our formulation, dispatchable generators compensate the deviation of wind farms from the forecasts through the primary frequency control, as described next. Once introduced, we proceed to derive the probabilistic formulation of conventional generators.

Primary frequency control modelling

Let $G \subset D$ be the set of dispatchable conventional generators of the system. As described in the previous chapter, the primary frequency control (PFC) aims at regulating the frequency of the power system by adapting the generation [ES13]. Following equations 4.3 and 4.4, the contribution of a generator $g \in G$ to primary response is determined by the ratio of its coefficient, K_g, and the frequency response characteristic of the system, $\sum_{g \in G} K_g$. Hence, the response Δp_g of a generator g due to a deviation from the power scheduled that imply a compensation: Δp, can be formally expressed by the following steady-state equation:

$$\Delta p_g = \frac{K_g}{\sum_{g' \in G} K_{g'}} \Delta p \tag{5.2}$$

Probabilistic formulation

We consider that the compensation of the forecast error of the wind farm is achieved by the generators following the primary frequency control described above. Thus, following Equation 5.2, the primary frequency response of a generator $g \in G$ results from the product of a constant and the aggregated forecast error of all wind farms in the

system. The aggregated forecast error of wind farms, turns into a sum of uncorrelated Gaussian variables:

$$\Delta p = -\sum_{w \in W} \Delta p_w \sim \mathcal{N}\left(0, \sum_{w \in W} \sigma_w^2\right) \tag{5.3}$$

Hence, the primary frequency response of a generator is also a random variable, following a normal distribution $\Delta p_g \sim \mathcal{N}(0, \sigma_g^2)$ with a variance correlated with the output power of wind farms as:

$$\sigma_g^2 = \left(\frac{K_g}{\sum_{g' \in G} K_{g'}}\right)^2 \cdot \sum_{w \in W} \sigma_w^2 \tag{5.4}$$

Therefore, under this probabilistic model, the cost function of the generator is defined as the expectation of cost of generation applied on the total power generation output variable. This actual power generation is equal to the sum of the forecast schedule of production, p_g, and the primary frequency response due to wind power deviation from forecast. The cost of generation is supposed quadratic, as in Equation 4.12, with quadratic coefficient β and linear coefficient γ, so that:

$$\begin{aligned} \mathbb{E}[f(p_g + \Delta p_g)] &= \mathbb{E}[\beta \cdot (p_g + \Delta p_g)^2 + \gamma \cdot (p_g + \Delta p_g)] \\ &= \beta \cdot \sigma_g^2 + \beta \cdot p_g^2 + \gamma \cdot p_g \end{aligned} \tag{5.5}$$

Moreover, following the chance-constrained approach [ROKA13], we constrain that the maximum and minimum capacity limits of the generator are not reached given a certain tolerance to a violation ϵ:

$$\begin{aligned} \mathbb{P}[P_g^{min} \leqslant p_g + \Delta p_g] > 1 - \epsilon \\ \mathbb{P}[p_g + \Delta p_g \leqslant P_g^{max}] > 1 - \epsilon \end{aligned} \tag{5.6}$$

where $\mathbb{P}(\cdot)$ is the probability to respect the constraint on the generator production.

Under the assumption of Gaussianity, these constraints are simplified using the quantile function of the standard Gaussian distribution $\Phi^{-1}(\cdot)$. The chance constraint then simplifies to:

$$\begin{aligned} P_g^{min} \leqslant p_g - \Phi^{-1}(1-\epsilon) \cdot \sigma_g \\ p_g + \Phi^{-1}(1-\epsilon) \cdot \sigma_g \leqslant P_g^{max} \end{aligned} \tag{5.7}$$

The ramp constraint, as defined in Chapter 4, cannot be integrated because the reserve is constant and thus, if the reserves needed are greater than the ramp capabilities, the problem becomes unfeasible from the beginning. We propose a solution to this issue in Section 5.4.

5.1.3 *Chance-constrained lines*

To formulate the chance-constraints on lines, we need to be able to evaluate the impact of the deviation of a wind farm from its forecast on the lines flows. We then first introduce the sensitivity factors that we use to formulate the lines sub-problems.

Generalised Generation Distribution Factors

The Generalised Generation Distribution factors (GGDFs), first introduced in [Ng81], are used to determine the lines flow changes due to a deviation of power injection in the system. Let $L \subset D$ be the set of lines of the system. Formally, for line $l \in L$ and a power injection change Δp_g at each generator $g \in G$, the power flow change Δp_l is determined by the GGDF coefficients GF_l^g:

$$\forall l \in L, \quad \Delta p_l = \sum_{g \in G} GF_l^g \cdot \Delta p_g \tag{5.8}$$

As we are considering that any deviation of power injection is linearly compensated by generators that participate in the primary frequency control, we can determine the GGDF of a line $l \in L$ due to the deviation from forecast Δp_w of a wind farm $w \in W$, i.e. GF_l^w, through the equation:

$$\Delta p_l^w = GF_l^w \cdot \Delta p_w \tag{5.9}$$

Moreover, the linearity of Eq. 5.9 allows the use of superposition, so that, for a set of wind farms W that deviate from their forecast by $\forall w \in W,\ \Delta p_w$, we can determine the power flow change in line l due to all those deviations with:

$$\Delta p_l = \sum_{w \in W} (GF_l^w \cdot \Delta p_w) \tag{5.10}$$

Probabilistic formulation

We use the GGDF to formulate the probabilistic optimal power flow, as in [ROKA13], by adding chance constraints in the line flow capacity constraints, as described next.

As for generators, the amount of power transmitted through a line is linearly affected by the deviations of the wind farms because the primary frequency response of generators is also linearly related to the wind deviations. Hence, the line flow changes is a random variable following a normal distribution:

$$\Delta p_l \sim \mathcal{N}(0, \sigma_l^2) \tag{5.11}$$

With the notation of the previous section on GGDF, we can determine the relationship between the variance on the lines flows and the variance of the wind farms:

$$\sigma_l^2 = \sum_{w \in W} \left(GF_l^w \cdot \sigma_w\right)^2 \tag{5.12}$$

It turns out that the variance of a line flow is a linear combination of the variance of the wind forecast errors, and that the coefficient are the GGDF.

The chance constraints applied on lines enforce that the line flow capacity p_l^{max} is not reached given a certain tolerance ϵ to violation:

$$\begin{aligned} \mathbb{P}[-P_l^{max} \leqslant p_{l_1} + \Delta p_l] > 1 - \epsilon \\ \mathbb{P}[p_{l_1} + \Delta p_l \leqslant P_l^{max}] > 1 - \epsilon \end{aligned} \tag{5.13}$$

where $\mathbb{P}(\cdot)$ is the probability distribution of the amount of power transmitted through the line.

As for generators, under the assumption of Gaussianity, these constraints are simplified using $\Phi^{-1}(\cdot)$, the quantile function of the standard Gaussian distribution, and becomes:

$$\begin{aligned} -P_l^{max} &\leqslant p_{l_1} - \Phi^{-1}(1-\epsilon)\cdot\sigma_l \\ p_{l_1} + \Phi^{-1}(1-\epsilon)\cdot\sigma_l &\leqslant P_l^{max} \end{aligned} \tag{5.14}$$

5.2 DISTRIBUTED ALGORITHMS

This section presents the two-step distributed algorithm for solving the CCOPF problem with PFC formulated in the previous section. First, we describe how we determine the sensitivity factors and the frequency response characteristic of the system, in Section 5.2.1. Then, we provide the ADMM updates for the CCOPF sub-problems in Section 5.2.2.

5.2.1 *Step 1: Distributed computation of sensitivity factors*

Notice that to define lines and generators problems, and in particular Eq. 5.14 and 5.4, line agents need to compute the GGDF with respect the deviation of the wind farms, as defined in Section 5.1.3, and conventional generators need to compute the frequency response characteristic $\sum_{g\in G} K_g$. We propose in this section a distributed protocol that determines the GGDF and the frequency response characteristic.

First, the frequency response characteristic ($\sum_{g\in G} K_g$) is determined by computing a distributed sum, using the efficient Push-Sum protocol [KDG03]. This protocol consists in determining in peer-to-peer: (i) the average of the local values (i.e. of the average coefficient K_g of all generators: $\frac{1}{|G|}\cdot\sum_{g\in G} K_g$), and, (ii) the number of generators participating in the primary frequency control ($|G|$). After convergence, each generator computes the frequency response characteristic by multiplying the average ($\frac{1}{|G|}\cdot\sum_{g\in G} K_g$) by the number of generators ($|G|$).

To determine the GGDF of the lines, we need to solve an initial power flow with a feasible power injection schedule in order to get the line flows $\forall l \in L,\ p_l^{(0)}$ and power injection schedules $\forall g \in G,\ p_g^{(0)}$. We also need to create one case per wind farm, in which, we apply a deviation Δp_w at one of the wind farm $w \in W$. We determine the new power injection schedule of conventional generators by spreading Δp_w, and with the frequency response characteristic of the system. We finally solve the power flow with this new injection schedule, for each line $l \in L$, we get $p_l^{(w)}$, the power flow of line l associated with the wind farm power deviation Δp_w. Then, in each scenario that

considers the deviation of one of the wind farms $w \in W$, we determine the GGDF, GF_l^w, of each line $l \in L$ by computing:

$$\forall w \in W,\ GF_l^w = \frac{\Delta p_l^{(w)}}{\Delta p_w} = \frac{p_l^{(0)} - p_l^{(w)}}{\Delta p_w} \tag{5.15}$$

In summary, this first step of the algorithm is divided into four different sub-steps that can be run by agents sequentially or in parallel:

s1.1 Run a distributed sum algorithm to calculate the frequency response characteristic, i.e. $\sum_{g \in G} K_g$.

s1.2 Determine a feasible power injection schedule ($\forall g \in G,\ p_g^{(0)}$) and power flows ($\forall l \in L,\ p_l^{(0)}$) with the ADMM.

s1.3 Create for each wind farm $w \in W$ a scenario in which a deviation of w (Δp_w) is applied and spread. The primary frequency response of each generator is computed based on that deviation ($\forall g \in G,\ p_g^{(w)} = p_g^{(0)} + \frac{K_g}{\sum_{g \in G} K_g} \cdot \Delta p_w$).

s1.4 Run the ADMM algorithm to compute the power flows in each of these scenarios ($\forall l \in L,\ \forall w \in W,\ p_l^{(w)}$).

After the sub-step 4, each line agent has all information needed to compute its GGDF factor for each wind farm, i.e. $\forall w \in W,\ GF_l^{(w)} = \frac{p_l^{(0)} - p_l^{(w)}}{\Delta p_w}$. Note that those steps can be computed in parallel and that we can use previous power flow solutions as base case (step 2) and as warm starts to carry out the distributed power flow (step 4).

5.2.2 *Step 2: Distributed CCOPF*

The outputs of the sensitivity analysis are now the inputs of CCOPF problem. We provide a description of the sub-problems implemented in devices and nets agents after applying the ADMM.

Net agents

Before updating the scaled dual variables following Eq. 2.14a-2.14b, each net agent solves its sub-problem, Eq. 2.13. Since nets agents are not different from [KCLB14], the ADMM updates are the same than the ones provided in Eq. 2.17 and 2.18.

Wind farm agents

The mean power injections of the wind farms are constant, there is nothing to optimise. However, the wind farms spread the value of their variance σ_w^2 in a peer-to-peer fashion, so that lines and generators can access it.

Chance-constrained generator agents

Each chance constrained generator $g \in G$ solves, at iteration $k+1$, the sub-problem:

$$\min_{p_g} \ \beta \cdot \sigma_g^2 + \beta \cdot p_g^2 + \gamma \cdot p_g + \frac{\rho}{2}||p_g - \dot{p}_g^k + u_g^k||_2^2 \tag{5.16a}$$

$$\text{subject to :} \quad \sigma_g = \frac{K_g}{\sum_{g' \in G} K_{g'}} \cdot \sqrt{\sum_{w \in W} \sigma_w^2} \tag{5.16b}$$

$$r_g = \Phi^{-1}(1-\epsilon) \cdot \sigma_g \tag{5.16c}$$

$$p_g + r_g \leqslant P_g^{max} \qquad p_g - r_g \geqslant P_g^{min} \tag{5.16d}$$

This problem consists in minimising a polynomial of order 2, with a linear inequality constraint, because the reserve r_g is constant. The problem can thus be solved analytically.

Chance-constrained line agents

We present the chance constrained sub-problem solved by lines, keeping in mind that we determined the GGDF, related to each wind farm, of the lines through the distributed sensitivity analysis. We then have:

$$\min_{(p_{l_1}, \theta_{l_1}, p_{l_2}, \theta_{l_2})} \quad \frac{\rho}{2}||p_{l_1} - \dot{p}_{l_1}^k + u_{l_1}^k||_2^2 + \frac{\rho}{2}||p_{l_2} - \dot{p}_{l_2}^k + u_{l_2}^k||_2^2 \tag{5.17a}$$

$$+\frac{\rho}{2}||\theta_{l_1} - \dot{\theta}_{l_1}^k + v_{l_1}^k||_2^2 + \frac{\rho}{2}||\theta_{l_2} - \dot{\theta}_{l_2}^k + v_{l_2}^k||_2^2 \tag{5.17b}$$

$$\text{subject to :} \quad p_{l_1} = -p_{l_2} = b \cdot (\theta_{l_2} - \theta_{l_1}), \tag{5.17c}$$

$$\sigma_l = \sqrt{\sum_{w \in W} \left(GF_l^w \cdot \sigma_w\right)^2}, \qquad m_l = \Phi^{-1}(1-\epsilon) \cdot \sigma_l \tag{5.17d}$$

$$-P_l^{max} \leqslant p_{l_1} + m_l \leqslant P_l^{max} \qquad -P_l^{max} \leqslant p_{l_1} - m_l \leqslant P_l^{max} \tag{5.17e}$$

We solve the line flow problem as in Section 4.2.2: we solve the unconstrained problem, check that the inequality constraint is respected, and, if not, we simplify the problem using the fact that the objective function is convex.

Loads

The loads are considered constant, the sub-problem solution is fixed.

5.3 SIMULATION RESULTS

The proposed distributed algorithm was implemented in the Java Agent DEvelopment[1] (JADE) platform [BBCP05], where each agent solves its corresponding sub-problem

1 jade.tilab.com

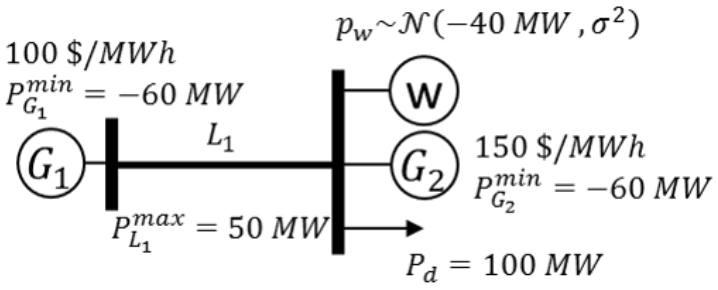

Figure 5.1: 2-bus test system.

in parallel. We tested our algorithm on two power systems: a small 2-bus test system to illustrate its operation and the IEEE 14-bus test system for validation on a realistic system. For each circuit, we tested it under scenarios with different percentages of wind forecast error, where the percentage forecast error is defined by setting the standard deviation (i.e. the square root of the variance) of the wind error distribution to a percentage of its mean value. For example, a 10% of forecast error for a wind farm with an expected value of $100MW$ leads to an error prediction distribution with a variance of 100. For each scenario, we enforce that the reserves and margins are sufficient in 99.7 % of the time, i.e. $\phi^{-1}(0.997) = 3$.

Next sections discusses the results obtained in the 2-bus test system (Section 5.3.1) and in the IEEE 14-bus test system (Section 5.3.2) as well as the limitations of the current formulation given by the fact that the uncertainty in the problem is considered as constant and not-controllable (Section 5.3.3).

5.3.1 *2-bus test system*

We tested our algorithm on a 2-bus test system with two conventional generators, a line, a load and a wind farm, as depicted in Figure 5.1. The two conventional generators are identical (same capacity limits, same coefficients i.e. $K_{g_1} = K_{g_2} = K_g$), except that the cost of generation of G_1 is cheaper than G_2. We selected this circuit because it is simple enough to allow an analytical solution.

First, we focus on the solution of the OPF problem (i.e. the one that minimises the cost of operation and enforces the line and generators constraints). The wind farm in this case is supposed to generate its mean power p_w, i.e. -40 MW. To minimise the cost, we need to maximise the use of generator G_1 (cheaper than G_2), but we also must ensure that the line L_1 is not overloaded. G_1 then generates the maximum power the line can carry $P_{L_1}^{max}$, i.e. 50 MW, and finally G_2 covers the remaining power needed, i.e. 10 MW.

Then, we consider the uncertainty in the wind farm forecast and the case in which the generators G_1 and G_2, and line L_1 enforce that they have sufficient reserves (Eq. 5.16c) or margins (Eq. 5.17d) to cover most of the wind farm deviations.

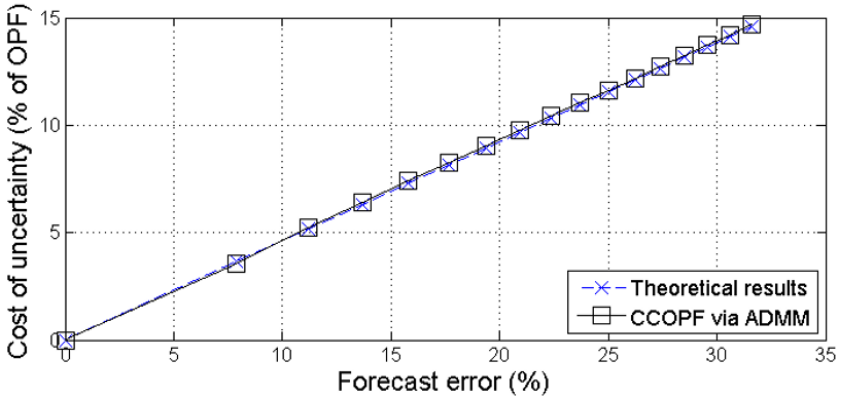

(a) Percentage error compare to theory.

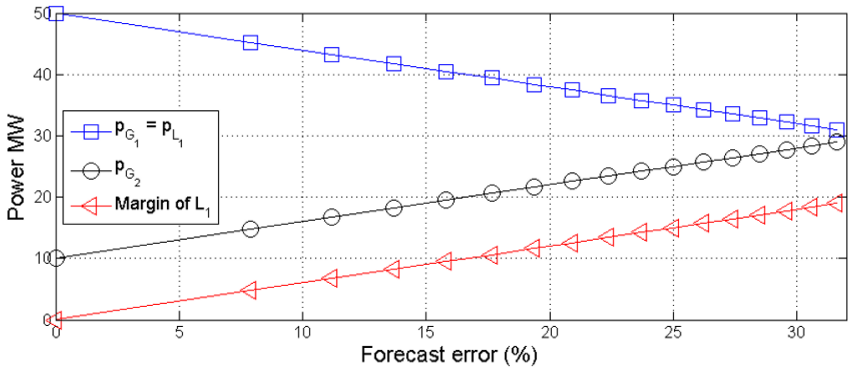

(b) Power scheduled in generators, in the line and the margin needed for the line.

Figure 5.2: Results on the 2-bus test system.

See that, in this simple example, there is only one line that transmits all the power generated by generator G_1 to the rest of the system, i.e. bus 2. The GGDF reflects the impact of a deviation of the wind farm on the line flow and thus, on the generation of generator G_1. Then, from Eq. 5.2, we get :
$\Delta p_{L_1} = \Delta p_{G_1} = \frac{K_G}{K_G+K_G} \cdot (-\Delta p_w) = \frac{1}{2} \cdot (-\Delta p_w) = GF^w_{L_1} \cdot \Delta p_w$.
The standard deviation for the (equal) generators is calculated using Eq. 5.16b, so that:
$\sigma_{G_1} = \sigma_{G_2} = \frac{K_G}{K_G+K_G} \cdot \sigma_w = \frac{1}{2} \cdot \sigma_w$;
whereas for lines, the standard deviation is computed through Eq. 5.17d, as
$\sigma_{L_1} = GF^w_l \cdot \sigma_w$.
The reserves and margins are defined in Eq. 5.16c and Eq. 5.17d, so that $r_{G_1} = r_{G_2} = \frac{3}{2} \cdot \sigma_w$ and $m_{L_1} = \frac{3}{2} \cdot \sigma_w$.
The limiting constraint, in this example, is the capacity of line L_1 because all the power generated by G_1 is flowing through L_1 that have lower capacity than G_1. It follows that the scheduled power output of generator G_1 is $p_{G_1} = -P^{max}_{L_1} + \frac{3}{2} \cdot \sigma_w$, and as this power can only be transmitted through line L_1, the expected power flow in line L_1 is equal to p_{G_1}. Generator G_2 covers the rest of power needed to fulfil the load consumption $p_{G_2} = P^{max}_{L_1} - \frac{3}{2} \cdot \sigma_w - p_w - p_d$.

We propose to compare the theoretical results, provided above, with the results obtained with our algorithm using a scaling parameter $\rho = 1$ and a tolerance equal to 10^{-4}.
Figure 5.2a depicts the cost of uncertainty, which represents the cost increase when considering the uncertainty on the wind production, for the analytical solution and for the two-step ADMM algorithm when varying the wind forecast error. The cost of uncertainty found by our algorithm matches well the analytical results, and the relative error of our results, compared to the analytical solution, is below 0.1% for all cases. It took 50 iterations for the ADMM algorithm to solve the OPF and between 57 and 59 iterations (i.e. depending on the particular wind forecast error) to find the solutions of the CCOPF, which shows that the addition of the chance constraints do not increase significantly the number of iterations needed.

Figure 5.2b depicts the generation of both generators and the margin of line L_1. We observe that when the uncertainty grows, the margin needed increases and thus the power generation is more and more scheduled on generator G_2 which increases the cost of operations.

5.3.2 *IEEE 14-bus test system*

This section tests the performance of the proposed algorithm on the IEEE-14-bus test system with data from the Power System Test Case Archive [2], where we replace the generators on bus 3 (G_3) and on bus 6 (G_4) by identical wind farms. The system, represented in Figure 4.1, is composed of 11 loads, 20 lines, 3 conventional generators

2 https://www2.ee.washington.edu/research/pstca/

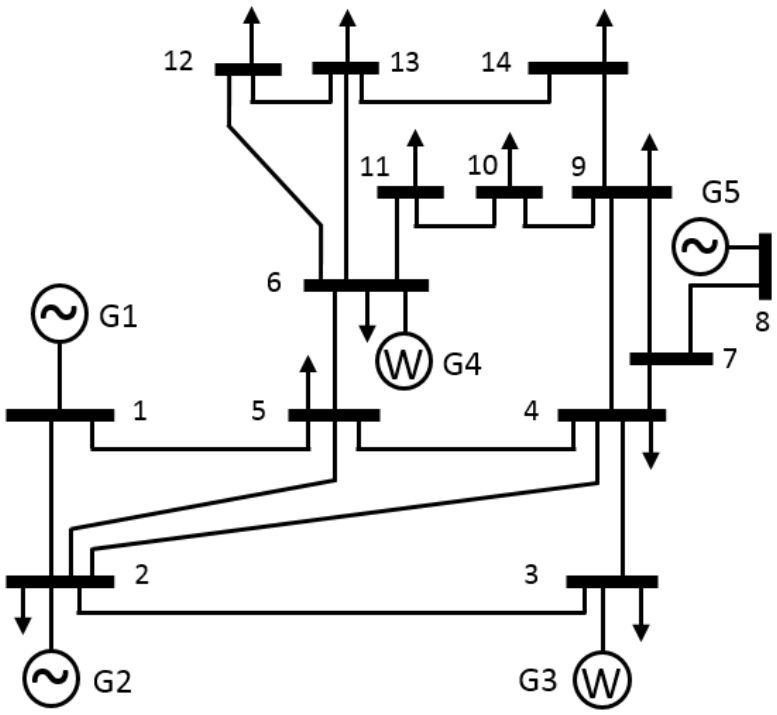

Figure 5.3: IEEE 14-bus test system with two wind farms.

and 2 wind farms. We completed the model by setting the line capacity limits to 50 MW, except for lines 1-2, 1-5, 2-3, 7-8 and 7-9 that were set to 110 MW, because those lines carry most of the power of the system. Table 4.2 details the parameters used for the different generators, and the cost of wind generation is assumed equal to zero. We compare the results obtained with our algorithm with the solution found by a centralised solver using MATLAB©[MAT14] and CVX: a package for solving convex programs [GB08, GB14]. Depending on the step of the algorithm, we use different scaling parameters, but we set for all ADMM processes a tolerance equal to 10^{-4}.

As the first sub-step s1.1 of the algorithm, agents compute the frequency response characteristic of the system in a distributed way, in 25 iterations, via the Push-Sum algorithm. In the sub-step s1.2, agents run ADMM to calculate an optimal power flow in a distributed manner. This initial feasible point was found in 761 iterations with a scaling parameter $\rho = 1$. This solution is then reused by agents as a warm start to solve the scenarios in which the wind farms deviate (sub-step s1.3), i.e. the power flow variables are initialised to the previously calculated solution. With two wind farms, this means to solve two power flows with deviations of the power injection schedule ruled by a shift of a wind farm and the primary frequency control. Solving these two scenarios in parallel by ADMM with a scaling parameter set to $\rho = 10^{-2}$ took 556 iterations until convergence.

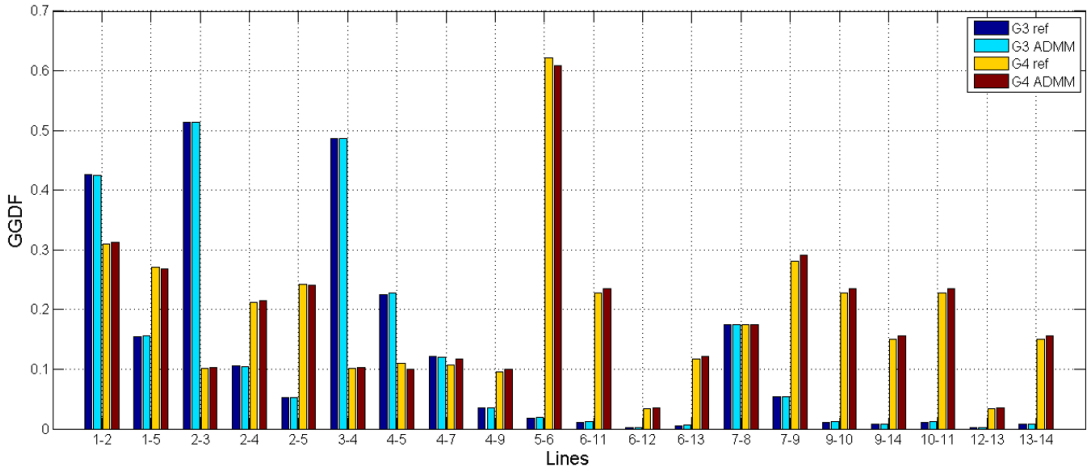

Figure 5.4: IEEE 14-bus absolute value of the GGDF compared to centralised calculation.

Hence, it took a total of 1342 iterations for the agents to compute the GGDF in a distributed manner. The results of the first step of the proposed algorithm are summarised and compared in Figure 5.4. We compare the GGDF obtained, for each wind farm ($G3$ and $G4$) and at each line, from our distributed algorithm with those from the reference calculated in a centralised manner. The lines most impacted by generator G_3 are lines 1-2, 2-3 and 3-4, when the most impacted by G_4 are lines 1-2, 5-6 and 7-9, then these lines see their capacity shrink more than the other lines of the system when the uncertainty grows. The difference between the results obtained with the ADMM and the reference can be explained by the tolerance and the fact that some power flows are small.
Note that this first step needs to be computed again only if the generators connected or the topology change and that we could have used a previous power flow solution instead of running an OPF in sub-step s1.2.

Finally, for the second step of the algorithm, we perform simulations with different wind penetrations levels and with different wind forecast errors. The term wind penetration level is defined here, as the ratio of the wind production and the total consumption of the system. In particular, we used 10 %, 20 %, 30 % and 40 % wind penetration levels and we vary the percentage forecast error between 0 % (no forecast error, i.e. OPF) and 40 %. The scaling parameter for ADMM in this case was set to $\rho = 10$.
We present the cost of uncertainty, in Figure 5.5a, defined as the cost increase in percentage of the OPF solution, for each wind penetration level and for different forecast errors. Observe that as the forecast error grows, the cost increases which is due to the rise of the margins and reserves needed. Under a wind penetration level as low as 10 %, the impact of the uncertainty on the cost of operation is limited, e.g. even with a 40 % forecast error, the cost of uncertainty does not exceed 1.4 %. However, with high

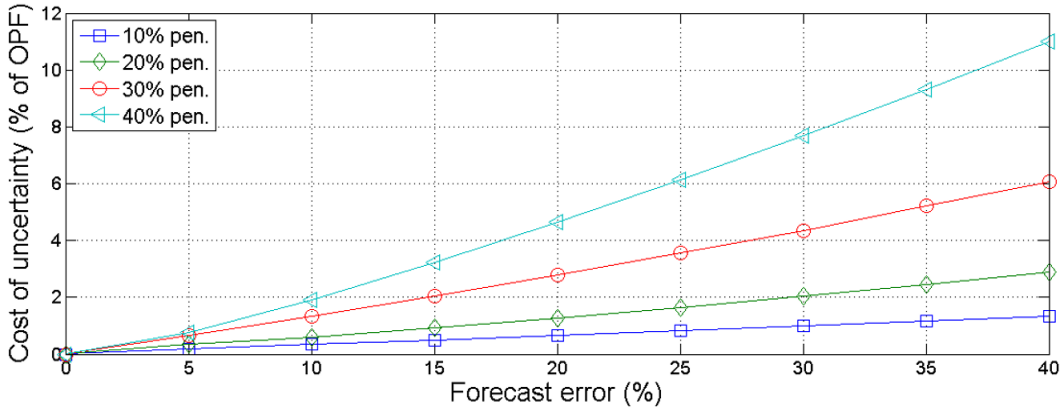

(a) Comparison of theoretical results and via our method based on ADMM.

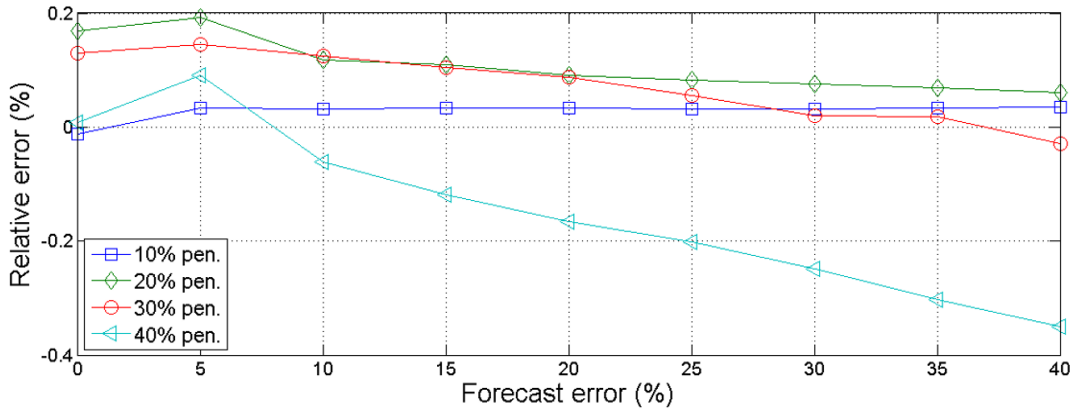

(b) Percentage error compare to theory.

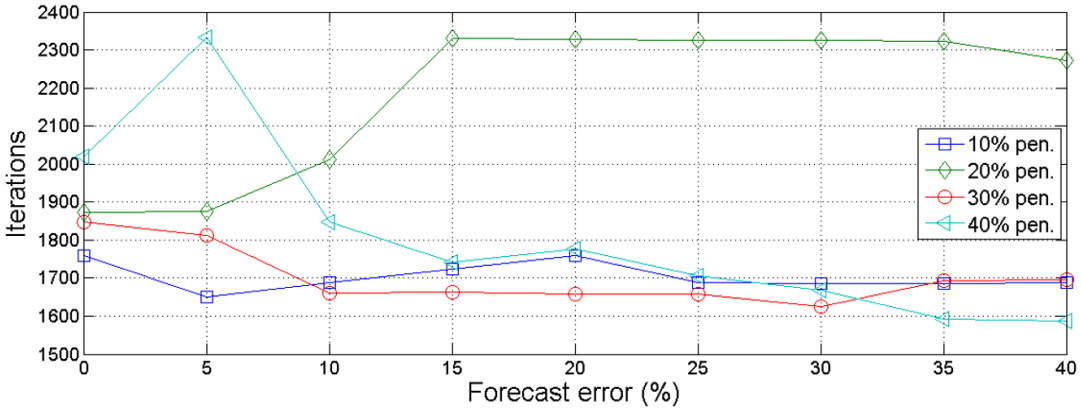

(c) Iterations needed to reach convergence.

Figure 5.5: Results on the 14-bus test system.

wind penetration and a forecast error of 40 %, the cost of security goes up to 11 % of the OPF cost of operation.

Figure 5.5b presents the relative error of our simulation compared to the reference. The error is below 0.2 % and is more conservative than the reference for wind penetration below 40 % wind penetration. For the case with a wind penetration of 40 %, the underestimation can be explained by the fact that, depending on the wind penetration, different constraints imposes the power injection schedule. In the 40 % wind penetration case, line 4-5 is the limiting line and this line GGDF is underestimated compared to the reference for generator G_4, as shown in Figure 5.4.
Finally, the number of iterations for each case is presented in Figure 5.5c. The number of iterations needed does not vary significantly and is not greater than the number of iterations to solve the optimal power flow (the OPF is 0 % forecast error).

5.3.3 *Discussion on the limits of the proposed CCOPF formulation*

The CCOPF formulation solved in the previous section considers the uncertainty as constant and hence non-optimisable by the algorithms. As we discuss next, this formulation has two main drawbacks, namely: the problem can easily become unfeasible and the generators reserves cannot be integrated.

As illustrating example, consider again the 2-bus test system from Section 5.3.1. In this circuit note that if the uncertainty on the wind farms forecast is too high, the problem can become unfeasible due to the maximum capacity of the generator G_2. As mentioned before, the power output plus[3] the reserve needed should be below the maximum output capacity ($-P^{min}_{G_2}$) of the generator. And, if we enforce that the line constraints are not violated, we have: $p_{G_2} - r_{G_2} = P^{max}_{L_1} - p_w - p_d - 3 \cdot \sigma_w \geqslant P^{min}_{G_2}$. Isolating the standard deviation results in $\sigma_w \leqslant \frac{1}{3} \cdot (-P^{min}_{G_2} + P^{max}_{L_1} - p_w - p_d) = 16.67$, which represents a 41.67% forecast error. Thus, above this limit, the problem becomes unfeasible because it is no longer possible to respect the line constraints and generator G_2 constraints. This unfeasibility may also come from the ramp constraints of generators. As mentioned in Section 5.1.2, the ramp constraints of generators are not included. Indeed, if the reserves needed are greater than the ramp capabilities of generators, there is no leverage to relieve the violation of the ramp constraint. In particular, if we include the ramp constraints, some of the problems solved previously are no longer feasible.

This discussion above clearly showed the limits of the proposed CCOPF formulation. To overcome these limitations, we propose in the next section to extend this formulation in order include the standard deviation (i.e. forecast error) as optimisation variable in the CCOPF problem through wind curtailment.

3 We are discussing here in absolute value while our sign convention imposes that the power injection into the grid is counted negatively.

5.4 EXTENSION OF THE CCOPF PROBLEM TO INCLUDE CURTAILMENT CAPABILITIES

As seen in the previous simulation section, the chance-constrained optimal power flow problem does not always have a feasible solution. When the uncertainty is large, the margins and reserves needed to cover most deviation from forecast can exceed the system capabilities. In that case, the schedule cannot satisfy the chance constraints of lines and generators and is thus not secure. In addition, the ramp constraints of generators cannot be enforced because the reserves needed are constant.

In some cases, wind power plants can be curtailed to mitigate the impact of the wind forecast errors, as mentioned in [AES10]. The possibility to curtail wind power plants increases the flexibility of the system, can reduce the reserves and margins needed and allows the integration of more wind farms. The objective of this extension is then to determine the optimal curtailment factor to apply at each wind farm, in addition to determining the optimal schedule of generation of the conventional generators.

In the next section, we include a curtailment model (Section 5.4.1), which is a linear curtailment of the wind farms generation, to the previous problem and we propose an extension of the CCOPF algorithm to solve this new problem (Section 5.4.2).

5.4.1 *Formulation of the extension*

This extension mainly modifies the model of the wind farms that is described next. The main difference being that the variances of the wind farms that were previously considered constant now they turn into variables of the problem. In contrast, the equations provided in Section 5.1 for the generators and lines remain unchanged.

Wind farms

In addition to the modelling of Section 5.1 where wind farms are not flexible, we introduce the possibility to curtail a part of the wind generation at a certain cost to relieve some violations. The curtailment is proportional regardless of the actual production of the wind farm (realisation of p_w), i.e. if the forecast overestimate the wind generation there would still be a curtailment. We introduce the curtailment factor ξ_w of the wind farm w, and we note p_w^{nc} the actual power production of the wind farm not curtailed and the p_w^c the wind production after curtailment such that:

$$\forall w \in W, \;\; p_w^c = (1 - \xi_w) \cdot p_w^{nc} \tag{5.18}$$

and with a forecast of the wind farm w initially equal to $\mathcal{N}\left(p_w^i, (\sigma_w^i)^2\right)$, this implies a probability distribution of the curtailed wind farm production p_w so that:

$$\forall w \in W, \;\; p_w \sim \mathcal{N}\left((1 - \xi_w) \cdot p_w^i, (1 - \xi_w)^2 \cdot (\sigma_w^i)^2\right) \tag{5.19}$$

We also introduce the vector of standard deviations of wind farms that is here a variable:

$$\mathbf{\Sigma} = \left[\sigma_w = (1-\xi_w)^2 \cdot (\sigma_w^i)^2\right]_{\forall w \in W} \tag{5.20}$$

We form a consensus problem on this variable similarly to the relative steady-state frequency variable introduced in Section 4.2. Each standard deviation is then determined collectively by all the agents of the system and can then impact the curtailment of the wind farms.

5.4.2 *Extension of step 2 of the algorithm*

The sub-problems implemented in the devices and nets agents after applying the ADMM are described in the following sections.

Net agents

Before updating the scaled dual variables following Eq. 2.14a-2.14b, each net agent solves its sub-problem, Eq. 2.13. The dual update for the active power and the angle is the same as in Chapter 2, except for the variable $\mathbf{\Sigma}$ representing the standard deviation of the wind farms forecast errors. In this case, the constraint enforced at the nets is that there should be a consensus on the standard deviation of the wind farms for all the devices connected to each net $n \in N$ which can be written as:

$$\dot{\mathbf{\Sigma}}_t = \dot{\mathbf{\Sigma}}_{t'}, \quad \forall t, t' \in n^2 \tag{5.21}$$

The net agent minimisation step is then augmented by:

$$\forall w \in W \quad \dot{\sigma}_{w(n)}^{k+1} = \frac{1}{|n|} \cdot \sum_{d \in n} \sigma_{w(d)}^{k+1} \tag{5.22}$$

with $\sigma_{w(a)}$ the standard deviation of the forecast error of the wind farm w, for the agent a.
Or:

$$\dot{\mathbf{\Sigma}}_n^{k+1} = \frac{1}{|n|} \cdot \sum_{d \in n} \mathbf{\Sigma}_d^{k+1} \tag{5.23}$$

in a more compact formulation.

We also introduce the vector of dual variables related to the wind farms forecast errors $\mathcal{W}$, which is updated as follows:

$$\mathcal{W}_n^{k+1} = \mathcal{W}_n^{k+1} + (\mathbf{\Sigma}_d^{k+1} - \dot{\mathbf{\Sigma}}_n^{k+1}) \tag{5.24}$$

Wind farm agents

The objective of the wind farm agents is to determine the optimal curtailment factor to apply. The problem can include a cost that depends on the curtailment applied with parameter β and can be formulated as follows:

$$\min_{p_w, \boldsymbol{\Sigma}_w} \ \beta \cdot (\sigma_w^i - \sigma_w)^2 + \frac{\rho}{2}||p_w - \dot{p}_w^k + u_w^k||_2^2 + \frac{\rho}{2}||\boldsymbol{\Sigma}_w - \dot{\boldsymbol{\Sigma}}^k{}_w + \mathcal{W}_w^k||_2^2 \tag{5.25a}$$

$$\text{subject to :} \quad p_w = (1-\xi)\cdot p_w^i \tag{5.25b}$$

$$\sigma_w = (1-\xi)\cdot \sigma_w^i \tag{5.25c}$$

It is a simple quadratic problem with linear constraints and can thus be solved analytically.

Chance-constrained generator agents

The generators problem is the same as in Section 5.2.2, except that the wind farms standard deviation are variables to determine. Each chance-constrained generator $g \in G$ then solves, at iteration $k+1$, the following sub-problem:

$$\min_{p_g, \boldsymbol{\Sigma}_g} \ \beta \cdot \left(\frac{K_g}{\sum_{g' \in G} K_{g'}}\right)^2 \cdot ||\boldsymbol{\Sigma}_g||_2^2 + \beta \cdot p_g^2 + \gamma \cdot p_g + \tag{5.26a}$$

$$\frac{\rho}{2}||p_g - \dot{p}_g^k + u_g^k||_2^2 + \frac{\rho}{2}||\boldsymbol{\Sigma}_g - \dot{\boldsymbol{\Sigma}}_g^k + \mathcal{W}_g^k||_2^2 \tag{5.26b}$$

$$\text{subject to :} \quad r_g = \Phi^{-1}(1-\epsilon)\cdot\left(\frac{K_g}{\sum_{g' \in G} K_{g'}}\right)\cdot||\boldsymbol{\Sigma}_g||_2 \tag{5.26c}$$

$$p_g + r_g \leqslant P_g^{max} \qquad p_g - r_g \geqslant P_g^{min} \tag{5.26d}$$

$$r_g \leqslant R_g^{max}\cdot\Delta t \tag{5.26e}$$

Thereafter, we propose to ignore the term $\alpha \cdot \left(\frac{K_g}{\sum_{g' \in G} K_{g'}}\right)^2 \cdot ||\boldsymbol{\Sigma}_g||_2^2$ of the objective function that represents the cost of use of the reserves related to the quadratic cost. Otherwise, the generators would tend to minimise this term, while we want to maximise the use of the wind farms production and only wish to use the curtailment capabilities to make the initially unfeasible CCOPF problem feasible. We finally solve this sub-problem using IPOPT solver that is an interior point solver able to solve non-convex problems.

Chance-constrained line agents

We present the chance constrained sub-problem solved by lines, keeping in mind that we determined the GGDF, related to each wind farm, of the lines through the distributed sensitivity analysis. For the sake of conciseness, we introduce the GGDF

matrix GF_l of line l that is diagonal, and the diagonal terms correspond to the GGDF related to the wind farms of $\mathbf{\Sigma}$. We then have the problem:

$$\begin{aligned}
\min_{p_{l_1},\theta_{l_1},p_{l_2},\theta_{l_2},\mathbf{\Sigma}} \quad & (\frac{\rho}{2}||p_{l_1} - \dot{p}_{l_1}^{k(s)} + u_{l_1}^{k(s)}||_2^2 + \frac{\rho}{2}||p_{l_2} - \dot{p}_{l_2}^{k(s)} + u_{l_2}^{k(s)}||_2^2 \\
& + \frac{\rho}{2}||\theta_{l_1} - \dot{\theta}_{l_1}^{k(s)} + v_{l_1}^{k(s)}||_2^2 + \frac{\rho}{2}||\theta_{l_2} - \dot{\theta}_{l_2}^{k(s)} + v_{l_2}^{k(s)}||_2^2 \\
& + \frac{\rho}{2}||\mathbf{\Sigma}_{l_1} - \dot{\mathbf{\Sigma}}_{l_1}^{k(s)} + \mathcal{W}_{l_1}^{k(s)}||_2^2 + \frac{\rho}{2}||\mathbf{\Sigma}_{l_2} - \dot{\mathbf{\Sigma}}_{l_2}^{k(s)} + \mathcal{W}_{l_2}^{k(s)}||_2^2) \qquad (5.27) \\
\text{subject to :} \quad & \mathbf{\Sigma}_{l_1} = \mathbf{\Sigma}_{l_2} = \mathbf{\Sigma} \\
& p_{l_1} = b_l \cdot (\theta_{l_2} - \theta_{l_1}), \quad p_{l_1} = -p_{l_2}, \\
& m_l = \Phi^{-1}(1-\epsilon) \cdot \sqrt{\mathbf{\Sigma} \cdot GF_l \cdot GF_l \cdot \mathbf{\Sigma}} \\
& p_{l_1} + m_l \leqslant P_l^{max} \qquad -P_l^{max} \leqslant p_{l_1} - m_l
\end{aligned}$$

The line agents sub-problems are then non-convex, we rely on IPOPT solver to solve this problem.

5.5 SIMULATIONS EXTENSION

This extension was also implemented in the Java Agent DEvelopment[4] (JADE) platform [BBCP05] and benchmarked on the small 2-bus test system and the IEEE 14-bus test system. We use the same parameters as in the simulation Section 5.3.

5.5.1 *2-bus test system*

As shown in Section 5.3.3, the problem becomes unfeasible if the standard deviation of the forecast error is greater than 41.67%. When we include the possibility to curtail the wind farms, the power output plus the reserves of G_2 can be written as:
$p_{G_2} - r_{G_2} = P_{L_1}^{max} - p_d - \xi \cdot (3 \cdot \sigma_w^i + p_w^i) \geqslant P_{G_2}^{min}$.

This calculation assumes that we respect the line constraints and minimise the cost of generation by maximising the production of generator G_2. Thus, the constraint that makes the infeasibility is the maximum power output of generator G_2. Which means that, to respect all the constraints, the curtailment must respect:

$$\xi \leqslant \frac{-P_{G_2}^{min} + P_{L_1}^{max} - p_d}{3 \cdot \sigma_w^i + p_w^i} \qquad (5.28)$$

As an example, for a 50 % standard deviation, the optimal curtailment factor is:
$\xi^* = \frac{60+50-100}{3 \cdot 20-40} = 0.5$.

We provide simulation results with different forecast error and we compare the results from our algorithm with the analytical results presented before. We use a scaling

4 jade.tilab.com

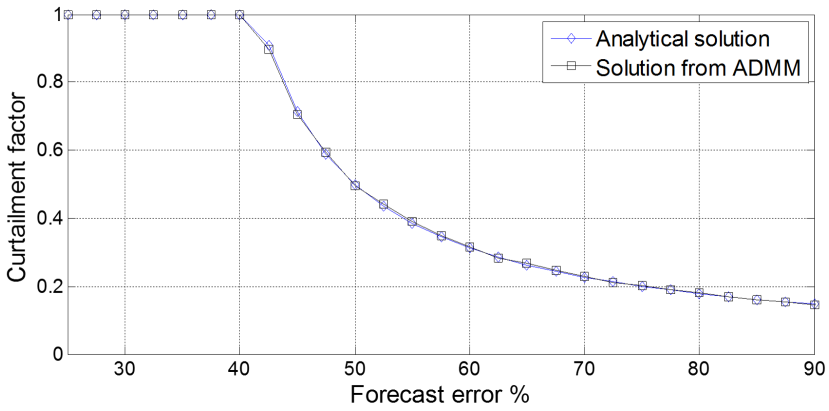

(a) Optimal curtailment factor.

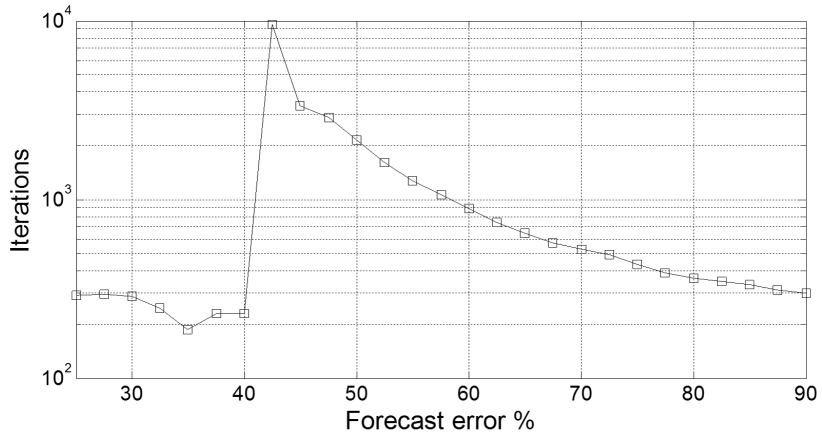

(b) Iterations.

Figure 5.6: Results for the 2-bus test systems.

parameter of $\rho = 1$ and a tolerance of $\epsilon_{abs} = 10^{-4}$.
Figure 5.6a presents the optimal curtailment factors that allow to respect all the constraints of the system, while minimising the cost of generation. The comparison proves that the solutions found are the optimal solution, and follow the inverse function given in Eq. 5.28, with a good precision.

The number of iterations to found those solutions is depicted in Figure 5.6b, and we note a sharp rise of the number of iterations when the forecast error starts to make the classic CCOPF problem unfeasible. After a 42.5 % forecast error, the less feasible the problem is, the less iterations is needed. Similar results have been obtained and discussed, in Section 4.3.2, illustrating the fact that when tightening the constraints, the feasible solution space is reduced and the solution can be found faster than if constraints are slightly reached.

This simple example illustrates the ability of this new algorithm to find feasible and optimal solutions through the curtailment of wind farms.

5.5.2 *IEEE 14-bus test system*

Now that we proved that the algorithm is able to solve the CCOPF with curtailment on a small system, we propose to evaluate it on the IEEE 14-bus test system. The ramps are set to 35 MW/min, as in Table 4.2. Then, for a 30 % penetration and with a forecast error greater than 35 % and for a 40 % penetration and with a forecast error greater than 25 %, the CCOPF problem becomes unfeasible. The absolute tolerance is still set to $\epsilon_{abs} = 10^{-4}$, and the scaling parameter to $\rho = 10$.

We reuse the results of step 1 obtained in Section 5.3 and provided in Figure 5.4. We then solve the CCOPF with the extension, for wind farms penetration of 10 %, 20 %, 30 % and 40 %, and for forecast errors from 0 % to 40 %. We remind that 10 % forecast error means that the standard deviation of the probability density function of the wind farm is equal to 10 % of its mean generation.

Figure 5.7 illustrates the results obtained with the curtailment compared to the results of the CCOPF modelling. Figure 5.7a compares the cost of uncertainty with the model of Section 5.1, in dashed lines, with the cost of uncertainty of the CCOPF with curtailment, in plain lines. The unfeasible point of the CCOPF formulation without curtailment, due to violations of the reserves constraints are marked with red crosses. First, we observe that there is a rise of the cost of uncertainty, when considering the ramp constraints, as well as the curtailment capabilities, for the penetrations and forecast errors that are not feasible for the CCOPF problem without curtailment. Moreover, the results, with and without the consensus problem on the standard deviation of the wind farms, reach the same solutions.
The curtailment factors, for both generators, are depicted in Figure 5.7b for 30 % and 40 % wind penetration. Note that, in each case, both curtailment factors are the same, which can be explained by the fact that the constraints reached that need to be relieved by the curtailments concern the maximum reserves of a generator. In more detail,

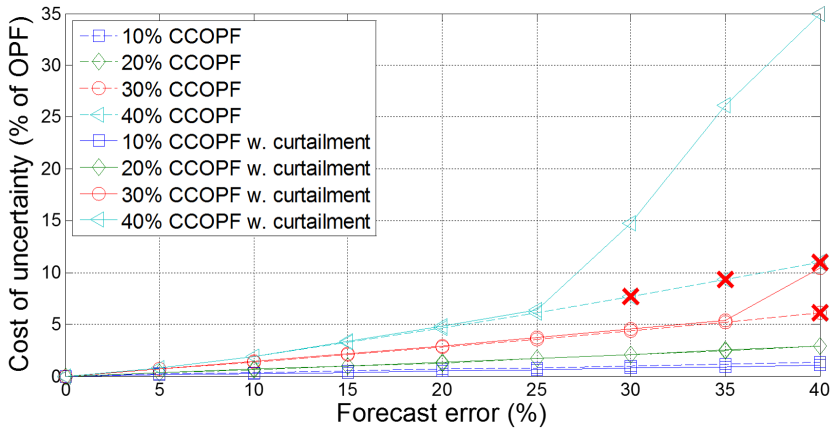

(a) Comparison of theoretical results of CCOPF without curtailment and with curtailment.

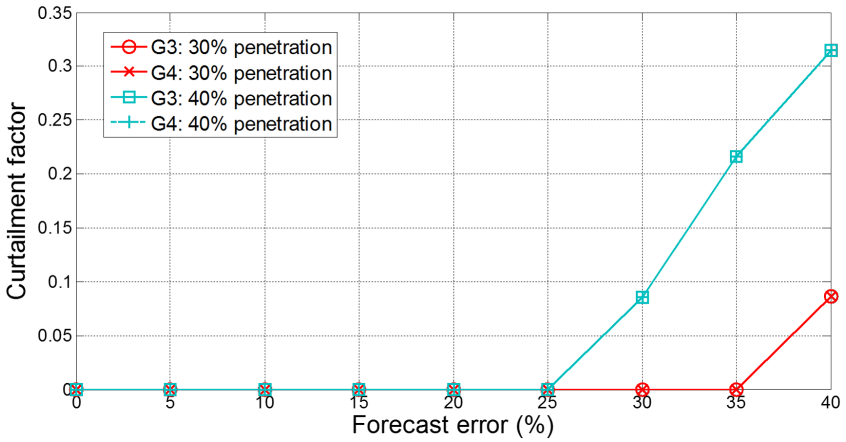

(b) Curtailment factors for 30 % and 40 % wind penetration.

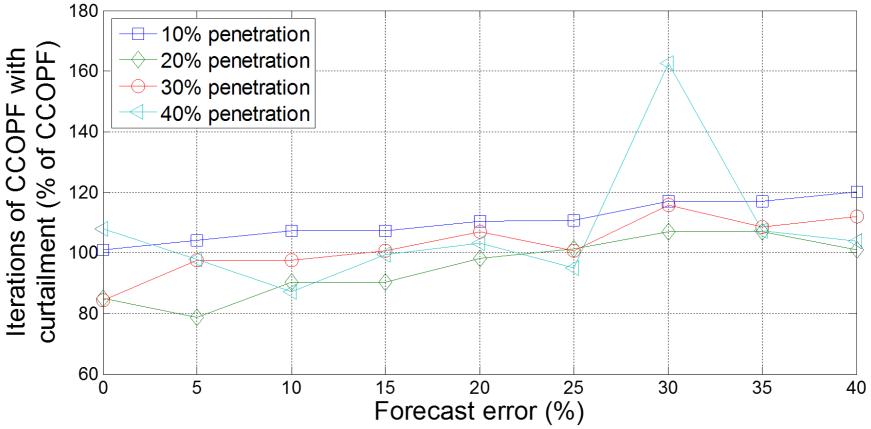

(c) (c) Comparison of the number of iterations needed to reach convergence.

Figure 5.7: Results on the 14-bus test system.

generators reserve is equally impacted by all the wind farms and, thus, the cheapest solution to reduce Eq. 5.26c is to apply the same curtailment factor to each generator.

Finally, we provide the percentage increase of iterations of the case with curtailment compared to the case without curtailment. The number of iterations are very similar because the number of iterations needed to converge for the case with curtailment is between 80 % and 120 % of the case without curtailment, except for one case. This case represents the first unfeasible point of the 40 % penetration case, similarly to the results on the 2-bus test system, which shows again that the problems which are unfeasible, but close to the feasible space, are the longest to solve.

The CCOPF with the possibility to curtail wind farms appears as a good extension of the classic CCOPF problem, introduced in Section 5.1. First, even when adding the consensus problem on the standard deviation of wind farms, the solutions found are the same and the number of iterations to reach them is similar. And finally, the inclusion of the curtailment capabilities allow to found feasible solutions even when the classic CCOPF problem is unfeasible, which allow for more wind power integration to grid.

5.6 CONCLUSIONS

This chapter presented a distributed two-step algorithm that solves the Chance-Constrained Optimal Power Flow problem (CCOPF) based on an exact reformulation of the problem assuming that wind power forecast errors follow independent Gaussian distributions.

The proposed method employs a distributed solution to cope with the inter-regional OPF problem, whilst previous works (i.e. [BCH14, ROKA13, LM15]) needed to adopt centralised strategies for both the computation of the sensitivity factors and the CCOPF solution. The distributed approach ensures the privacy and autonomy of the actors of interconnected systems and enables the parallelisation of the computation. The first step of the algorithm aims at determining the generalised generation distribution factors and the frequency response characteristic of the system, whereas the second step is the distributed CCOPF solution in itself. We provide simulation results on a two-bus test system and on the IEEE 14-bus test system, and show the ability of this algorithm to solve our problem. However, we also show that the problem can be unfeasible due to large uncertainties and that the ramp limits of generators cannot be taken into account.

We thus provide a formulation of a CCOPF problem that includes the possibility to curtail the generation of the wind farms of the system. It provides enough flexibility to make the original CCOPF problems feasible when it would be unfeasible without curtailment. To determine this flexibility in a distributed manner, we introduce a consensus problem on the wind farms standard deviations. The new agent problems are detailed and we show that the problem becomes non-convex. We evaluate this extension of the algorithm on the two-bus test system and on the IEEE 14-bus test system, and proved the effectiveness of the method. In fact, despite the inclusion of the con-

sensus problem on the standard deviation of the wind farms, the number of iterations stays similar to the first CCOPF formulation and the solutions reached are the same.

6

CONCLUSIONS AND FUTURE WORKS

This final chapter summarises the work and main results presented in this thesis as well as introduces future works that could enhance the methods developed and help addressing further the requirements of Section 1.1.

6.1 CONCLUSIONS

The need for an energy transition implies a development of power systems and especially a change in the type of energy sources, from mainly fossil fuel to renewable energy sources whose emissions are very low. However, the replacement of conventional energy sources by renewable energy sources is challenging for power systems. In addition, the enhancement of power systems implies having more interconnections between power systems, forming large-scale interconnected power systems. Interconnections allow to reduce the cost of operations and to share the power reserves needed in case an incident occurs. But the coordination of power systems actors is compulsory and comes with privacy, interoperability and scalability issues. The security regarding incidents that can happen on devices of the system or regarding the deviation from forecast of renewable energy sources is then challenging in this context.

To identify the correct and most up-to-date requirements for the design of secure OPF algorithms, Chapter 3 of this thesis analysed 9 recent major blackouts that happened in the period from 2005 to 2016. Our analysis revealed that most blackouts from the last decade happened in periods of normal loading with some important equipment out of service and with highly dependent transmission system regions. In addition to this, it highlighted that recent blackouts have a tendency to enter directly the fast cascade (with the loss of interconnections among highly dependent regions playing an important role in this high speed), leaving system operators with hardly any time to take any countermeasure. This final conclusion supported the focus of this thesis on the prevention rather than on determining potential corrective actions because it is more suited to mitigate the risk of blackouts due to their high speed. It also raised the need to consider interconnected systems as a whole and thus the need to enhance the coordination of the different power system actors, in particular in the context of security.

We thus developed, in Chapter 4, an algorithm that solve the preventive Security Constrained Optimal Power Flow (SCOPF) problem in a fully distributed manner.

The preventive SCOPF problem consists in adding constraints that ensure that, after the loss of any major device of the system, the new steady-state reached, as a result of the primary frequency control, does not violate any constraint. The developed algorithm uses a fine-grained decomposition and it was implemented under the multi-agent system paradigm based on two categories of agents: devices and buses. This multi-agent fine-grained decomposition ensures the autonomy and privacy of the different actors of the system and provides good scalability with respect to the size of the problem. These agents are coordinated using the Alternating Direction Method of Multipliers (ADMM), in conjunction with a consensus problem that aims at modelling the primary frequency response of conventional generators. Extensive simulation results on several standard IEEE systems showed the good performance of the proposed model and algorithm in terms of convergence speed and accuracy because the optimal solution was found in a similar number of iterations compared to the OPF problem. These results also proved the capacity of the algorithm to deal with the disconnection of areas in interconnected systems without propagating the origin of the disturbance.

The risk related to the uncertainty of production of wind farms is integrated, in Chapter 5, through chance constraints. We formulated the Chance-Constrained Optimal Power Flow (CCOPF) problem that consists in including constraints on the probability that network constraints are violated. In more detail, it enforces that the constraints are respected with a high probability, given the probability density function associated with the production of each wind farm. The resulting schedule provides in this way probabilistic guarantees that the constraints are respected. Chapter 5 presented a distributed two-step algorithm to solve this problem based on the same fine-grained decomposition than the one presented in Chapter 4. The first step of the algorithm aims at determining, in a distributed manner, the sensitivity factors employed in the formulation, i.e. the generalised generation distribution factors and the frequency response characteristic of the system. The second step consists in solving the CCOPF problem with the ADMM algorithm, using the sensitivity factors to define the constraints of this problem. The algorithm was tested on a two-bus test system and on the IEEE 14-bus test system. The results were compared with the solution found using a centralised optimisation tool and prove the effectiveness of the method.
However, this first model cannot include the ramp capabilities of generators because the needed generators reserves are considered constant, and consequently, in highly uncertainty cases, the problem can become unfeasible. To overcome this issue, we formulated a second model that considers some flexibility from the wind farms, through the inclusion of the possibility to curtail the wind production, in order to reduce the uncertainty. This allows to make the CCOPF problems feasible, and to determine how much each wind farm should be curtailed, by including a consensus problem on the wind farms uncertainty, in addition to the ADMM. Simulations are conducted on the test systems to prove the effectiveness of both methods. We compared the results of the CCOPF with curtailment capabilities with an analytical solution, for a two-bus test system. The algorithm was also tested on the IEEE 14-bus test system and proved to be able to find solutions to this non-convex problem.

In conclusion, the developed methods fulfil, each, some the requirements listed in Section 1.1. Particularly, they are both scalable, and they allow the coordination of the power systems actors while maintaining their privacy. Chapter 4 fulfils the security requirements regarding the loss of devices of the system due to an incident, and Chapter 5 fulfils the security requirements regarding the uncertainty on the wind farms production.

6.2 FUTURE WORKS

In order to foster the real-world deployment and commercial use of the techniques presented in this thesis, a number of improvements should be conducted. First, the formulation of the problems described should be improved to capture more accurately power systems phenomenon and to integrate more complex devices and controls. Second, we discuss the main algorithmic improvements needed before a real deployment on power systems.

6.2.1 *Enhancement of problem formulation*

The first track of improvement of this thesis consists in enhancing the formulation of the SCOPF and CCOPF problems.

Modelling of AC power flow equations

In this thesis, we employed the DC power flow equations that are linearisations of the non-convex AC power flow equations. It is essential to consider those non-convex equations to reach the correct level of accuracy needed to operate power systems. The AC power flow equations have been used in [ST15], for an AC power flow energy management problem, and could be employed in the formulation of the SCOPF and of the CCOPF. The reactive power and voltage magnitude variables should then be integrated and as a result the line-sub-problems become non-convex and cannot be solved analytically (for the rest of devices and the nets, sub-problems are similar to the ones presented in this thesis and can still be solved either analytically or using Dykstra's method to project the solution on the constraints). Thus, to solve the AC-SCOPF and AC-CCOPF, it is important to solve line sub-problems in an efficient way.

More complex device models

Another extension of the proposed models consists in enhancing the devices of the systems. For example, under the AC power flow equations, the generators can regulate the voltage magnitude by controlling their reactive power injection. The transformers can be equipped with on-load-tap changers that also control the voltage magnitude. However, on-load-tap changers involves discrete tap changes that make the problem mix-integer non-convex. Finally, with the increase interest of Smart-Grids systems

that allow pro-sumers to provide services to the grid, the fixed loads could be replaced by distribution systems. One of the advantages of using the ADMM to solve transmission system problems is that this method is often used to coordinate pro-sumers in Smart-Grid and, thus, the connection of those optimisation tools should be eased.

Optimising the speed droop of generators

In the SCOPF problem, the speed droop of the generators is traditionally supposed fixed because it depends on the characteristics of the electric machine. And yet, as shown in [DHKP16] this droop can be slightly modified and optimised, within the mechanical and electrical limits of the machine.

An extension of the SCOPF then consists in optimising the generators speed droops to enforce the security of the operations and minimise the network operation cost. The main impact would be on the complexity of the generators sub-problems, but the framework to solve the SCOPF proposed in this thesis can be adapted to this extended case.

Non-Gaussian distributions

To be able to reformulate the problem analytically, this thesis assumed that the random fluctuations in wind energy can be represented by means of Gaussian distributions. However, the wind farms generation forecast uncertainty is, in fact, not following a Gaussian distribution, but rather a Weibull distribution [GTPDF98, Wai17]. Thus, a line of future work consists in extending the CCOPF problem formulation of this thesis to handle more general (non-Gaussian) distributions.
A more straightforward extension would be to model the forecast error as a Gaussian Mixture Model which prevents from computing the convolution of many probability density functions. The main impact would be that the computation of the reserves and margins would become a weighted Kronecker product of the Gaussian Mixture Model parameters, which requires more computation than the Gaussian models.

Integration of the curtailed power into the primary frequency control

As mentioned in Chapter 5, curtailment capabilities are proposed in [RMC$^+$16], where the curtailed power is used as a reserve for the primary frequency control (PFC). This would help reducing the cost of uncertainty by fully taking advantage of the flexibility provided by the curtailment of wind farms.
The main issue, however, comes from the fact that the wind farms need to determine how much they should curtail and their primary frequency control factor (i.e. K_w). Moreover, changing the PFC factors should modify the GGDF of the system which should be included in the optimisation.

Address all requirements at once: Chance Security Constrained OPF

Addressing all the requirements at the same time is a natural extension of this work and consists in tackling a security-constrained optimal power flow problem with chance constraints. However, this is challenging and the main issue comes from the fact that the GGDF would need to be computed for each scenario of the SCOPF problem. It means that for each scenario of the SCOPF problem, we would need as many extra scenarios as wind farms to compute the sensitivity factors. On the other hand, the CCOPF and SCOPF algorithm can be merged more easily if the first of the CCOPF algorithm is replaced by specific scenarios whose objectives would be to determine the sensitivity factors and not to enforce additional constraints.

6.2.2 *Improvement of the ADMM performance and real deployment*

The validation of the distributed performance of the algorithm is crucial before a real deployment of the methods developed in this thesis. Different approaches can enhance the (distributed) performance of the ADMM algorithm (in particular, the convergence rate) and these are mentioned next.

Fast ADMM

An accelerated version of the ADMM, based on Nesterov acceleration, is proposed in [GOSB14] and has been applied to the DC-OPF problem in [WWW17b]. However, the acceleration step necessitates a central coordinator. Hence, adapting this accelerated ADMM to a fully decentralised approach seems a promising direction of future work.

Tuning of the scaling parameter

The rate of convergence of the ADMM algorithm highly depends on the value of the scaling parameter. Given this, different methods can be found in the literature to dynamically update the scaling parameter. For example, self-adaptive methods relying on the assumption that the fastest convergence of the ADMM is achieved when the primal and dual residuals are of the same order of magnitude are proposed in [HYW00] and [KCLB14]. Another method, developed in [FB15], consists in setting the scaling parameter so that the primal residual is minimised, until the solution becomes feasible and then to adapt the scaling parameter to reach the optimality via the dual residual.

However, all these above-cited references need to be tuned themselves, so, to apply them it is necessary to study how those parameters influence the performances.

Pre-conditioning

Pre-conditioning a problem consists in applying a transformation that eases the solving, usually, by reducing the condition number of the problem. For example, [FB15]

and [TJ16] explore the impact of preconditioning problems on the convergence speed of the ADMM. The improvements in terms of performances appeared promising on the applications of those references. Hence, pre-conditioning could be investigated in the context of SCOPF and CCOPF problems.

Optimising the level of decomposition

We discussed the level of decomposition of the problem in Section 2.4.1, and the existing works basically proved that the way the problem is decomposed impacts the performance of the ADMM. It is also emphasized that there is a trade-off between the quantity of information exchanged per iteration (larger when the decomposition is finer) and the complexity of the sub-problems to solve at each iteration (greater when the decomposition is coarser). A thorough study of the best level of decomposition should be conducted, because it impacts the performances and also the deployment.

Real deployment

To be able to deploy this framework in real-world power systems, a number of challenges remains. For example, the communication framework is crucial for the good functioning of the method and should be carefully integrated. Moreover, the robustness of the method to communication failures or errors should be investigated. For instance, [ZNCX16] proposes an asynchronous version of the ADMM that can be employed to improve this robustness.

BIBLIOGRAPHY

[20004] Major Grid Blackouts of 2003 in North America and Europe. Panel session conducted at the Power Engineering Society General Meeting, 2004.

[20006] Power System Blackouts. Panel session conducted at the Power Systems Conference and Exposition, 2006.

[ADF+05] G. Andersson, P. Donalek, R. Farmer, N. Hatziargyriou, I. Kamwa, P. Kundur, N. Martins, J. Paserba, P. Pourbeik, J. Sanchez-Gasca, R. Schulz, A. Stankovic, C. Taylor, and V. Vittal. Causes of the 2003 major grid blackouts in North America Europe, and recommended means to improve system dynamic performance. *IEEE Transactions on Power Systems*, 20(4):1922–1928, 2005.

[AEM16] AEMO. Update report: black system event in South Australia on 28 September 2016. Technical report, Australian Energy Market Operator (AEMO), 2016.

[AES10] M. Albadi and E. El-Saadany. Overview of wind power intermittency impacts on power systems. *Electric Power Systems Research*, 80(6):627–632, 2010.

[AGG+12] C. B. Antonio, P. Gomes, A. Guarini, F. Alves, N. Martins, D. Falcão, G. Taranto, and C. Ribeiro. C2-214 CIGRE 2012 Lessons Learned in Restoration from Recent Blackout Incidents in Brazilian Power System TARANTO COPPE / UFRJ CEP : 22283-900. Technical report, CIGRE, 2012.

[And08] G. Andersson. Modelling and analysis of electric power systems. *ETH Zurich, september*, 2008.

[AS74] O. Alsac and B. Stott. Optimal load flow with steady-state security. *IEEE Transactions on Power Apparatus and Systems*, PAS-93(3):745–751, May 1974.

[AS09] A. Atputharajah and T. K. Saha. Power system blackouts - literature review. In *2009 International Conference on Industrial and Information Systems (ICIIS)*, pages 460–465, Dec 2009.

[BB03] A. G. Bakirtzis and P. N. Biskas. A decentralised solution to the dc-opf of interconnected power systems. *IEEE Transactions on Power Systems*, 18(3):1007–1013, 2003.

[BBCP05] F. Bellifemine, F. Bergenti, G. Caire, and A. Poggi. JADE - A java agent development framework. In *Multi-Agent Programming: Languages, Platforms and Applications*, pages 125–147. Springer, 2005.

[BCD+08] R. Baldick, B. Chowdhury, I. Dobson, Z. Dong, B. Gou, D. Hawkins, H. Huang, M. Joung, D. Kirschen, F. Li, J. Li, Z. Li, C.-C. Liu, L. Mili, S. Miller, R. Podmore, K. Schneider, K. Sun, D. Wang, Z. Wu, P. Zhang, W. Zhang, and X. Zhang. Initial review of methods for cascading failure analysis in electric power transmission systems IEEE PES CAMS task force on understanding, prediction, mitigation and restoration of cascading failures. In *Power and Energy Society General Meeting - Conversion and Delivery of Electrical Energy in the 21st Century, 2008 IEEE*, pages 1–8. IEEE, July 2008.

[BCH14] D. Bienstock, M. Chertkov, and S. Harnett. Chance-constrained optimal power flow: Risk-aware network control under uncertainty. *SIAM Review*, 56(3):461–495, 2014.

[BD86] J. P. Boyle and R. L. Dykstra. A method for finding projections onto the intersection of convex sets in hilbert spaces. In *Advances in order restricted statistical inference*, pages 28–47. Springer, 1986.

[BGL10] H. Bevrani, A. Ghosh, and G. Ledwich. Renewable energy sources and frequency regulation: survey and new perspectives. *IET Renewable Power Generation*, 4(5):438–457, 2010.

[BPC+11] S. Boyd, N. Parikh, E. Chu, B. Peleato, and J. Eckstein. Distributed optimisation and Statistical Learning via the Alternating Direction Method of Multipliers. *Foundations and Trends in Machine Learning*, 3(1):1–122, 2011.

[BSJ+15] Z. Bo, O. Shaojie, Z. Jianhua, S. Hui, W. Geng, and Z. Ming. An analysis of previous blackouts in the world: Lessons for china's power industry. *Renewable and Sustainable Energy Reviews*, 42:1151–1163, 2015.

[Cap16] F. Capitanescu. Critical review of recent advances and further developments needed in ac optimal power flow. *Electric Power Systems Research*, 136:57–68, 2016.

[Car62] J. Carpentier. Contribution a l'etude du dispatching economique. *Bulletin de la Societe Francaise des Electriciens*, 3(1):431–447, 1962.

[CD17] M. Chertkov and Y. Dvorkin. Chance constrained optimal power flow with primary frequency response. *arXiv preprint arXiv:1703.06724*, 2017.

[CDE11] CDEC-SIC. Estudio para análisis de falla EAF 300/2011: Apertura intempestiva de los interruptores 52K1 y 52K2 de S/E Ancoa. Technical report, Power System Operator of Central Interconnected System Chile (CDEC-SIC), 2011.

[Cer12] Cerc. Report on the Grid Disturbance on 30 Th July and Grid Disturbance on 31 St July. Technical Report 167, CERC, 2012.

[CKC+14] S. Chakrabarti, M. Kraning, E. Chu, R. Baldick, and S. Boyd. Security Constrained Optimal Power Flow via proximal message passing. *2014 Clemson University Power Systems Conference*, pages 1–8, 2014.

[CND16] B. A. Carreras, D. E. Newman, and I. Dobson. North american blackout time series statistics and implications for blackout risk. *IEEE Transactions on Power Systems*, 31(6):4406–4414, 2016.

[COC12] M. B. Cain, R. P. O'neill, and A. Castillo. History of optimal power flow and formulations. *Federal Energy Regulatory Commission*, pages 1–36, 2012.

[Coh80] G. Cohen. Auxiliary problem principle and decomposition of optimisation problems. *Journal of optimisation Theory and Applications*, 32(3):277–305, 1980.

[CRP+11] F. Capitanescu, J. M. Ramos, P. Panciatici, D. Kirschen, A. M. Marcolini, L. Platbrood, and L. Wehenkel. State-of-the-art, challenges, and future trends in security constrained optimal power flow. *Electric Power Systems Research*, 81(8):1731–1741, 2011.

[CVL00] J.-P. Clerfeuille, S. Vitet, and C. Lebrevelec. *Plan de defense des reseaux contry les incidents majeurs*. Ed. Techniques Ingénieur, 2000.

[CW08] F. Capitanescu and L. Wehenkel. A new iterative approach to the corrective security-constrained optimal power flow problem. *IEEE transactions on power systems*, 23(4):1533–1541, 2008.

[CW11] F. Capitanescu and L. Wehenkel. Redispatching active and reactive powers using a limited number of control actions. *IEEE Transactions on Power Systems*, 26(3):1221–1230, 2011.

[Dag06] J. E. Dagle. Postmortem analysis of power grid blackouts - the role of measurement systems. *IEEE Power and Energy Magazine*, 4(5):30–35, Sept 2006.

[DBT17] P. Du, R. Baldick, and A. Tuohy. *Integration of Large-Scale Renewable Energy into Bulk Power Systems*. Springer, 2017.

[DHKP16] Y. Dvorkin, P. Henneaux, D. S. Kirschen, and H. Pandžić. optimising primary response in preventive security-constrained optimal power flow. *IEEE Systems Journal*, PP(99):1–10, 2016.

[DO05] R. Doherty and M. O'malley. A new approach to quantify reserve demand in systems with significant installed wind capacity. *IEEE Transactions on Power Systems*, 20(2):587–595, 2005.

[DZG13] E. Dall'Anese, H. Zhu, and G. B. Giannakis. Distributed optimal power flow for smart microgrids. *IEEE Transactions on Smart Grid*, 4(3):1464–1475, Sept 2013.

[EB05] I. Erlich and U. Bachmann. Grid code requirements concerning connection and operation of wind turbines in germany. In *Power Engineering Society General Meeting, 2005. IEEE*, pages 1253–1257, 2005.

[EE15] ENTSO-E's. Where the energy union starts: regions. `https://www.entsoe.eu/Documents/Publications/vision/entsoe_vision04_regions_web.pdf`, November 2015.

[EES15] W. T. Elsayed and E. F. El-Saadany. A fully decentralised approach for solving the economic dispatch problem. *IEEE Transactions on Power Systems*, 30(4):2179–2189, July 2015.

[Ers14] T. Erseghe. Distributed optimal power flow using admm. *IEEE Transactions on Power Systems*, 29(5):2370–2380, Sept 2014.

[Ers15] T. Erseghe. A distributed approach to the opf problem. *EURASIP Journal on Advances in Signal Processing*, 2015(1):45, 2015.

[ES13] M. Eremia and M. Shahidehpour. *Handbook of electrical power system dynamics: modelling, stability, and control*, volume 92. John Wiley & Sons, 2013.

[Eur07] European Regulators Group for Electricity and Gas. Final Report The lessons to be learned from the large disturbance in the European power system on the 4th of November 2006. Technical Report February, European Regulators Group for Electricity and Gas, 2007.

[FB15] C. Fougner and S. Boyd. Parameter selection and pre-conditioning for a graph form solver. *arXiv preprint arXiv:1503.08366*, 2015.

[FN12] Ferc and Nerc. Arizona-Southern California Outages on September 8 2011. Technical report, Federal Energy Regulatory Commission (FERC) & North American Electric Reliability Corporation (NERC), 2012.

[For99] R. T. Force. The ieee reliability test system-1996. *IEEE Trans. Power Syst*, 14(3):1010–1020, 1999.

[FSR12] S. Frank, I. Steponavice, and S. Rebennack. Optimal power flow: a bibliographic survey i. *Energy Systems*, 3(3):221–258, 2012.

[GB08] M. Grant and S. Boyd. Graph implementations for nonsmooth convex programs. In V. Blondel, S. Boyd, and H. Kimura, editors, *Recent Advances in Learning and Control*, Lecture Notes in Control and Information Sciences, pages 95–110. Springer-Verlag Limited, 2008. `http://stanford.edu/~boyd/graph_dcp.html`.

[GB14] M. Grant and S. Boyd. CVX: Matlab software for disciplined convex programming, version 2.1. `http://cvxr.com/cvx`, March 2014.

[GHT16a] J. Guo, G. Hug, and O. K. Tonguz. Enabling distributed optimisation in large-scale power systems. *CoRR*, abs/1605.09785, 2016.

[GHT16b] J. Guo, G. Hug, and O. K. Tonguz. Intelligent partitioning in distributed optimisation of electric power systems. *IEEE Transactions on Smart Grid*, 7(3):1249–1258, 2016.

[GOSB14] T. Goldstein, B. O'Donoghue, S. Setzer, and R. Baraniuk. Fast alternating direction optimisation methods. *SIAM Journal on Imaging Sciences*, 7(3):1588–1623, 2014.

[GTPDF98] A. Garcia, J. Torres, E. Prieto, and A. De Francisco. Fitting wind speed distributions: a case study. *Solar energy*, 62(2):139–144, 1998.

[Gut09] M. Gutierrez. Colombian Blackout 2007 Blackout Watch. *PAC world magazine*, pages 36–37, 2009.

[HDDC17] A. Hassan, Y. Dvorkin, D. Deka, and M. Chertkov. Chance-constrained admm approach for decentralised control of distributed energy resources. *arXiv preprint arXiv:1710.09738*, 2017.

[HG91] M. Huneault and F. Galiana. A survey of the optimal power flow literature. *IEEE transactions on Power Systems*, 6(2):762–770, 1991.

[HP06] S. H. Horowitz and A. G. Phadke. Blackouts and relaying considerations - relaying philosophies and the future of relay systems. *IEEE Power and Energy Magazine*, 4(5):60–67, Sept 2006.

[HPK02] D. Hur, J.-K. Park, and B. H. Kim. Evaluation of convergence rate in the auxiliary problem principle for distributed optimal power flow. *IEE Proceedings-Generation, Transmission and Distribution*, 149(5):525–532, 2002.

[HYW00] B. He, H. Yang, and S. Wang. Alternating direction method with self-adaptive penalty parameters for monotone variational inequalities. *Journal of optimisation Theory and applications*, 106(2):337–356, 2000.

[HZ15] L. Hirth and I. Ziegenhagen. Balancing power and variable renewables: Three links. *Renewable and Sustainable Energy Reviews*, 50:1035–1051, 2015.

[IEE07] IEEE Task Force on Blackout Experience, Mitigation and Role of New Technologies. Blackout experiences and lessons, best practices for system dynamic performance, and the role of new technologies. Technical report, IEEE Task Force, 2007.

[Ilh10] J. M. O. F. Ilho. Brazilian Blackout 2009 Blackout Watch. *PAC World Magazine*, 2010.

[Jab13] R. A. Jabr. Adjustable robust opf with renewable energy sources. *IEEE Transactions on Power Systems*, 28(4):4742–4751, 2013.

[JWW+17] X. Jin, Z. Wen, L. Weidong, L. Yan, T. Xinshou, L. Chao, and W. Linjun. Study on the driving force and challenges of developing power grid with high penetration of renewable energy. In *Transportation Electrification Asia-Pacific (ITEC Asia-Pacific), 2017 IEEE Conference and Exp*, pages 1–5, 2017.

[KB97] B. H. Kim and R. Baldick. Coarse-grained distributed optimal power flow. *IEEE Transactions on Power Systems*, 12(2):932–939, 1997.

[KB00] B. H. Kim and R. Baldick. A comparison of distributed optimal power flow algorithms. *IEEE Transactions on Power Systems*, 15(2):599–604, 2000.

[KCLB14] M. Kraning, E. Chu, J. Lavaei, and S. P. Boyd. Dynamic network energy management via proximal message passing. *Foundations and Trends in optimisation*, 1(2):73–126, 2014.

[KCP10] K. Karoui, H. Crisciu, and L. Platbrood. Modeling the primary reserve allocation in preventive and curative security constrained opf. In *Transmission and Distribution Conference and Exposition, 2010 IEEE PES*, pages 1–6, 2010.

[KDG03] D. Kempe, A. Dobra, and J. Gehrke. Gossip-based computation of aggregate information. In *Foundations of Computer Science, 2003. Proceedings. 44th Annual IEEE Symposium on*, pages 482–491, 2003.

[KF14] A. Kargarian and Y. Fu. System of systems based security-constrained unit commitment incorporating active distribution grids. *IEEE Transactions on Power Systems*, 29(5):2489–2498, 2014.

[KFL15] A. Kargarian, Y. Fu, and Z. Li. Distributed security-constrained unit commitment for large-scale power systems. *IEEE Transactions on Power Systems*, 30(4):1925–1936, 2015.

[KMG+16] A. Kargarian, J. Mohammadi, J. Guo, S. Chakrabarti, M. Barati, G. Hug, S. Kar, and R. Baldick. Toward distributed/decentralised dc optimal power flow implementation in future electric power systems. *IEEE Transactions on Smart Grid*, 2016.

[KPA+04] P. Kundur, J. Paserba, V. Ajjarapu, G. Andersson, A. Bose, T. Van Cutsem, C. Canizares, N. Hatziargyriou, D. Hill, V. Vittal, A. Stankovic, and C. Taylor. Definition and Classification of Power System Stability IEEE/CIGRE Joint Task Force on Stability Terms and Definitions. *IEEE Transactions on Power Systems*, 19(3):1387–1401, 2004.

[KSM18] F. Karbalaei, H. Shahbazi, and M. Mahdavi. A new method for solving preventive security-constrained optimal power flow based on linear network compression. *International Journal of Electrical Power & Energy Systems*, 96:23–29, 2018.

[LBD15] E. Loukarakis, J. W. Bialek, and C. J. Dent. Investigation of maximum possible opf problem decomposition degree for decentralised energy markets. *IEEE Transactions on Power Systems*, 30(5):2566–2578, Sept 2015.

[LBZR06] W. Lu, Y. Besanger, É. Zamaï, and D. Radu. Blackouts: Description, Analysis and Classification. In *WSEAS International Conference on Power Systems*, Lisbonne, Portugal, September 2006.

[LDB16] M. Lubin, Y. Dvorkin, and S. Backhaus. A robust approach to chance constrained optimal power flow with renewable generation. *IEEE Transactions on Power Systems*, 31(5):3840–3849, 2016.

[LKYH13] L. Liu, A. Khodaei, W. Yin, and Z. Han. A distribute parallel approach for big data scale optimal power flow with security constraints. In *Smart Grid Communications (SmartGridComm), 2013 IEEE International Conference on*, pages 774–778, 2013.

[LM15] B. Li and J. L. Mathieu. Analytical reformulation of chance-constrained optimal power flow with uncertain load control. In *PowerTech, 2015 IEEE Eindhoven*, pages 1–6, 2015.

[LSW+15] Z. Li, M. Shahidehpour, W. Wu, B. Zeng, B. Zhang, and W. Zheng. Decentralised multiarea robust generation unit and tie-line scheduling under wind power uncertainty. *IEEE Transactions on Sustainable Energy*, 6(4):1377–1388, 2015.

[LWZ+16] Z. Li, W. Wu, B. Zeng, M. Shahidehpour, and B. Zhang. Decentralised Contingency-Constrained Tie-Line Scheduling for Multi-Area Power Grids. *IEEE Transactions on Power Systems*, pages 1–14, 2016.

[MAEH99] J. A. Momoh, R. Adapa, and M. El-Hawary. A review of selected optimal power flow literature to 1993. i. nonlinear and quadratic programming approaches. *IEEE transactions on power systems*, 14(1):96–104, 1999.

[MAT14] MATLAB. *version 7.10.0 (R2014a)*. The MathWorks Inc., Natick, Massachusetts, 2014.

[MDC+07a] S. D. McArthur, E. M. Davidson, V. M. Catterson, A. L. Dimeas, N. D. Hatziargyriou, F. Ponci, and T. Funabashi. Multi-agent systems for power engineering applications—part i: Concepts, approaches, and technical challenges. *IEEE Transactions on Power systems*, 22(4):1743–1752, 2007.

[MDC+07b] S. D. McArthur, E. M. Davidson, V. M. Catterson, A. L. Dimeas, N. D. Hatziargyriou, F. Ponci, and T. Funabashi. Multi-agent systems for power engineering applications—part ii: Technologies, standards, and tools for building multi-agent systems. *IEEE Transactions on Power Systems*, 22(4):1753–1759, 2007.

[MDS+17] D. K. Molzahn, F. Dörfler, H. Sandberg, S. H. Low, S. Chakrabarti, R. Baldick, and J. Lavaei. A survey of distributed optimisation and control algorithms for electric power systems. *IEEE Transactions on Smart Grid*, 8(6):2941–2962, 2017.

[MEHA99] J. A. Momoh, M. El-Hawary, and R. Adapa. A review of selected optimal power flow literature to 1993. ii. newton, linear programming and interior point methods. *IEEE Transactions on Power Systems*, 14(1):105–111, 1999.

[MGL14] K. Margellos, P. Goulart, and J. Lygeros. On the road between robust optimisation and the scenario approach for chance constrained optimisation problems. *IEEE Trans. Automat. Contr.*, 59(8):2258–2263, 2014.

[MHH+12] K. Margellos, T. Haring, P. Hokayem, M. Schubiger, J. Lygeros, and G. Andersson. A robust reserve scheduling technique for power systems with high wind penetration. In *International conference on probabilistic methods applied to power systems*, 2012.

[MHK14] J. Mohammadi, G. Hug, and S. Kar. Role of communication on the convergence rate of fully distributed dc optimal power flow. In *Smart Grid Communications (SmartGridComm), 2014 IEEE International Conference on*, pages 43–48, 2014.

[MHK15] J. Mohammadi, G. Hug, and S. Kar. Asynchronous distributed approach for dc optimal power flow. In *PowerTech, 2015 IEEE Eindhoven*, pages 1–6, 2015.

[MKH14] J. Mohammadi, S. Kar, and G. Hug. Distributed approach for dc optimal power flow calculations. *arXiv preprint arXiv:1410.4236*, 2014.

[MKH17] J. Mohammadi, S. Kar, and G. Hug. Fully distributed corrective security constrained optimal power flow. In *PowerTech, 2017 IEEE Manchester*, pages 1–6, 2017.

[MPG87] A. Monticelli, M. V. F. Pereira, and S. Granville. Security-constrained optimal power flow with post-contigency corrective rescheduling. *IEEE Transactions on Power Systems*, 2(1):175–180, 1987.

[MRM16] M. H. Moradi, S. Razini, and S. Mahdi Hosseinian. State of art of multiagent systems in power engineering: A review. *Renewable and Sustainable Energy Reviews*, 58:814–824, 2016.

[MRSV05] Y. V. Makarov, V. I. Reshetov, A. Stroev, and I. Voropai. Blackout prevention in the United States, Europe, and Russia. *Proceedings of the IEEE*, 93(11):1942–1955, November 2005.

[MSK16] C. Murphy, A. Soroudi, and A. Keane. Information gap decision theory-based congestion and voltage management in the presence of uncertain wind power. *IEEE Transactions on Sustainable Energy*, 7(2):841–849, 2016.

[MWF15] S. Magnússon, P. C. Weeraddana, and C. Fischione. A distributed approach for the optimal power-flow problem based on admm and sequential convex approximations. *IEEE Transactions on Control of Network Systems*, 2(3):238–253, 2015.

[NER11] NERC. Balancing and frequency control. Technical report, North American Electric Reliability Corporation (NERC), jan 2011.

[Ng81] W. Y. Ng. Generalised generation distribution factors for power system security evaluations. *IEEE Transactions on Power Apparatus and Systems*, (3):1001–1005, 1981.

[ODK11] R. P. O'Neill, T. Dautel, and E. Krall. Recent iso software enhancements and future software and modelling plans. *Federal Energy Regulatory Commission, Washington, DC, Tech. Rep*, 2011.

[oEotRoI05] M. of Energy and M. R. of the Republic of Indonesia. Investigation Report on the Java-Madura-Bali Power System Blackout on 18 August 2005. Technical report, Ministry of Energy and Mineral Resources of the Republic of Indonesia, December 2005.

[ONS09] ONS. Análise da perturbação do dia 10/11/2009 às 22h13min, envolvendo o desligamento dos três circuitos da LT 765 kV Itaberá - Ivaiporã. Technical report, Operador Nacional do Sistema Elétrico (ONS), 2009.

[ONS11] ONS. Análise da perturbaçâo do dia 04/02/2011 à 00h21min envolvendo os estados da região nordeste. Technical report, Operador Nacional do Sistem Elétrico, 2011.

[P. 07] P. C. Avella, Á. M. Cabra, N. D. Montoya, A. B. Barreto, L. S. Botero, and J. Vargas. Evento del 26 de abril de 2007 en el sistema interconectado nacional sin colombiano. Technical report, XM Compañía de expertos en mercados, 2007.

[PB+14] N. Parikh, S. Boyd, et al. Proximal algorithms. *Foundations and Trends® in optimisation*, 1(3):127–239, 2014.

[PBJW06] P. Pourbeik, M. Bahrman, E. John, and W. Wong. Modern countermeasurus to blackouts. *IEEE Power and Energy Magazine*, 4(5):36–45, Sept 2006.

[PJ08] K. Pandya and S. Joshi. A survey of optimal power flow methods. *Journal of Theoretical & Applied Information Technology*, 4(5), 2008.

[PK06] J. Paserba and P. Kundur. Guest editorial - power grid blackouts remembering and fighting grid failures. *IEEE Power and Energy Magazine*, 4(5):16–21, Sept 2006.

[PK12] D. Phan and J. Kalagnanam. Distributed methods for solving the security-constrained optimal power flow problem. In *Innovative Smart Grid Technologies (ISGT), 2012 IEEE PES*, pages 1–7, 2012.

[PK14] D. Phan and J. Kalagnanam. Some efficient optimisation methods for solving the security-constrained optimal power flow problem. *IEEE Transactions on Power Systems*, 29(2):863–872, 2014.

[PKT06] P. Pourbeik, P. S. Kundur, and C. W. Taylor. The anatomy of a power grid blackout - root causes and dynamics of recent major blackouts. *IEEE Power and Energy Magazine*, 4(5):22–29, Sept 2006.

[PL14] Q. Peng and S. H. Low. Distributed algorithm for optimal power flow on a radial network. In *53rd IEEE Conference on Decision and Control*, pages 167–172, Dec 2014.

[PMDL10] A. Pinar, J. Meza, V. Donde, and B. Lesieutre. optimisation strategies for the vulnerability analysis of the electric power grid. *SIAM Journal on optimisation*, 20(4):1786–1810, 2010.

[Pro15] Project Group Turkey. Report on Blackout in Turkey on 31st March 2015. Technical report, ENTSO-E, 2015.

[PS15] D. T. Phan and X. A. Sun. Minimal impact corrective actions in security-constrained optimal power flow via sparsity regularization. *IEEE Transactions on Power Systems*, 30(4):1947–1956, 2015.

[RAM+16] L. Roald, G. Andersson, S. Misra, M. Chertkov, and S. Backhaus. Optimal power flow with wind power control and limited expected risk of overloads. In *Power Systems Computation Conference (PSCC), 2016*, pages 1–7, 2016.

[RKF16] P. Ringler, D. Keles, and W. Fichtner. Agent-based modelling and simulation of smart electricity grids and markets–a literature review. *Renewable and Sustainable Energy Reviews*, 57:205–215, 2016.

[RMC+16] L. Roald, S. Misra, M. Chertkov, S. Backhaus, and G. Andersson. Chance constrained optimal power flow with curtailment and reserves from wind power plants. *arXiv preprint arXiv:1601.04321*, 2016.

[ROG08] C. A. Ruiz, N. J. Orrego, and J. F. Gutierrez. The colombian 2007 black out. In *2008 IEEE/PES Transmission and Distribution Conference and Exposition: Latin America*, pages 1–5, Aug 2008.

[ROKA13] L. Roald, F. Oldewurtel, T. Krause, and G. Andersson. Analytical reformulation of security constrained optimal power flow with probabilistic constraints. *PowerTech (POWERTECH)*, 2013.

[RRRSR10] E. Romero-Ramos, J. Riquelme-Santos, and J. Reyes. A simpler and exact mathematical model for the computation of the minimal power losses tree. *Electric Power Systems Research*, 80(5):562–571, 2010.

[SPG13] A. X. Sun, D. T. Phan, and S. Ghosh. Fully decentralised ac optimal power flow algorithms. In *2013 IEEE Power Energy Society General Meeting*, pages 1–5, July 2013.

[ST15] P. Scott and S. Thiébaux. Distributed multi-period optimal power flow for demand response in microgrids. In *Proceedings of the 2015 ACM Sixth International Conference on Future Energy Systems, e-Energy 2015, Bangalore, India, July 14-17, 2015*, pages 17–26, 2015.

[SV05] W. Shao and V. Vittal. Corrective switching algorithm for relieving overloads and voltage violations. *IEEE Transactions on Power Systems*, 20(4):1877–1885, 2005.

[TEPR06] S. Tosserams, L. Etman, P. Papalambros, and J. Rooda. An augmented lagrangian relaxation for analytical target cascading using the alternating direction method of multipliers. *Structural and multidisciplinary optimisation*, 31(3):176–189, 2006.

[TJ16] R. Takapoui and H. Javadi. Preconditioning via diagonal scaling. *arXiv preprint arXiv:1610.03871*, 2016.

[VBC+12] M. Vaiman, K. Bell, Y. Chen, B. Chowdhury, I. Dobson, P. Hines, M. Papic, S. Miller, and P. Zhang. Risk assessment of cascading outages: Methodologies and challenges. *IEEE Transactions on Power Systems*, 27(2):631–641, 2012.

[VML12] M. Vrakopoulou, K. Margellos, and J. Lygeros. Probabilistic guarantees for the N-1 security of systems with wind power generation. *Proceedings of PMAPS 2012*, pages 858–863, 2012.

[VS16] O. P. Veloza and F. Santamaria. Analysis of major blackouts from 2003 to 2015: Classification of incidents and review of main causes. *The Electricity Journal*, 29(7):42–49, 2016.

[Wai17] P. Wais. Two and three-parameter weibull distribution in available wind power analysis. *Renewable energy*, 103:15–29, 2017.

[WM06] L. Wang and K. Morison. Implementation of online security assessment. *IEEE Power and Energy Magazine*, 4(5):46–59, Sept 2006.

[WMZL13] Q. Wang, J. D. McCalley, T. Zheng, and E. Litvinov. A computational strategy to solve preventive risk-based security-constrained opf. *IEEE Transactions on Power Systems*, 28(2):1666–1675, 2013.

[WMZL16] Q. Wang, J. D. McCalley, T. Zheng, and E. Litvinov. Solving corrective risk-based security-constrained optimal power flow with lagrangian relaxation and benders decomposition. *International Journal of Electrical Power & Energy Systems*, 75:255–264, 2016.

[Woo01] M. Wooldridge. Intelligent agents: The key concepts. In *ECCAI Advanced Course on Artificial Intelligence*, pages 3–43, 2001.

[WWW17a] Y. Wang, S. Wang, and L. Wu. Distributed optimisation approaches for emerging power systems operation : A review. *Electric Power Systems Research*, 144:127–135, 2017.

[WWW17b] Y. Wang, L. Wu, and S. Wang. A fully-decentralised consensus-based admm approach for dc-opf with demand response. *IEEE Transactions on Smart Grid*, 8(6):2637–2647, Nov 2017.

[YLZL09] K. Yamashita, J. Li, P. Zhang, and C. C. Liu. Analysis and control of major blackout events. *2009 IEEE/PES Power Systems Conference and Exposition, PSCE 2009*, pages 2–5, 2009.

[Yok97] M. Yokoo. Why adding more constraints makes a problem easier for hill-climbing algorithms: Analysing landscapes of csps. In *Proceedings of the 3rd International Conference on Principles and Practice of Constraint Programming*, CP'97, pages 356–370, Berlin, Heidelberg, 1997. Springer-Verlag.

[ZC12] Z. Zhang and M.-Y. Chow. Convergence analysis of the incremental cost consensus algorithm under different communication network topologies in a smart grid. *IEEE Transactions on power systems*, 27:1761–1768, 2012.

[ZNCX16] J. Zhang, S. Nabavi, A. Chakrabortty, and Y. Xin. Admm optimization strategies for wide-area oscillation monitoring in power systems under asynchronous communication delays. *IEEE Transactions on Smart Grid*, 7(4):2123–2133, July 2016.

RÉSUMÉ / ABSTRACT

TITRE : MÉTHODES D'OPTIMISATION DISTRIBUÉE POUR L'EXPLOITATION SÉCURISÉE DES RÉSEAUX ÉLECTRIQUES INTERCONNECTÉS

Notre société étant plus dépendante que jamais au vecteur d'énergie électrique, la moindre perturbation du transport ou de l'acheminement de l'électricité a un impact social et économique important. La fiabilité et la sécurité des réseaux électriques sont donc cruciales pour les gestionnaires de réseaux, en plus des aspects économiques. De plus, les réseaux de transport sont interconnectés pour réduire les coûts des opérations et pour améliorer la sécurité. Un des grands défis des gestionnaires des réseaux de transport est ainsi de se coordonner avec les réseaux voisins, ce qui soulève des problèmes liés à la taille du problème, à l'interopérabilité et à la confidentialité des données.

Cette thèse se focalise principalement sur la sécurité des opérations sur les réseaux électriques, c'est pourquoi l'évolution des principales caractéristiques des blackouts, qui sont des échecs de la sécurité des réseaux, sont étudiés sur la période 2005-2016. L'approche de cette étude consiste à déterminer quelles sont les principales caractéristiques des incidents de ces 10 dernières années, afin d'identifier ce qui devrait être intégré pour réduire le risque que ces incidents se reproduisent. L'évolution a été étudiée et comparée avec les caractéristiques des blackouts qui se sont produit avant 2005. L'étude se focalise sur les préconditions qui ont mené à ces blackouts et sur les cascades, et particulièrement sur le rôle de la vitesse des cascades. Les caractéristiques importante sont extraites et intégrées dans la suite de notre travail.

Un algorithme résolvant un problème préventif d'Optimal Power Flow avec contraintes de sécurité (SCOPF) de manière distribuée est ainsi développé. Ce problème consiste en l'ajout de contraintes qui assure qu'après la perte de n'importe quel équipement majeur (ligne, transformateur, générateur, le nouveau point d'équilibre, atteint suite au réglage primaire en fréquence, respecte les contraintes du système. L'algorithme développé utilise une décomposition fine du problème et est implémenté sous le paradigme multi-agent, basé sur deux catégories d'agents : les appareils et les bus. Les agents sont coordonnés grâce à l' "Alternating Direction Method of Multipliers (ADMM)" et grâce à un problème de consensus. Cette décomposition procure l'autonomie et la confidentialité nécessaire aux différents acteurs du système, mais aussi, un bon passage à l'échelle par rapport à la taille du problème. Cet algorithme a aussi pour avantage d'être robuste à n'importe quelle perturbation, incluant la séparation du système en plusieurs régions.

Puis, pour prendre en compte l'incertitude sur la production créée par les erreurs de prédiction des fermes éoliennes, une approche distribuée à deux étapes est développée pour résoudre un problème d'Optimal Power Flow avec contraintes probabilistes (CCOPF), d'une manière complétement distribuée. Les erreurs de prédiction des fermes éoliennes sont modélisées par des lois normales indépendantes et les écarts par rapport aux plannings de production sont considérés compensés par le réglage primaire en fréquence. La première étape de l'algorithme a pour but de déterminer des paramètres de sensibilités nécessaires pour formuler le problème. Les résultats de cette étape sont ensuite des paramètres d'entrée de la seconde étape qui, elle, résout le problème de CCOPF. Une extension de cette formulation permet d'ajouter de la flexibilité au problème en permettant la réduction de la production éolienne. Cet algorithme est basé sur la même décomposition fine que précédemment où les agents sont également coordonnés par l'ADMM et grâce à un problème de consensus. En conclusion, cet algorithme en deux étapes garantit la confidentialité et l'autonomie des différents acteurs, et est parallèle et adaptée aux plateformes hautes performances.

TITLE: DISTRIBUTED OPTIMISATION METHODS TO MANAGE THE SECURITY OF INTERCONNECTED POWER SYSTEMS

Our societies are more dependent on electricity than ever, thus any disturbance in the power transmission and delivery has major economic and social impact. The reliability and security of power systems are then crucial to keep, for power system operators, in addition to minimising the system operating cost. Moreover, transmission systems are interconnected to decrease the cost of operation and improve the system security. One of the main challenges for transmission system operators is therefore to coordinate with interconnected power systems, which raises scalability, interoperability and privacy issues. Hence, this thesis is concerned with how TSOs can operate their networks in a decentralised way but coordinating their operation with other neighbouring TSOs to find a cost-effective scheduling that is globally secure.

The main focus of this thesis is the security of power systems, this is why the evolution of the main characteristics of the blackouts that are failures in power system security, of the period 2005-2016 is studied. The approach consists in determining what the major characteristics of the incidents of the past 10 years are, to identify what should be taken into account to mitigate the risk of incidents. The evolution have been studied and compared with the characteristics of the blackouts before 2005. The study focuses on the pre-conditions that led to those blackouts and on the cascades, and especially the role of the cascade speed. Some important features are extracted and later integrated in our work.

An algorithm that solve the preventive Security Constrained Optimal Power Flow (SCOPF) problem in a fully distributed manner, is thus developed. The preventive SCOPF problem consists in adding constraints that ensure that, after the loss of any major device of the system, the new steady-state reached, as a result of the primary frequency control, does not violate any constraint. The developed algorithm uses a fine-grained decomposition and is implemented under the multi-agent system paradigm based on two categories of agents: devices and buses. The agents are coordinated with the Alternating Direction method of multipliers in conjunction with a consensus problem. This decomposition provides the autonomy and privacy to the different actors of the system and the fine-grained decomposition allows to take the most of the decomposition and provides a good scalability regarding the size of the problem. This algorithm also have the advantage of being robust to any disturbance of the system, including the separation of the system into regions.

Then, to account for the uncertainty of production brought by wind farms forecast error, a two-step distributed approach is developed to solve the Chance-Constrained Optimal Power Flow problem, in a fully distributed manner. The wind farms forecast errors are modelled by independent Gaussian distributions and the mismatches with the initials are assumed to be compensated by the primary frequency response of generators. The first step of this algorithm aims at determining the sensitivity factors of the system, needed to formulate the problem. The results of this first step are inputs of the second step that is the CCOPF. An extension of this formulation provides more flexibility to the problem and consists in including the possibility to curtail the wind farms. This algorithm relies on the same fine-grained decomposition where the agents are again coordinated by the ADMM and a consensus problem. In conclusion, this two-step algorithm ensures the privacy and autonomy of the different system actors and it is de facto parallel and adapted to high performance platforms.